



HAL
open science

Sur de nouveaux verres conducteurs ioniques de l'argent : matériaux, modèles, applications

Jun Liu

► **To cite this version:**

Jun Liu. Sur de nouveaux verres conducteurs ioniques de l'argent : matériaux, modèles, applications. Matériaux. Université Sciences et Technologies - Bordeaux I, 1989. Français. NNT : 1989BOR10555 . tel-00620693

HAL Id: tel-00620693

<https://theses.hal.science/tel-00620693>

Submitted on 8 Sep 2011

HAL is a multi-disciplinary open access archive for the deposit and dissemination of scientific research documents, whether they are published or not. The documents may come from teaching and research institutions in France or abroad, or from public or private research centers.

L'archive ouverte pluridisciplinaire **HAL**, est destinée au dépôt et à la diffusion de documents scientifiques de niveau recherche, publiés ou non, émanant des établissements d'enseignement et de recherche français ou étrangers, des laboratoires publics ou privés.

THÈSE

PRÉSENTÉE A

L'UNIVERSITÉ DE BORDEAUX I

POUR OBTENIR LE GRADE DE

DOCTEUR

Spécialité : SCIENCES DES MATÉRIAUX

PAR

LIU Jun

**SUR DE NOUVEAUX VERRES CONDUCTEURS IONIQUES DE L'ARGENT :
MATÉRIAUX, MODÈLES, APPLICATIONS**

Soutenu le 15 juin 1989, devant la Commission d'examen :

MM. P. HAGENMULLER	<i>Président.</i>
J. DURAND	} <i>Examineurs.</i>
J. ETOURNEAU	
J. PORTIER	
J. SALARDENNE	
C. SOURISSEAU	
J.M. REAU	
B. TANGUY	
J.J. VIDEAU	

A ma patrie

A ma mère, à mon père

A ma femme, ZHOU FANG et à ma fille

A mon frère

A toute ma famille

A mes amis

A tous ceux qui me sont chers

Témoignage de ma profonde affection

**A Monsieur le Professeur Paul Hagenmuller, fondateur
du Laboratoire de Chimie du Solide, hommage de notre
profond respect.**

**A Monsieur le Professeur Jean Etourneau, directeur du
Laboratoire de Chimie du Solide, témoignage de notre
gratitude.**

**A Monsieur le Professeur Bernard Tanguy, à Monsieur Josik
Portier, Directeur de recherche au CNRS, témoignage de
notre sincère amitié.**

Ce travail a été réalisé au Laboratoire de Chimie du Solide du CNRS. Monsieur le Professeur Hagenmuller, son fondateur, Monsieur le Professeur Etourneau son directeur, ont permis qu'il se réalise en nous invitant et en créant les conditions matérielles nécessaires à son achèvement. Qu'ils en soient remerciés.

Nous exprimons notre reconnaissance a Bernard Tanguy et à Josik Portier qui ont dirigé notre travail avec gentillesse et efficacité nous faisant profiter de leur expérience et partager leur enthousiasme pour la découverte. Qu'ils acceptent notre amitié.

Monsieur le Professeur Jean Salardenne, messieurs Jean Durand et Claude Sourisseau, Directeurs de recherche au CNRS nous ont fait l'honneur de juger notre travail. Nous les prions d'accepter notre respectueuse reconnaissance.

Nous tenons à remercier tout particulièrement Jean Maurice Réau pour sa contribution aux études de transport ionique, Jean Jacques Videau pour son étroite participation aux études structurales par spectroscopie infrarouge, Jean Salardenne pour la réalisation de couches minces.

Monsieur le Professeur Austen Angell nous a fait profiter de ses compétences dans la science du verre. Nous le remercions d'avoir bien voulu s'intéresser à notre travail.

Christian Cros, vice directeur du LCS, nous a aidé à résoudre nos problèmes matériels. Anne Marie Berdin nous a guidé au travers des arcanes administratifs. Nous les en remercions.

Notre reconnaissance s'adresse enfin à tous nos camarades techniciens, chercheurs et étudiants pour leur amicale sollicitude et leur disponibilité :

Lucien Lozano pour les manipulations sous atmosphère de chlore

Louis Trut et Jean Pierre Cazorla pour les caractérisations par diffraction X

Michel Lahaye pour les analyses par microsonde

Louis Rabardel et Joel Villot pour les analyses thermiques

Jean Michel Dance pour les études par RPE.

TABLE DES MATIERES

	page
CHAPITRE 1: INTRODUCTION	1
CHAPITRE 2: LES VERRES CONDUCTEURS IONIQUES DE L'ARGENT	5
2.1. GENERALITES SUR LES CONDUCTEURS IONIQUES VITREUX	5
2.1.1. ABREGE DE L'HISTOIRE DES VERRES	5
2.1.2. LES MATERIAUX	5
2.1.3. MECANISMES DE TRANSPORT IONIQUE DANS LES VERRES	8
2.1.3.1 L'APPROCHE DE ANDERSON-STUART (A-S)	8
2.1.3.2 LA THEORIE DE L'ELECTROLYTE FAIBLE (R-S)	10
2.1.3.3 COMPARAISON DES MODELES A-S ET R-S	12
2.2. LES VERRES CONDUCTEURS DE L'ION ARGENT	13
2.3. CHOIX DES MATERIAUX	15
CHAPITRE 3: PROPRIETES ET STRUCTURES DE VERRES THIOIODES A BASE D'ARSENIC	18
3.1. LES VERRES DU SYSTEME $As-Ag-S$	18
3.2. PROPRIETE DE TRANSPORT DES VERRES DU SYSTEME $As_2S_3-Ag_2S-AgI$	31
3.3. COMPARAISON DES PROPRIETES DE TRANSPORT DES VERRES DES SYSTEMES $As_2S_3-Ag_2S-AgI$ ET $Sb_2S_3-Ag_2S-AgI$	38
3.4. STRUCTURE DES VERRES DU SYSTEME $As_2S_3-Ag_2S-AgI$	41
3.5. CONCLUSION DU CHAPITRE 3	57
CHAPITRE 4: VERRES THIO-OXYPHOSPHATES	59
4.1. LE SYSTEME $Ag_2S-AgPO_3$	59
4.2. CONCLUSION DU CHAPITRE 4	77
CHAPITRE 5: REMPLACEMENT DE L'ARGENT DANS LES VERRES SULFURES ET PHOSPHATES	82
5.1. INTRODUCTION	82
5.2. INCORPORATION ELECTROCHIMIQUE DU CUIVRE DANS UN VERRE CONDUCTEUR IONIQUE DE L'ION ARGENT	83
5.3. LE SYSTEME $TII-AgPO_3$	90
5.4. LE SYSTEME $Tl_2S-AgPO_3$	100
5.5. CONCLUSIONS DU CHAPITRE 5	108
CHAPITRE 6: APPLICATIONS ELECTROCHIMIQUES DES	

	page
VERRES CONDUCTEURS DE L'ION ARGENT110
6.1. INTRODUCTION110
6.2. APPLICATIONS ELECTROCHIMIQUES DES VERRES CONDUCTEURS DE L'ION ARGENT110
CHAPITRE 7: CONCLUSIONS GENERALES125
LISTE DES FIGURES 127
LISTE DES TABLEAUX 131

Chapitre 1 INTRODUCTION

Table des Matières

Chapitre 1 INTRODUCTION

1

Chapitre 1

INTRODUCTION

Depuis un demi siècle, la chimie et la physique du solide ont subi un immense développement en raison sans doute de l'intérêt économique que représentent les applications des matériaux dans le monde moderne. Les conducteurs ioniques, bien que découverts il y a plus d'un siècle, étaient restés cependant des curiosités de laboratoire. La crise de l'énergie des années 60-70, a suscité un intérêt renouvelé pour ces matériaux susceptibles d'être utilisés dans des applications, notamment de stockage de l'énergie.

De nos jours, les recherches concernant la conductivité ionique des verres connaissent elles-mêmes un développement considérable qui porte à la fois sur la recherche de nouveaux matériaux aux performances élevées et sur la modélisation de la conductivité.

Les verres inorganiques étudiés sont très divers : verres d'oxydes (silicates, borates , etc.), verres halogénés (fluorures, chlorures, etc.), verres de chalcogénures (sulfures, sélénures, etc.). Les ions mobiles sont également variés. Parmi les cations on peut citer les alcalins et notamment le lithium et le sodium, le proton, Ag^+ , Cu^+ , Tl^+ , etc. , parmi les anions O^{2-} , F^- , etc. .

Les performances de ces matériaux sont parfois exceptionnelles; dans le cas des verres à l'argent, la conductivité peut dépasser $10^{-2} (\Omega\text{cm})^{-1}$ à température ambiante, ce qui correspond à celle d'une solution aqueuse de nitrate

d'argent de normalité N/10. En règle générale, les performances des matériaux sont largement suffisantes pour la réalisation de dispositifs électrochimiques "tout solide". En conséquence de nombreux prototypes ont été réalisés : piles et batteries, dispositifs électrochromes, capteurs chimiques (capteurs de gaz, électrodes sélectives, ISFET), temporisateurs, etc. . Notons cependant que ces nombreuses recherches ont rarement abouti à des fabrications industrielles. Cet état de fait résulte soit de problèmes techniques (échanges ioniques ou électroniques difficiles aux interfaces électrode / électrolyte, vieillissement prématuré du solide isolant électronique sous tension électrique, etc.) soit économiques (prix réduit et performances élevées des dispositifs électrochimiques utilisant des électrolytes liquides).

Corrélativement aux recherches précédentes, les mécanismes de la conductivité ionique dans les verres ont fait l'objet d'études approfondies [1, 2]. Le but ultime de ces travaux concerne la mise en évidence du chemin de conduction des ions dans le solide vitreux et les caractéristiques temporelles et énergétiques corrélées (barrière(s) de potentiel, fréquences des sauts). Les étapes nécessaires à cette modélisation sont, bien entendu, les relations entre la conductivité et la composition du verre, sa structure, ses caractéristiques thermiques et mécaniques, etc. .

Le présent travail est consacré à de nouveaux matériaux vitreux, conducteurs de l'ion Ag^+ . Nous ne souhaitons pas ajouter à la surabondance de la littérature consacrée à ce type de verre, même sous prétexte de nouveauté. Nous désirions créer des matériaux nouveaux dans le but de rechercher des réponses ou, du moins, d'apporter des éléments de réponse aux questions suivantes :

- y-a-t'il une limite physique à la conductivité ionique dans le solide amorphe comme il en existe pour la conductivité électronique? C'est dans ce cadre que nous avons préparé des verres à base de sulfure d'arsenic. Nous avons adjoint à ce dernier l'iodure et de sulfure d'argent, qui possèdent, à l'état cristallin, des performances exceptionnelles. Pour augmenter le nombre de porteurs, nous avons synthétisés les verres par hypertrempe.

- dans les superconducteurs ioniques vitreux formés d'une matrice et d'un sel, siège de la conduction, y-a-t'il formation de microdomaines du sel? Lorsque cette matrice est formée de chaînes, la longueur de celles-ci influence-t'elle la conductivité? C'est l'objet de la troisième partie de ce travail où nous étudions les verres issus du système $\text{AgPO}_3\text{-Ag}_2\text{S}$.

Enfin, bien que ce travail ait eu à l'origine un but fondamental, nous avons finalement souhaité évaluer les potentialités d'applications des nouveaux électrolytes étudiés. En conséquence, nous avons réalisés et testés des prototypes de batteries et de capteurs chimiques.

REFERENCES DU CHAPITRE

- [1] C. A. Angell, *Solids State Ionics*, 18-19, 72 (1986)
- [2] M. D. Ingram, *Physics and Chemistry of Glasses*, 26, 8, 215 (1987)

**Chapitre 2 LES VERRES CONDUCTEURS IONIQUES DE
L'ARGENT**

Table des Matières

Chapitre 2 LES VERRES CONDUCTEURS IONIQUES DE L'ARGENT	5
2.1 GENERALITES SUR LES CONDUCTEURS IONIQUES VITREUX	5
2.1.1 ABREGE DE L'HISTOIRE DES VERRES	5
2.1.2 LES MATERIAUX	5
2.1.3 MECANISMES DE TRANSPORT IONIQUE DANS LES VERRES	8
2.1.3.1 L'APPROCHE DE ANDERSON-STUART (A- S)	8
2.1.3.2 LA THEORIE DE L'ELECTROLYTE FAIBLE (R-S)	10
2.1.3.3 COMPARAISON DES MODELES A-S ET R-S	12
2.2 LES VERRES CONDUCTEURS DE L'ION ARGENT	13
2.3 CHOIX DES MATERIAUX	15

Chapitre 2

LES VERRES CONDUCTEURS IONIQUES DE L'ARGENT

2.1 GENERALITES SUR LES CONDUCTEURS IONIQUES VITREUX

2.1.1 ABREGE DE L'HISTOIRE DES VERRES

Les dates essentielles de l'histoire de la conductivité ionique des verres sont réunies au tableau I. A titre de repère, nous y avons noté également les évènements marquants concernant les cristaux.

2.1.2 LES MATERIAUX

Les matériaux concernés sont essentiellement des oxydes, des chalcogénures, des halogénures et des verres à anions mixtes. Le tableau II décrit les principales classes de verre étudiés.

Les études les plus nombreuses concernent les alcalins et notamment le lithium ainsi que l'argent. L'ion mobile est introduit soit sous forme du composé correspondant du formateur soit, souvent, sous forme d'halogénures. Dans ce dernier cas, on observe fréquemment une exaltation de la conductivité due à un effet d'anions mixtes.

Tableau I : Un siècle de l'histoire de la conductivité ionique.

Warburg observe le transport du sodium à travers un verre séparant deux amalgames	1884	[1]
Utilisation d'une membrane de verre dans une électrode sélective à pH	1906	[2]
Compilation des verres conducteurs ioniques Corrélations conductivité composition	1932	[3]
Découverte par Strock de la conductivité ionique de AgI- α	1935	[4] [5]
Utilisation de la zircone dans une pile à combustible	1950	
Synthèse par Reuter et Hardel de Ag ₃ SI, le premier solide possédant, à température ambiante, la conductivité d'un électrolyte liquide	1961	[6]
Découverte de RgAg ₄ I ₅ et d'autres matériaux riches en Ag ⁺ et I ⁻	1961 1963	[7]
Découverte de la conductivité ionique de l'alumine β	1967	[8]
En vingt ans, les performances ($\sigma_{25^{\circ}\text{C}}$) des verres progressent de 10^{-5} à $10^{-2}(\Omega.\text{cm})^{-1}$	1969 1989	

Tableau II : Ions mobiles et formateurs dans les principaux verres conducteurs ioniques.

	oxydes			chalcogénures			fluorures	
ions mobiles	Li ⁺ Ag ⁺	Na ⁺ Cu ⁺	K ⁺ F ⁻	Li ⁺ Ag ⁺	Na ⁺ Cu ⁺	K ⁺	F ⁻	Li ⁺
cations du (des) formateur(s)	Si ⁴⁺ B ³⁺ Al ³⁺ Sb ³⁺	Ge ⁴⁺ P ⁵⁺ As ³⁺ Te ⁴⁺		Si ⁴⁺ B ³⁺ Al ³⁺ Sb ³⁺	Ge ⁴⁺ P ⁵⁺ As ³⁺		Be ²⁺ U ⁴⁺	Zr ⁴⁺

La conductivité ionique à température ambiante peut être inférieure à $10^{-10} (\Omega.cm)^{-1}$ dans les silicates et peut dépasser $10^{-2} (\Omega.cm)^{-1}$ dans les verres de chalcogénures à base d'argent.

Une étude exhaustive de la conductivité ionique dans les verres a été réalisée par Ravaine [9].

2.1.3 MECANISMES DE TRANSPORT IONIQUE DANS LES VERRES

La découverte, depuis une vingtaine d'années, d'un nombre considérable de nouveaux conducteurs vitreux a entraîné corrélativement le développement de recherches théoriques sur les mécanismes de transport. Une compilation de ces travaux a été réalisée récemment par Ingram [10]. Nous en donnerons ici un bref aperçu.

Deux modèles ont été essentiellement proposés : l'approche de Anderson-Stuart, la théorie de l'électrolyte faible.

2.1.3.1 L'APPROCHE DE ANDERSON-STUART (A-S)

Anderson et Stuart considèrent que l'énergie d'activation de la migration d'un ion E_A peut être décomposée en deux parties [11] :

E_b est l'énergie pour vaincre les forces électrostatiques qui retiennent l'ion dans son site,

E_s est une énergie supplémentaire pour déformer localement la structure de telle sorte que l'ion mobile puisse passer dans le site voisin sans contrainte stérique.

$$E_A = E_b + E_s \quad (1)$$

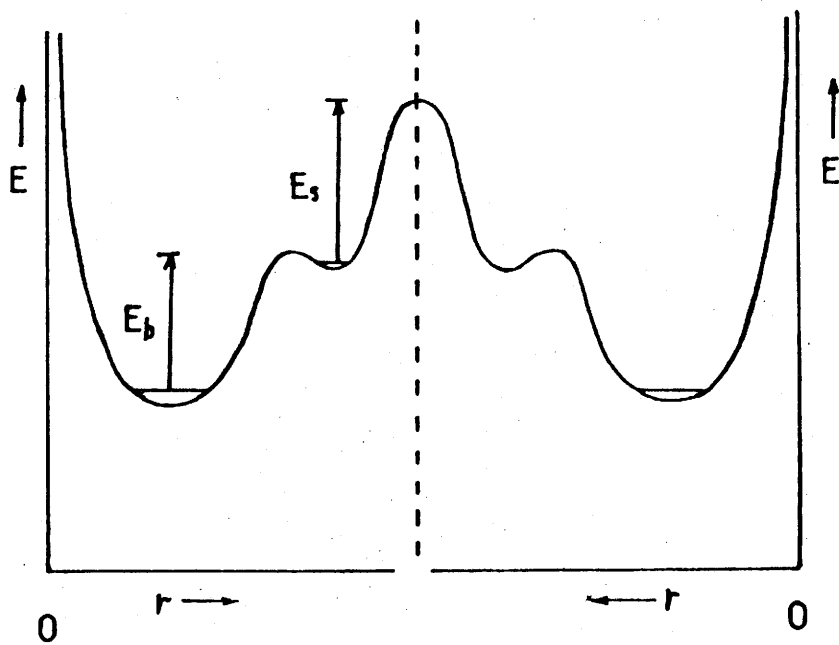
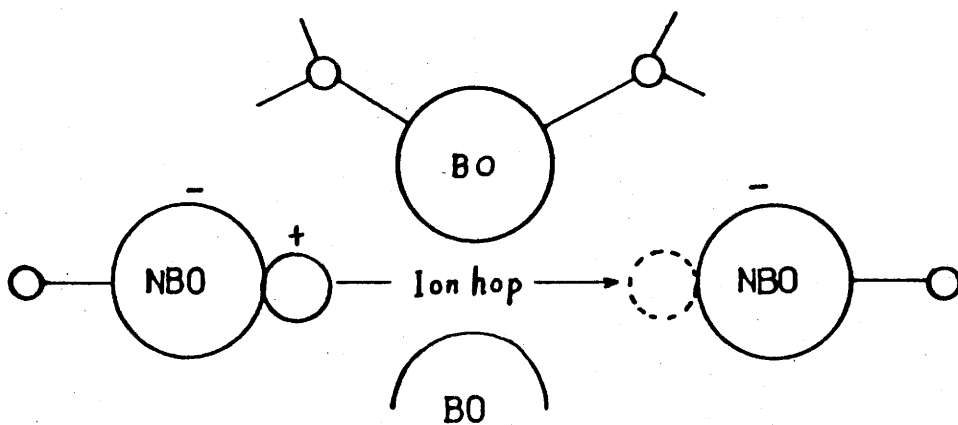


Fig. 1 Schématisation du modèle de Anderson-Stuart d'après Martin et Angell [12]

La figure 1 symbolise graphiquement ce mécanisme. Après diverses approximations, les auteurs proposent, dans le cas de verres silicatés, de calculer E_A par l'expression :

$$E_A = \frac{\beta z z_o e^2}{\gamma(r + r_o)} + 4 \pi G r_D (r - r_D)^2 \quad (2)$$

ou β est un paramètre de réseau dépendant de la distance entre sites voisins

r le rayon du cation mobile

z et z_o respectivement les charges du cation mobile et de l'oxygène

r_D le rayon, en l'absence de contrainte, du passage qu'aura à franchir l'ion mobile

G le module élastique du verre

γ un paramètre de covalence.

Cette théorie a permis d'expliquer la variation de l'énergie d'activation en fonction de la composition de verres silicates alcalins.

2.1.3.2 LA THEORIE DE L'ELECTROLYTE FAIBLE (R-S)

Ravaine et Souquet ont mis en évidence des corrélations entre la conductivité ionique et les potentiels chimiques des oxydes ou halogénure dissous dans les verres [13, 14].

La conductivité ionique des électrolytes s'exprime fréquemment sous la forme :

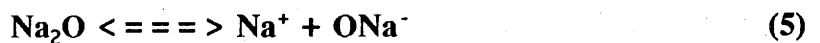
$$\sigma = n^* z e u \quad (3)$$

ou z est le nombre de charge, e la charge électronique, u la mobilité et n^* le nombre d'ions mobiles par unité de volume. Dans le modèle R-Q, pour les électrolytes faibles, n^* est plus petit que le nombre d'ions calculé à partir de la stoechiométrie.

Ravaine et Souquet ont observé que les variations de conductivité en fonction de la concentration de sodium dans les verres du système $\text{Na}_2\text{O-SiO}_2$ étaient liées à celles de l'activité de Na_2O :

$$\sigma = \text{const.} \cdot a(\text{Na}_2\text{O})^{1/2} \quad (4)$$

Ils postulèrent qu'au sein du verre existe un équilibre :



Suivant la thermodynamique traditionnelle, on peut en déduire :

$$\mu_{\text{Na}_2\text{O}} = \mu_{\text{Na}^+} + \mu_{(\text{ONa})^-} \quad (6)$$

si les concentrations des espèces dissociées sont faibles, les coefficients d'activité sont constants pour une température donnée quelle soit la composition. On peut écrire alors :

$$\mu_{\text{Na}_2\text{O}} = \text{const.} + RT \ln[\text{Na}^+][\text{ONa}^-] \quad (7)$$

$$= \mu_{\text{Na}_2\text{O}}^0 + RT \ln[\text{Na}^+]^2 \quad (8)$$

Mais comme :

$$\mu_{\text{Na}_2\text{O}} = \mu_{\text{Na}_2\text{O}}^D + RT \ln a(\text{Na}_2\text{O}) \quad (9)$$

Alors pour deux verres de composition différente le rapport des concentrations d'ions Na^+ mobiles s'écrit :

$$\frac{[\text{Na}^+]_1 [\text{ONa}^-]_1}{[\text{Na}^+]_2 [\text{ONa}^-]_2} = \frac{[\text{Na}_2\text{O}]_1^{1/2}}{[\text{Na}_2\text{O}]_2^{1/2}} \quad (10)$$

La comparaison des équations (2) et (8) conduit à :

$$\frac{\sigma_1 \left| \text{Na}^+ \right|_1}{\sigma_2 \left| \text{Na}^+ \right|_2} = \frac{\sigma_1 \left| \text{Na}^+ \right|_1}{\sigma_2 \left| \text{Na}^+ \right|_2} \quad (11)$$

et implique que $\sigma = \text{const.} \left| \text{Na}^+ \right|$. (12)

En comparant les équations (3) et (12), on voit que la mobilité des ions sodium est indépendante de la composition du verre.

Isard et al. [15] montrent que l'énergie d'activation peut s'écrire :

$$E_A(\sigma) = \Delta H/2 + E_m$$

où ΔH est l'enthalpie de l'équilibre (5) et E_m , la "vraie" énergie d'activation liée au mécanisme de conduction. Si $\Delta H/2$ est $\gg E_m$, la conductivité est gouvernée par la dissociation du modèle R-S.

2.1.3.3 COMPARAISON DES MODELES A-S ET R-S

Le modèle A-S est un modèle microscopique alors que le second est un formalisme macroscopique. Cependant, Angell a suggéré que ces deux modèles étaient équivalents. En effet, l'énergie de dissociation $\Delta H/2$ peut s'identifier à l'énergie E_b dans le modèle A-S et l'énergie de migration E_m à l'énergie E_s .

2.2 LES VERRES CONDUCTEURS DE L'ION ARGENT

Les performances exceptionnelles des verres à l'argent ont été mises en évidence pour la première fois en 1973 par Kunze lors de l'étude du système $\text{AgI-Ag}_2\text{O-SeO}_3$ [16]. Ces travaux ont conduit les chercheurs à tenter de faire réagir l'iodure d'argent avec des composés contenant des oxyanions (Fig.2). Minami et al. obtinrent des verres dans le système $\text{AgI-Ag}_2\text{O-P}_2\text{O}_5$ [17]. Simultanément Malugani et al. préparèrent des verres entre AgPO_3 et AgI [18]. Dans les deux cas la conductivité des matériaux étaient très élevées. L'extrapolation de celle-ci pour des taux d'iodure d'argent élevés conduisait à des valeurs voisines de celle de $\text{AgI-}\alpha$. Les auteurs précédents proposèrent alors l'hypothèse de la formation au sein du réseau vitreux de clusters possédant une structure de type $\text{AgI-}\alpha$. Ce problème sera discuté au chapitre 4 de ce mémoire.

Ces travaux furent étendus aux systèmes $\text{AgI-Ag}_2\text{MoO}_4$ [19], $\text{AgI-Ag}_2\text{O-As}_2\text{O}_3$ [20], $\text{AgI-Ag}_2\text{O-B}_2\text{O}_3$ [21].

Les verres chalcogénés ont généralement des performances supérieures à celles des verres d'oxydes. En conséquence, les chercheurs tentèrent de préparer des verres de ce type riches en argent. On peut citer les verres du système $\text{AgI-Ag}_2\text{Se-P}_2\text{Se}_5$ [22], $\text{AgI-Ag}_2\text{S-P}_2\text{S}_5$ [23], $\text{AgI-Ag}_2\text{S-GeS}_2$ [24], $\text{AgI-Ag}_2\text{S-As}_2\text{S}_3$ [25].

Les performances les plus élevées furent obtenues par Sun et al sur des matériaux préparés par hypertrempe dans le système $\text{AgI-Ag}_2\text{S-Sb}_2\text{S}_3$ [26].

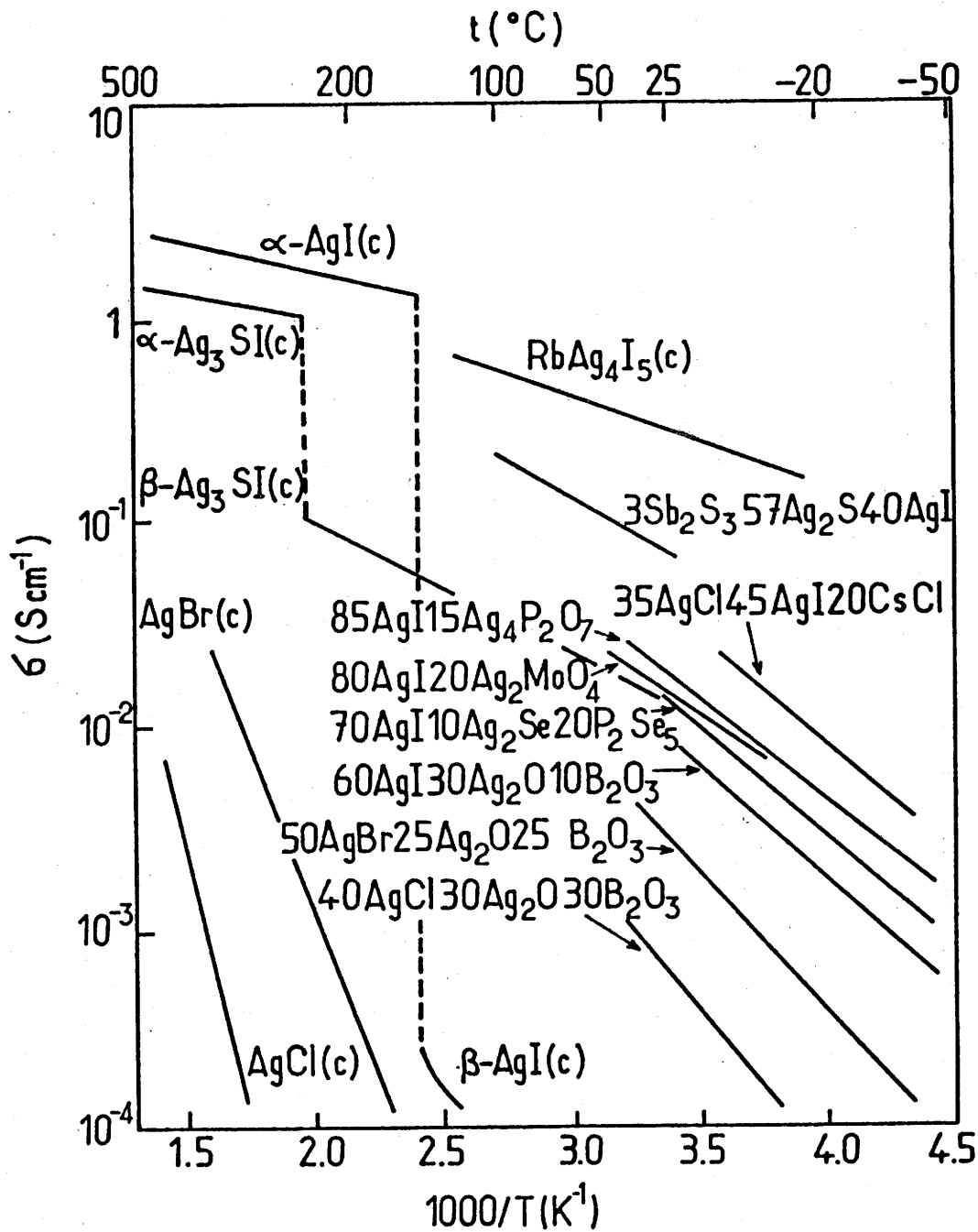


Fig.2 Variation de la conductivité en fonction de la température réciproque pour les verres conducteurs de l'ion argent. Comparaison avec quelques phases cristallisées.

2.3 CHOIX DES MATERIAUX

Compte tenu des travaux antérieurs et des buts que nous nous étions fixés (recherche des performances maximales, modélisation de la conductivité), nous nous sommes intéressés à deux types de matériaux : les verres chalcobalcohalogénés et les verres thio-oxyphosphates.

Il était tentant d'étendre les travaux de Sun et al. sur les verres du système $\text{AgI-Ag}_2\text{S-Sb}_2\text{S}_3$ à l'arsenic. En effet, une covalence renforcée de la matrice vitreuse peut parfois exalter la conductivité ionique par l'effet de la liaison antagoniste.

Par ailleurs, les variétés de haute température de l'iodure d'argent et du sulfure d'argent sont isotypes. Il était donc d'étendre les travaux sur les verres obtenus par réaction de AgI sur AgPO_3 au cas du sulfure d'argent. En particulier, nous étions intéressés de savoir si dans ce cas les propriétés de transport pouvait s'expliquer par la formation de clusters.

REFERENCES DU CHAPITRE II

- [1] G. Warburg Ann. Phys., 21, 622 (1884)
- [2] M. Cremer, Z. Biol. 47, 562 (1906)
- [3] E. Seddon, E.J. Trippet et W.E.S. Turner, J. Soc. Glass. Tech., 16, 450 (1932)
- [4] L.W. Strock, Z. Phys. Chem., B25, 441 (1934)
- [5] L.W. Strock, Z. Phys. Chem., B31, 132 (1936)
- [6] B. Reuter et K. Hardel, Z. Anorg. Allg. Chem., 340, 168 (1965)
- [7] J.N. Bradley et P.D. Greene, Trans. Faraday Soc., 62, 2069 (1966)

- [8] N. Weber et J.T. Kummar, Proc. Ann. Power Sources Conf. 21, 37 (1967)
- [9] D. Ravaine, J. Non-Cryst. Solids, 73, 215 (1985)
- [10] M.D. Ingram, Phys. Chem. of glasses, 28, 215 (1987)
- [11] O.L. Anderson et D.A. Stuart, J. Am. Ceram. Soc., 37, 573 (1954)
- [12] S.W. Martin et C.A. Angell, Solid State Ionics, 23, 185 (1986)
- [13] D. Ravaine et J.L. Souquet Physics Chem. Glasses, 18, (2), 27 (1977)
- [14] D. Ravaine et J.L. Souquet Physics Chem. Glasses, 19, (5), 115 (1978)
- [15] J. O. Isard, M. Jagla et K. K. MALICK, J. Phys., 43, C9, 387 (1982)
- [16] D. Kunze in "Fast ion transport", Van Gool ed., Noth Holland, Amsterdam 1973
- [17] T. Minami et M. Tanaka, Rev. Chim. Miné., 16, 283 (1979)
- [18] J.P. Malugani, A. Wasniewski, M. Doreau, G. Robert et A. Al Rikaki, Mat. Res. Bull., 13, 42 (1978)
- [19] [16] T. Minami, H. Nambu et M. Tanaka, J. Am. Cer. Soc. , 60, 467 (1977)
- [20] S.W. Martin et A. Schiraldi, J. Phys. Chem. , 89, 2071 (1985)
- [21] T. Minami, J. Non-Cryst. Solids, 73, 293 (1985)
- [22] T. Minami, J. Non-Cryst. Solids, 56, 15 (1983)
- [23] Y. Kawamoto et M. Nishida, J. Non-Cryst. Solids, 20, 383 (1976)
- [24] E. Robinel, B. Carette et M. Ribes, J. Non-Cryst. Solids, 57, 49 (1983)
- [25] Y. Kawamoto, N. Nagura et S. Tsuchihashi, J. Am. Ceram. Soc., 57, 489 (1974)
- [26] H. W. Sun, B. Tanguy, J.M. Réau, J.J. Videau, J. Portier et P. Hagemuller, J. Solid State Chem. , 70, 141 (1987)

**Chapitre 3 PROPRIETES ET STRUCTURES DE VERRES
THIOIDES A BASE D'ARSENIC**

Table des Matières

Chapitre 3 PROPRIETES ET STRUCTURES DE VERRES

THIOIODES A BASE D'ARSENIC	18
3.1 LES VERRES DU SYSTEME As-Ag-S	18
3.2 PROPRIETE DE TRANSPORT DES VERRES DU SYSTEME $As_2S_3-Ag_2S-AgI$	31
3.3 Comparaison des propriétés de transport des verres des systèmes $As_2S_3-Ag_2S-AgI$ et $Sb_2S_3-Ag_2S-AgI$	38
3.4 STRUCTURE DES VERRES DU SYSTEME $As_2S_3-Ag_2S-$ AgI	41
3.5 CONCLUSION DU CHAPITRE 3	57

Chapitre 3

PROPRIETES ET STRUCTURES DE VERRES THIOIODES A BASE D'ARSENIC

3.1 LES VERRES DU SYSTEME As-Ag-S

published in Mat. Res. Bull., Vol.23, pp.1315-1320, 1988.

INVESTIGATION ON GLASSES IN THE As-Ag-S SYSTEM

Liu Jun, J.J.Videau, B.Tanguy, J.Portier, J.M.Reau and P. Hagemuller

Laboratoire de Chimie du Solide du CNRS, Université de BORDEAUX I, 351
cours de la Libération, 33405 TALENCE Cedex (France)

Abstract: Novel glasses have been prepared in the $\text{As}_2\text{S}_3\text{-Ag}_2\text{S}$ system by splat cooling. A glass domain is obtained from As_2S_3 to $0.1 \text{As}_2\text{S}_3\text{-}0.9\text{Ag}_2\text{S}$. Thermal properties, ionic conductivity and transport number have been determined. A model based on IR absorption spectroscopy measurements has been proposed to account for the structure and the related properties.

MATERIALS INDEX: Silver,Arsenic,Sulfides.

INTRODUCTION

In a previous study, the properties of glasses obtained by hyperquenching in the $\text{Sb}_2\text{S}_3\text{-Ag}_2\text{S}$ system had been described [1].

The ionic conductivity of those materials was relatively high in particular for the composition $0.1\text{Sb}_2\text{S}_3\text{-}0.9\text{Ag}_2\text{S}$ ($\sigma_{25^\circ\text{C}} = 5.6 \times 10^{-3} \Omega^{-1}\text{cm}^{-1}$) due to a glass structure analogous to that of silver sulfide. Taking into account the fact that arsenic compounds are more covalent than the homologous antimony ones it seemed relevant to extend the previous work to the $\text{As}_2\text{S}_3\text{-Ag}_2\text{S}$ system in an attempt to enhance the conductivity. This system has already been investigated using classical preparation methods [2] and the authors found the composition $0.33\text{As}_2\text{S}_3\text{-}0.67\text{Ag}_2\text{S}$ as the highest silver glass limit.

EXPERIMENTAL

Glass Preparation

The starting materials were silver sulfide (purity 99.9%; Aldrich Co) and As_2S_3 (ventron UP). The mixtures once well homogenized and pressed into pellets of about 2g are put into a graphite crucible. They were melted then under argon atmosphere. The flake-like glass samples have been obtained from melts with a quenching rate of about 10^6K.s^{-1} [3]. The vitreous state of the sample is confirmed by X-ray diffraction.

Characterization

The various techniques used (thermal analysis, electrical conductivity, transport number, IR absorption spectroscopy) have been described in detail in ref[1].

RESULTS

Glass Formation Domain and Thermal Properties

In the $(1-x)\text{As}_2\text{S}_3-x\text{Ag}_2\text{S}$ pseudo-system, with the sealed tube technique, the glass domain stretches from $x=0$ to about $x=0.67$. For $0.04 < x < 0.33$ the sample was identified as a two glass mixture by visual examination as well as optical microscopy. These results agree with those obtained by KAWAMOTO et al.[2] The splat cooling technique allowed us to extend the glass domain up to a 0.1 $\text{As}_2\text{S}_3-0.9\text{Ag}_2\text{S}$ composition. The silver rich limit of the arsenic sulfide glass domain is similar to that observed by SUN HONG WEY in the $(1-x)\text{Sb}_2\text{S}_3-x\text{Ag}_2\text{S}$ system [1]. The variation of the glass transition temperature T_g and the crystallisation temperature T_c with composition (in the homogeneous glass domain) is given in table I.

Electrical Conductivity

The transport numbers determined for $x=0.67$ and $x=0.90$ are given in table II.

For both glasses they are quite close to 1, which shows that the electrical conductivity is mainly of ionic type, arsenic (III) sulfides being usually electronic insulators.

Fig.1 gives the variation of the logarithm of the conductivity vs. reciprocal temperature for various compositions. Arrhenius laws have been observed over the whole glass domain.

Fig.2 and 3 report the respective variation of the ionic conductivity at 25°C and of the activation energy vs. x . A conductivity maximum $\sigma = 3 \times 10^{-3} \Omega^{-1}\text{cm}^{-1}$ together with the lowest activation energy, $\Delta E_{\min} = 0.27\text{eV}$, has been obtained for the upper limit composition $0.10\text{As}_2\text{S}_3-0.90\text{Ag}_2\text{S}$. The results are

TABLE I Tg and Tc values for some compositions of the As₂S₃-Ag₂S system

Compositions	Tg(°C)	Tc(°C)
As ₂ S ₃	195	-
(As ₂ S ₃) _{0.50} -(Ag ₂ S) _{0.50}	118	158
(As ₂ S ₃) _{0.33} -(Ag ₂ S) _{0.67}	114	154
(As ₂ S ₃) _{0.20} -(Ag ₂ S) _{0.80}	98	118
(As ₂ S ₃) _{0.10} -(Ag ₂ S) _{0.90}	82	92

TABLE II Transport numbers of two glasses in the As₂S₃-Ag₂S system

Compositions	E _o (V)	E _{th} (V)	t=E _o /E _{th}
(As ₂ S ₃) _{0.33} -(Ag ₂ S) _{0.67}	0.682	0.687	0.992
(As ₂ S ₃) _{0.10} -(Ag ₂ S) _{0.90}	0.681	0.687	0.991

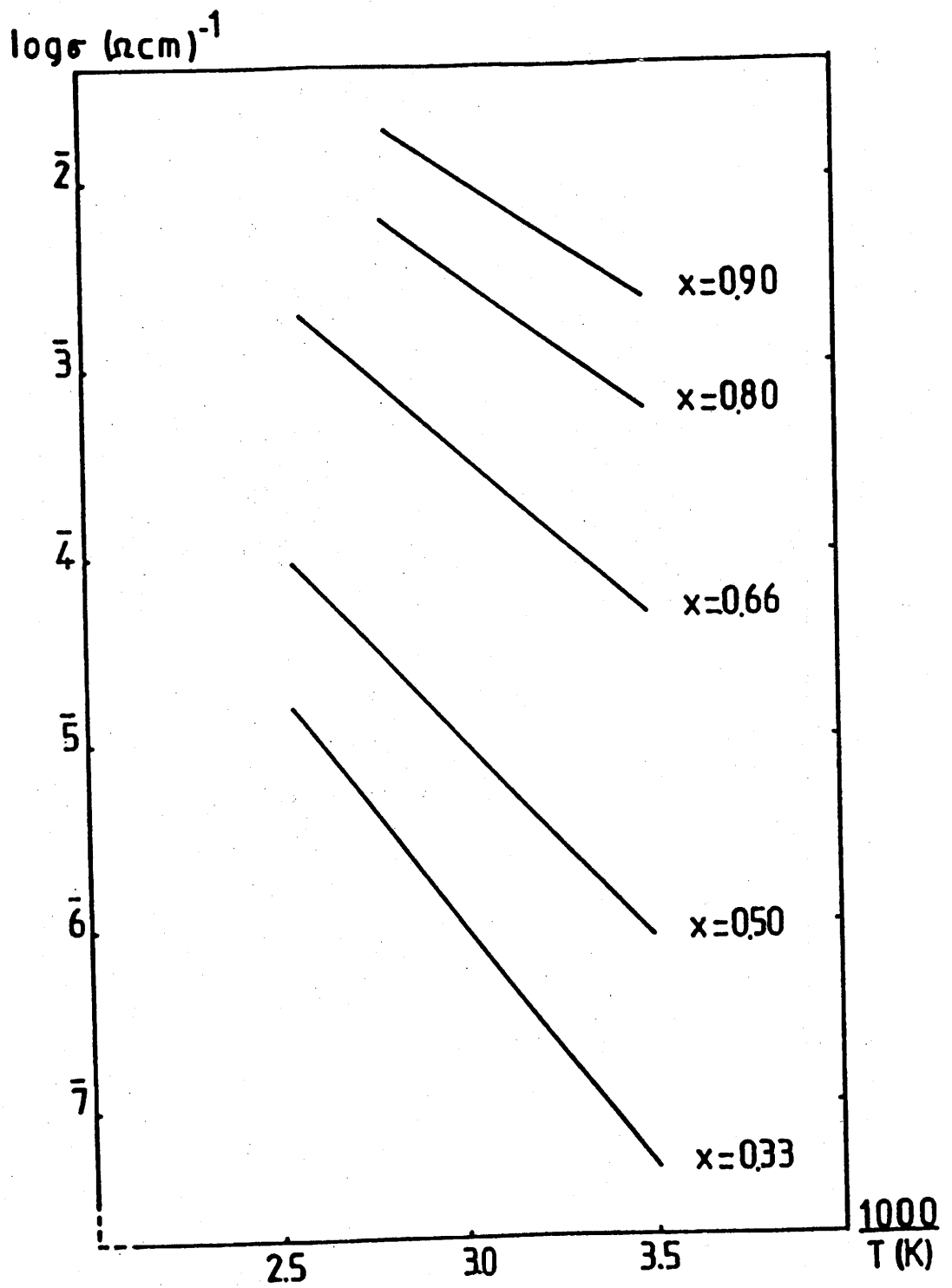


Fig.1 Variation of $\log \sigma$ vs. reciprocal temperature for various glasses belonging to the $(1-x) \text{As}_2\text{S}_3-x\text{Ag}_2\text{S}$ system.

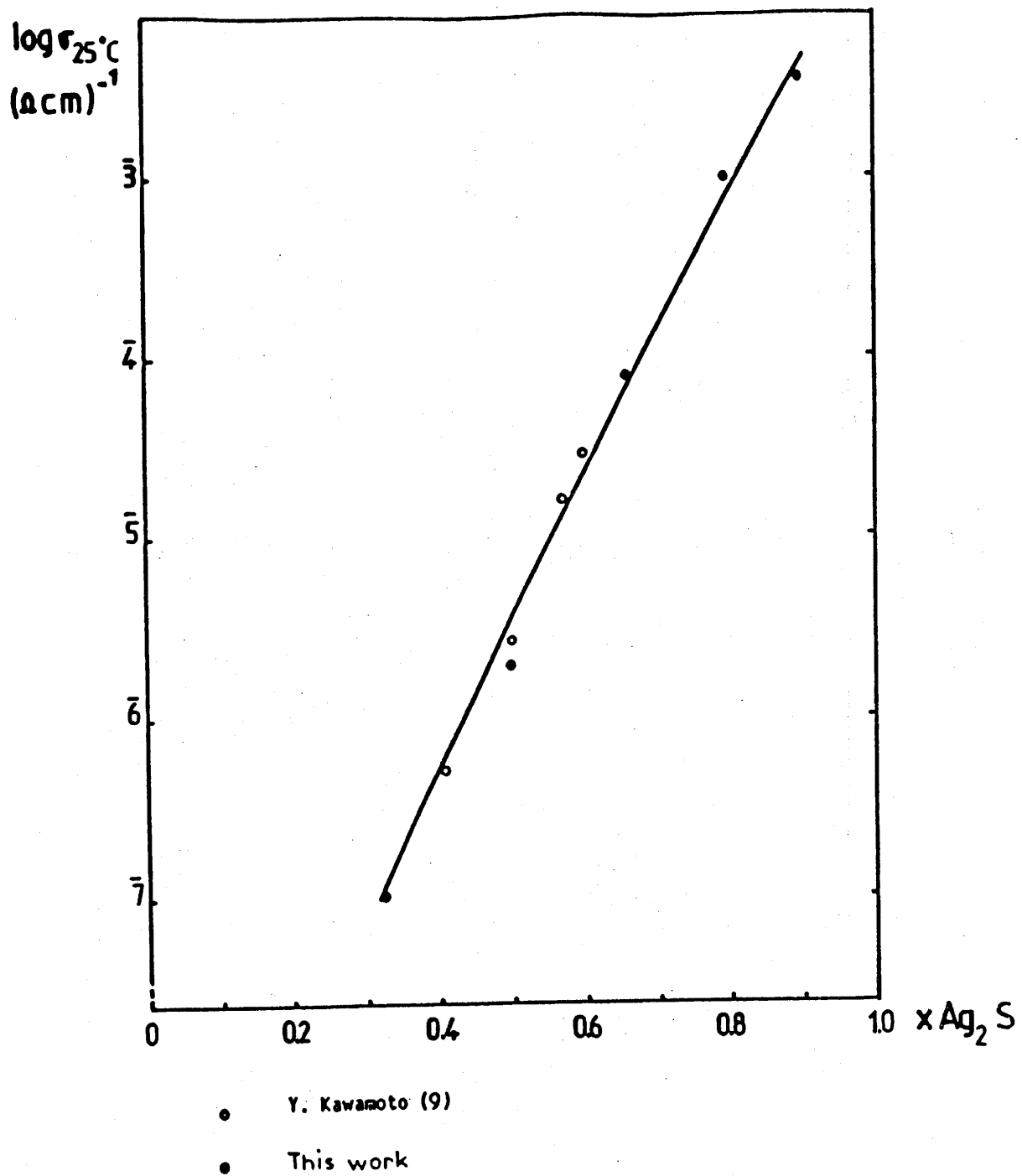


Fig.2 Variation of $\log \sigma_{25^\circ\text{C}}$ vs. molar rate of Ag_2S . Comparison with KAWAMOTO's results [9].

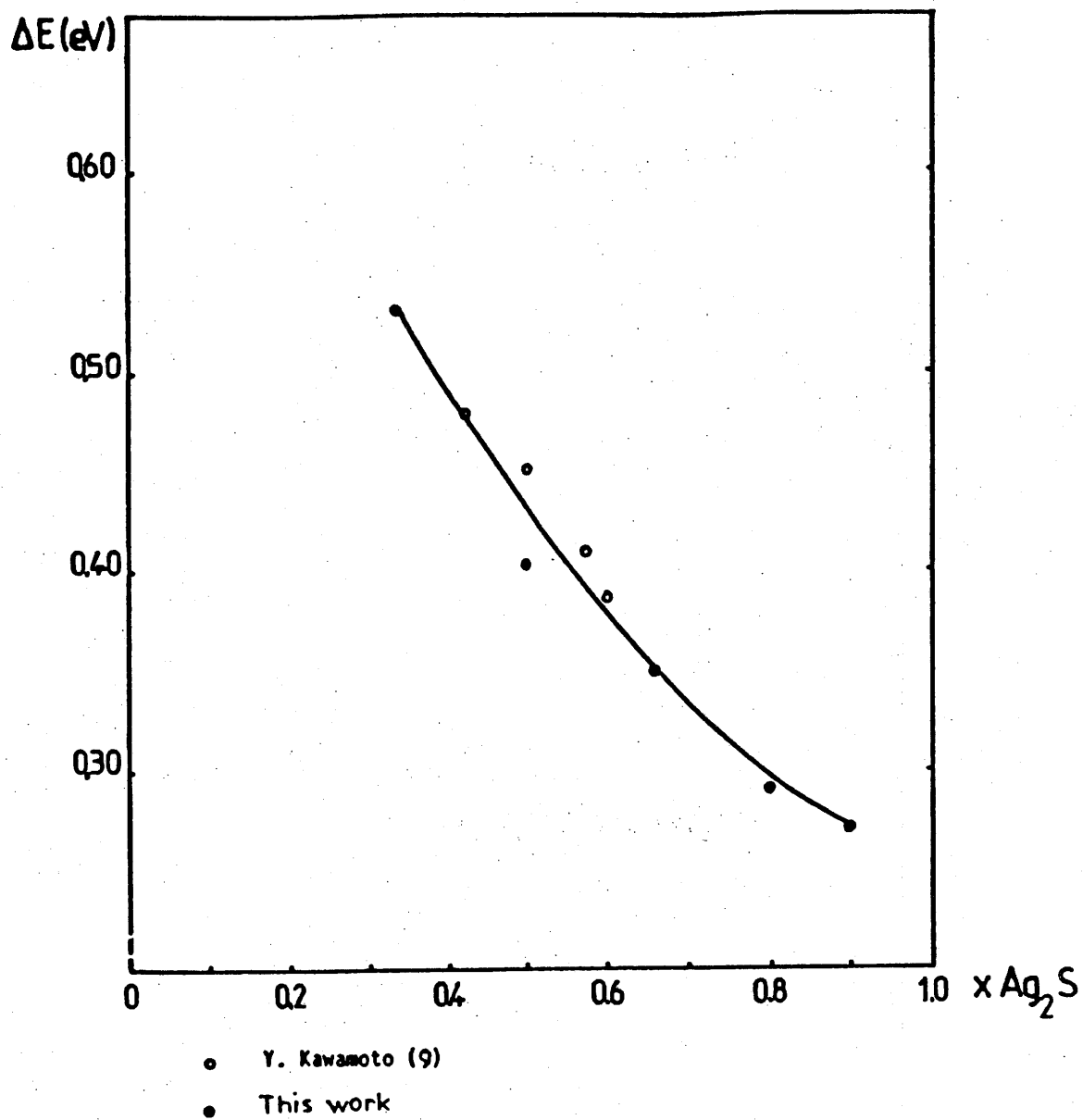


Fig.3 Variation of the activation energy at 25°C vs. molar rate of Ag_2S . Comparison with KAWAMOTO's results [9].

similar to those of KAWAMOTO [2] and don't differ much of those previously found for the homologous antimony system [1].

IR Absorption Spectroscopy

Figure 4 gives the IR absorption spectra of samples with compositions varying from As_2S_3 to Ag_2S in the $(1-x)\text{As}_2\text{S}_3-x\text{Ag}_2\text{S}$ binary system. As_2S_3 and the b,c,d samples are pure glasses, while Ag_2S is a ceramic. The a sample corresponds to a mixture of two glasses.

Vitreous As_2S_3 is characterized by a strong absorption band around 310 cm^{-1} with shoulders at 345 cm^{-1} and 385 cm^{-1} and a weaker band centered at 170 cm^{-1} corresponding respectively to the stretching and bending As-S vibrations [4]. The shoulder at 220 cm^{-1} can be assigned to a weak intermolecular coupling of $\text{S}_2\text{As-S-AsS}_2$ type.

The Ag_2S spectrum shows a strong absorption band with a maximum at 180 cm^{-1} and a weaker band around 110 cm^{-1} respectively assigned to Ag-S stretching and S-Ag-S bending vibrations.

Following observations can be made on the ternary glass samples:

(i) The intensity of the As-S stretching band decreases with rising x and its maximum shifts to 325 cm^{-1} ,

(ii) The S-As-S bending band disappears while two other weak bands arise around 200 cm^{-1} ,

(iii) The spectrum of the silver rich d sample strongly differs from those of the other glasses. It presents several peaks in the $350\text{-}200\text{ cm}^{-1}$ region and a strong band at 150 cm^{-1} .

Investigation of a,b and c samples

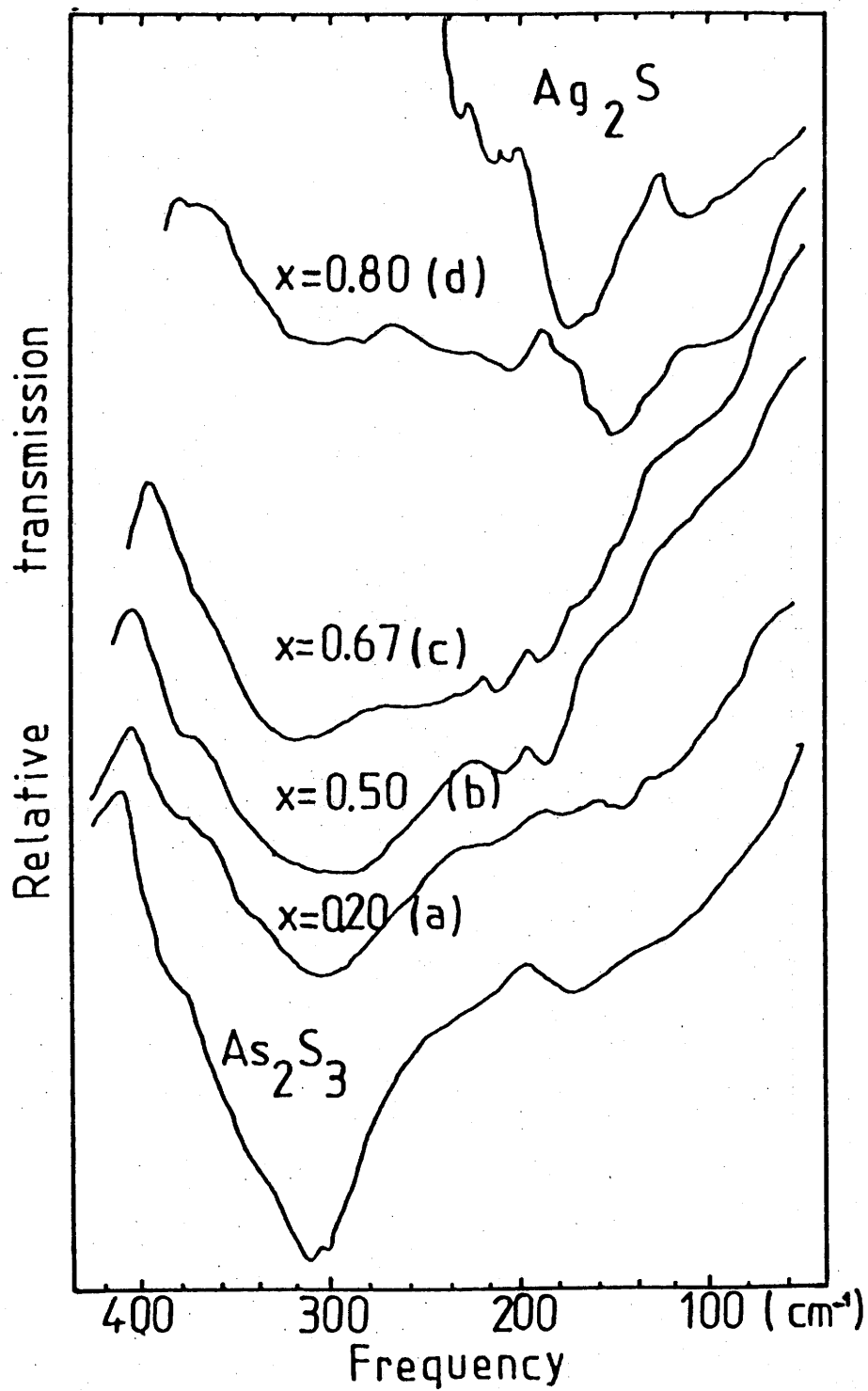


Fig.4 Far-infrared spectra for the crystallized compounds As_2S_3 and Ag_2S and various glasses belonging to the $(1-x)As_2S_3-xAg_2S$ system

Sample b (i.e. the two glass mixture) has in fact a spectrum similar to that of the homogeneous glasses.

The presence of the shoulder at 325 cm^{-1} appears to result from a shortening of the $(\text{AsS}_{3/2})_n$ chains. Indeed, one can observe that sample b with composition AgAsS_2 and the corresponding smithite crystallized phase have common features (Fig.5) in spite of the band broadening observed for the glass spectra. The network of smithite is built up with rings of six As_3S_6 groups linked to each other by Ag atoms[5].

For $x=2/3$ (sample C), the stretching As-S₃ absorption band presents only one maximum at 325 cm^{-1} as in the crystallized proustite Ag_3AsS_3 (fig.5). Hence this frequency characterizes an isolated AsS_3 pyramid[8].

Investigation of the d sample

The shift of S-Ag-S bending from 180 cm^{-1} (Ag_2S crystal) to 150 cm^{-1} (c sample) implies weakening of Ag-S bending. An analogous result had been observed for silver rich glasses in the $\text{Sb}_2\text{S}_3\text{-Ag}_2\text{S}$ system. Moreover, isolated As_2S_3 pyramids with a lone pair appear (325 cm^{-1}).

STRUCTURAL DISCUSSION

The silver poor glasses appear to present structural features analogous to those of arsenic sulfide, i.e. a network of vitreous As_2S_3 built up with triangular pyramids As_2S_3 forming both layers typical of crystalline orpiment As_2S_3 (pyramidal AsS_3 units sharing sulfur corners and chains constituted by $-\text{As} < \text{S}_s > \text{As}-$ units[4].

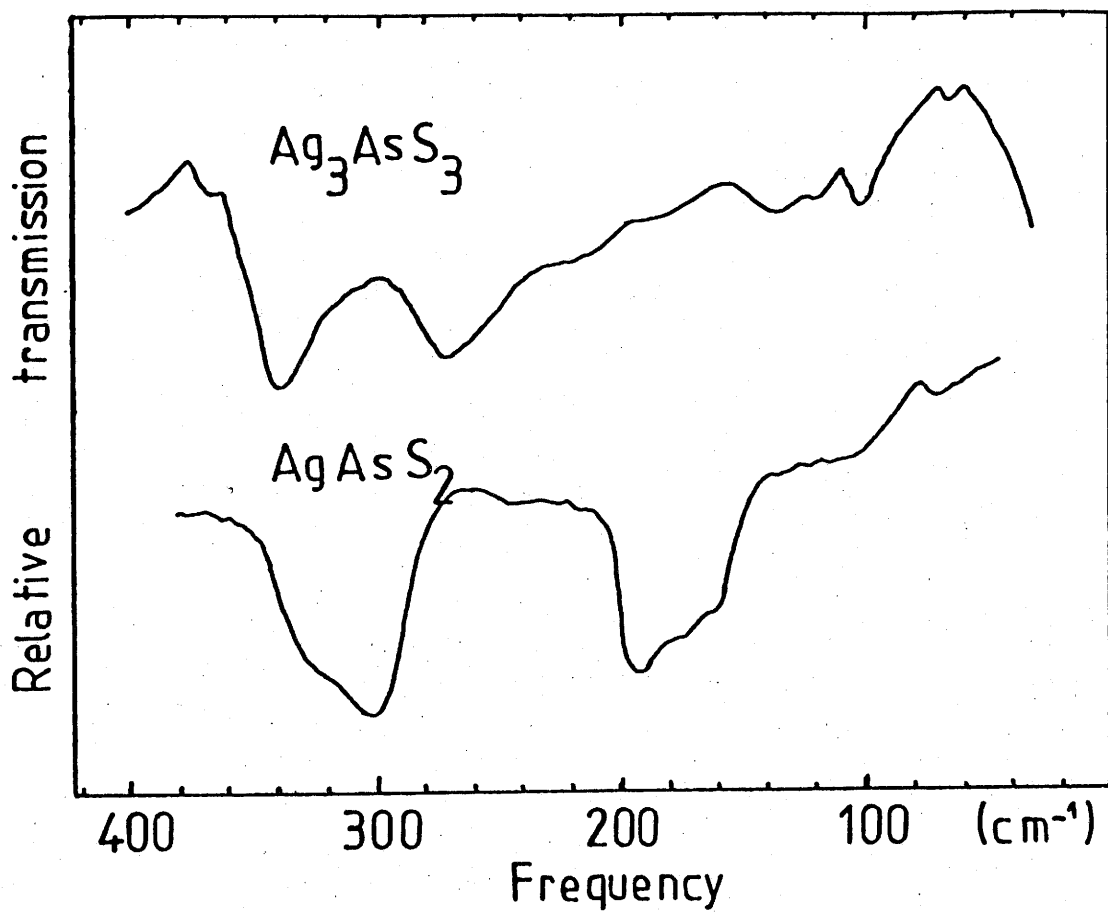


Fig.5 Infrared absorption spectra for the AgAsS_2 and Ag_3AsS_3 crystallized phases.

The introduction of silver sulfide leads to depolymerization. Silver ions connect the shortening AsS_3 pyramid chains. As the silver concentration becomes close to $x=0.6$ only isolated pyramids occur.

For the silver rich glasses, the As atoms should belong to a network probably based on the $\alpha\text{-Ag}_2\text{S}$ crystal structure [8]. They are likely bonded to neighboring sulfur atoms in such a way that they form structural units of the $\text{AsS}_{3/2}$ type as already suggested by KAWAMOTO et al.[9].

Increasing x -values lead to enhancement of the character of the As-S bonds and as a consequence to weakening of the competing Ag-S bonds in agreement with the observed IR spectra. Such a phenomenon accounts for enhancement of the silver ion conductivity with increasing number of carriers.

References:

1. H.W.SUN,B.TANGUY,J.M.REAU,J.J.VIDEAU and J.PORTIER, Mat. Res. Bull.,22,923(1987)
2. Y.KAWAMOTO,N.NAGURA and S.TSUCHINASHI,J.Amer.Ceram.Soc., 57,498(1974)
3. B.TANGUY,J.PORTIER and P.HAGENMULLER, J.Fluorine Chem.,25,1(1984)
4. G.LUCOVSKY and R.M.MARTIN , J.Non.Cryst. Solids 8-10, 185 (1972)
5. E.HELLUER and H.BURZLAFF,Die Natur-Wiss,Heft 2 Jg 51,35(1964)
6. C.R.KNOWLES , Acta Cryst. 17,847(1964)
7. H.H.BYER, Ferroelectrics,5, 207 (1973)
8. J.S.KASPER,"Inorganic Silver Ion Conductors" 14,217(1978)

9. Y.KAWAMOTO and M.NISHIDO, J.Non-Cryst.Solids 20,393(1976).

3.2 PROPRIETE DE TRANSPORT DES VERRES DU SYSTEME $\text{As}_2\text{S}_3\text{-Ag}_2\text{S-AgI}$

1. Introduction

Silver ion conductors , crystalline solids or glasses, involve high electrical performance and are among the best solid electrolytes[1-6].

In the field of applications, glasses offer a number of advantages over crystalline solids : ionic conductivity is isotropic, electronic contribution is generally weak, there is no grain boundary effect... Moreover the conduction properties of sulfide glasses are better than those of oxide glasses[7,8]. The polarizability of the sulphide ion, higher than that of the oxide ion, involves an increase of covalent character of non-conducting framework and consequently a weaker bonding between anion and Ag^+ which then becomes more mobile.

On the other hand, the ionic conductivity in glasses is strongly connected to mobile ion content. Hyperquenching techniques could allow isolation of glasses that cannot be obtained by classical methods and could enlarge notably the vitreous domains.

Glassy materials with high performance have been obtained by classical methods in the ternary systems : $\text{P}_2\text{S}_5\text{-Ag}_2\text{S-AgI}$ [9], $\text{GeS}_2\text{-Ag}_2\text{S-AgI}$ [8], $\text{As}_2\text{S}_3\text{-Ag}_2\text{S-AgI}$ [10]. Using the twin-roller quenching techniques, Sun et al. have investigated glasses inside the $\text{Sb}_2\text{S}_3\text{-Ag}_2\text{S-AgI}$ system [11]. It was tempting to study glasses in the corresponding $\text{As}_2\text{S}_3\text{-Ag}_2\text{S-AgI}$ system. The comparison of both systems could allow to determine the relative influence on silver ion transport

properties of cations forming the glass network having the same charge but different electronegativity.

2. Experimental

The starting materials were Ag_2S (purity 99.9%), AgI (purity 99%) and the chalcogenide As_2S_3 (purity 99%).

The mixtures once well homogenized are pressed into pellets. The batches of about 2g are melted. The pellets put into a graphite crucible are heated at 700°C under argon atmosphere. The flake-like glassy samples have been obtained from melts with a quenching rate of about 10^6K/s . On the other hand some glasses have also been prepared in sealed silica tubes quenched in water at 0°C . In all cases, the temperature of the melt has been 700°C .

The various techniques used to determine electrical conductivity and to obtain the infrared absorption spectra have been previously described in ref.[12].

3. Results

3.1. Glass forming region and thermal properties

The glass forming regions is shown in figs 1. In the vicinity of the $\text{As}_2\text{S}_3\text{-AgI}$ line, the rapid quenching method could not be used due to the formation of volatile thioiodide AsSI . When the silver sulfide content in the starting mixture becomes high enough ($\text{Ag}_2\text{S}/(\text{AgI}+\text{As}_2\text{S}_3) > 0.10$) the rapid roller quenching method has been used without significant losses. In fig. 1a, a solid line represents the limit of the glass domain obtained by rapid quenching, a dotted line corresponds to the limit of glasses obtained in sealed tubes. For comparison, Fig. 1b shows the diagram obtained by Sun et al. in the case of antimony glasses [11].

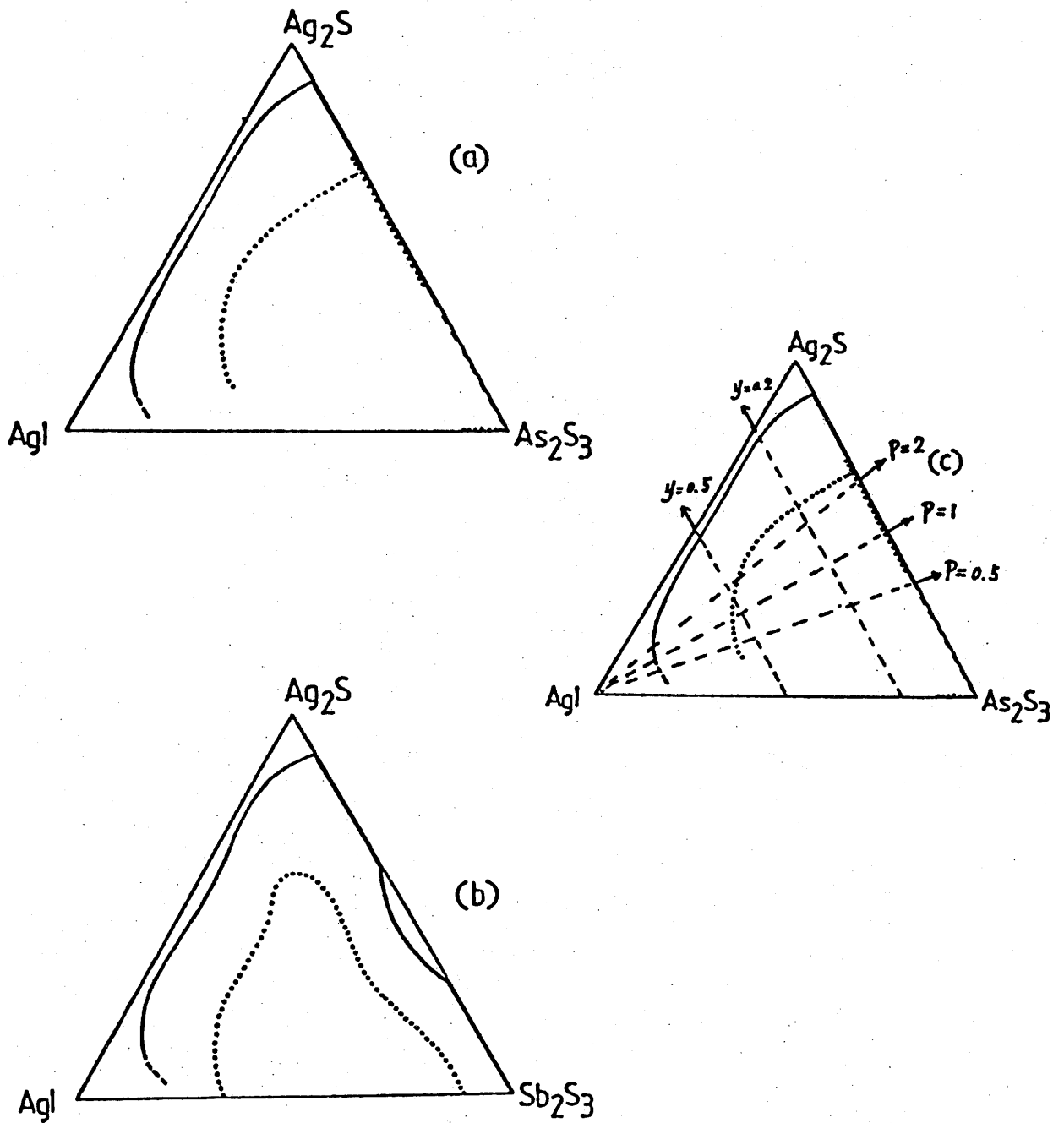


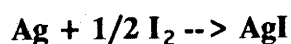
Fig.1: (1a) Glassy domain in the As_2S_3 - Ag_2S - AgI system
 \longleftrightarrow Glasses obtain by rapid quenching
 $\langle \dots \rangle$ Glasses prepared in a silica tube.
 (1b) Corresponding domain in the Sb_2S_3 - Ag_2S - AgI system
 (1c) Location in the ternary system of glasses described
 with the general formula: $(\text{As}_2\text{S}_3 - p\text{Ag}_2\text{S})_{1-y}(\text{AgI})_y$

AgI, Ag₂S and Ag₃SI cannot be obtained in the glassy form. Nevertheless compositions close to Ag₃SI have been achieved in the vitreous state.

The T_g of some glasses are given in table I.

3.2. Ionic conductivity

The transport number has been measured by an EMF method using the electrical chain : (-)Ag/Ag glass/C,I₂(+). The thermodynamic potential of this cell is E_{th} = 0.687 at 20°C and corresponds to the overall potential of :



The data for some glasses are shown in Tab. II. The transport number is close to unity indicating that the conductivity is mainly of ionic type.

The electrical properties have been determined as a function of temperature and composition. An Arrhenius behavior is verified for all the investigated samples below T_g.

Influence on the transport properties of the introduction of AgI into sulfide glasses has been studied for different glasses corresponding to a constant value of ratio $p = \text{As}_2\text{S}_3/\text{Ag}_2\text{S}$. The composition of the glasses can then be represented by the general formula $(\text{As}_2\text{S}_3 - p\text{Ag}_2\text{S})_{1-y}(\text{AgI})_y$.

Fig. 2a and 2b give the variation of $\log \sigma_{25^\circ\text{C}}$ and ΔE as a function of y ($p = \text{fixed}$) for the $(\text{As}_2\text{S}_3 - p\text{Ag}_2\text{S})_{1-y}(\text{AgI})_y$ glasses.

Transport properties depend strongly on p :

- for low values of p ($p < 1$), ΔE decreases rapidly and $\log \sigma_{25^\circ\text{C}}$ increases when y increases.

Table I. T_g values for some glasses in the As_2S_3 - Ag_2S - AgI system.

Composition	T_g °C
As_2S_3 (0.41)- Ag_2S (0.20)- AgI (0.39)	104
As_2S_3 (0.27)- Ag_2S (0.20)- AgI (0.53)	78
As_2S_3 (0.03)- Ag_2S (0.57)- AgI (0.40)	98

Table II. Transport number of some glasses in the As_2S_3 - Ag_2S - AgI system.

Composition	$E_{exp.}$ (V)	$t = E_{exp.}/E_{th.}$
As_2S_3 (0.03)- Ag_2S (0.57)- AgI (0.40)	0.681	0.991
As_2S_3 (0.33)- Ag_2S (0.52)- AgI (0.15)	0.686	0.998

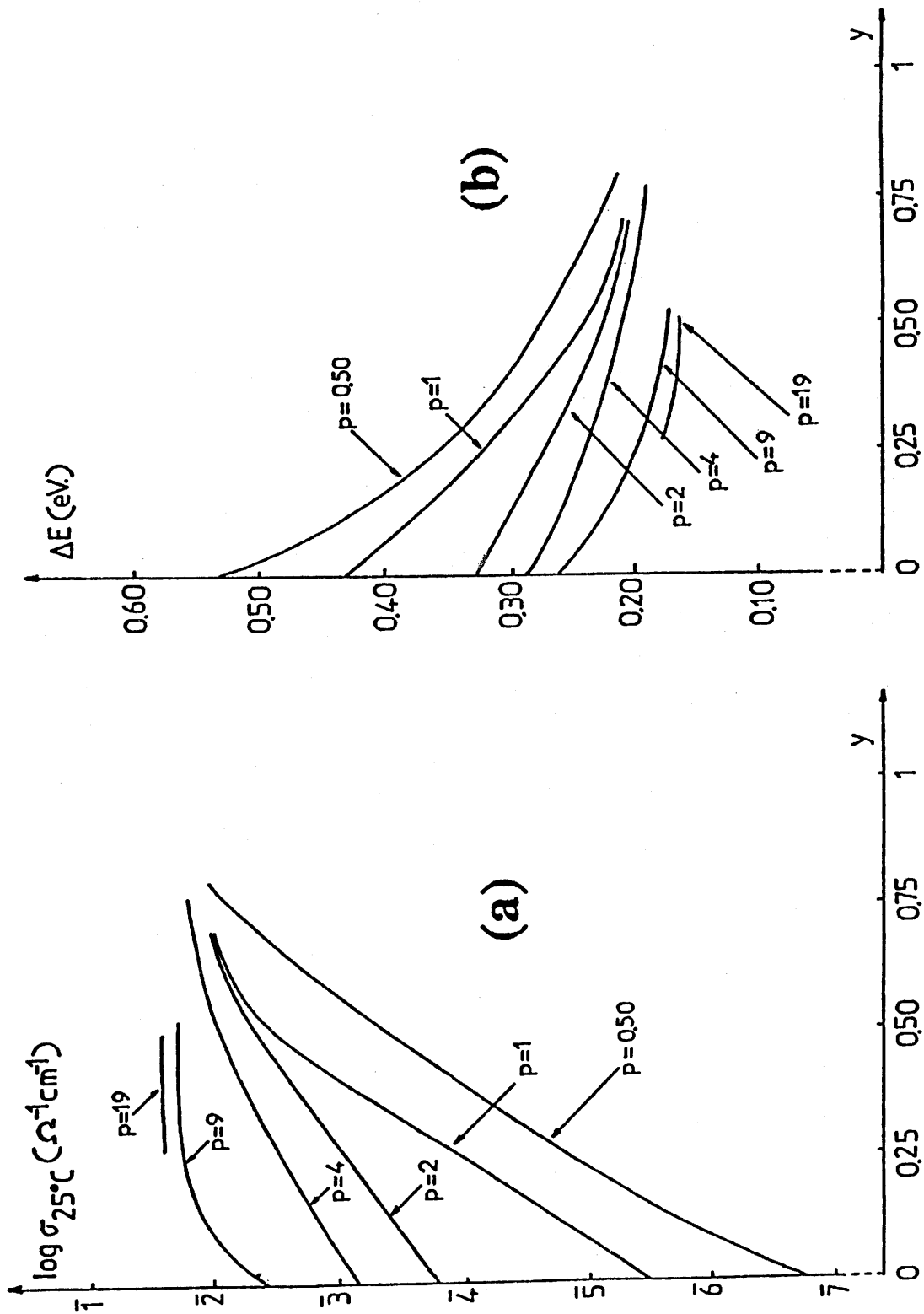


Fig.2 Variation of $\log \sigma_{25^\circ C}$ (a) and ΔE (b) versus y for glasses $(As_2S_3-pAg_2S)_{1-y}(AgI)_y$ corresponding to constant values of p .

- for higher values of p ($1 < p < 2$), the experimental points relative to $p = \text{const.}$ can be located on a straight line when $y < 0.50$ in agreement with the results of previous authors [9]. However, for $y > 0.50$ the data deviates strongly from linearity.
- for values of p higher than 2, ΔE decreases and $\log \sigma_{25^\circ\text{C}}$ increases when y increases. Variations of transport properties are yet lower and lower as p and y increases.

Study of transport properties of the $(\text{As}_2\text{S}_3-p\text{Ag}_2\text{S})_{1-y}(\text{AgI})_y$ glasses has shown that the linear variations of $\log \sigma_{25^\circ\text{C}}$ and ΔE as a function of AgI rate, previously reported [8-10], are only a first approach. Such behavior is obtained only for some particular values of p ($1 < p < 2$) and for $y < 0.50$.

The best performance have been obtained for glass involving the lowest As_2S_3 content and with a composition close to Ag_3SI :

$$(\text{As}_2\text{S}_3)_{0.03} (\text{Ag}_2\text{S})_{0.47} (\text{AgI})_{0.50} : \sigma_{25^\circ\text{C}} = 2 \times 10^{-2} (\Omega \cdot \text{cm})^{-1}; \Delta E = 0.16 \text{eV.}$$

References

1. C.Tubandt and E.Lorrenz, Z.Physik. Chem. 87 (1914) 513.
2. J.N.Bradley and P.D.Greene, Trans. Faraday Soc.63 (1967) 424.
3. B.Owens and G.Argue, Science 157 (1967) 308.
4. T.Mirami and M.Tanaka, J.Non-Cryst. Solids 38/39 (1980) 289.
5. T.Mirami, H.Nambu and M.Tanaka, J.Am.Ceram. Soc. 60 (1977) 467.
6. M.Sayer, S.L.Segel, I.Noad, J.Corey, T.Boyle, R.D.Heyding and A.Mansingh, J.Solid State Chem. 42 (1982) 191.
7. D.Ravaine, J.Non-Cryst. Solids 73 (1985) 287.
8. E.Robinel, B.Carette and M.Ribes, J.Non-Cryst. Solids 57(1983)49.
9. J.P.Malugani, G.Robert and R.Mercier, Mater.Res.Bull. 15 (1980) 715.
10. J.P.Malugani, A.Saida, A.Wasniewski and G.Robert, C.R.Acad. Sci.(Paris) 289C (1979) 69.
11. H.W.Sun, B.Tanguy, J.M.Reau, J.J.Videau and J.Portier and P. Hagenmuller, J. Solid State Chem. , 70 (1987) 141.
12. H.W.Sun, B.Tanguy, J.M.Reau, J.J.Videau and J.Portier Mater.Res.Bull. 22 (1987) 923.

3.3 Comparaison des propriétés de transport des verres des systèmes $\text{As}_2\text{S}_3\text{-Ag}_2\text{S-AgI}$ et $\text{Sb}_2\text{S}_3\text{-Ag}_2\text{S-AgI}$

La figure 1 représente le résultats obtenus par Sun et al. dans le cas du système $\text{Sb}_2\text{S}_3\text{-Ag}_2\text{S-AgI}$.

Pour les valeurs de $p \geq 1$ les variations des propriétés électriques des deux séries de verres sont semblables (Fig. 2 section 3-2 de ce chapitre). Ce comportement résulte d'une analogie structurale qui sera décrite plus loin.

Pour les valeurs de $p < 1$ peu de compositions de verres arséniés ont pu être étudiée en raison soit de leur démixion soit de la volatilité de AsI d'autant plus importante que Y croît. On note cependant que pour les faibles valeurs de p , le comportement des deux séries de verre est différent pour des valeurs de y inférieures ou égales à 0,30. Il s'agit de compositions riches en As_2S_3 et Sb_2S_3 pour lesquelles les structures sont différentes comme il sera montré dans le paragraphe suivant. En effet dans le cas de l'antimoine, l'iode participe au réseau vitreux en ce qui n'est pas le cas pour les verres à base d'arsenic. En conséquence, dans les verres arséniés, l'argent sera lié essentiellement à l'iode tandis que, dans les verres antimoniés, il sera lié au soufre. Il en résulte une mobilité plus grande dans le cas de l'arsenic.

Dans les deux séries les meilleures performances sont obtenues pour des compositions proches de Ag_3SI .

Le remplacement de l'antimoine par l'arsenic n'a pas permis d'obtenir des matériaux systématiquement plus performants. Si pour $p = 2$, par exemple, les

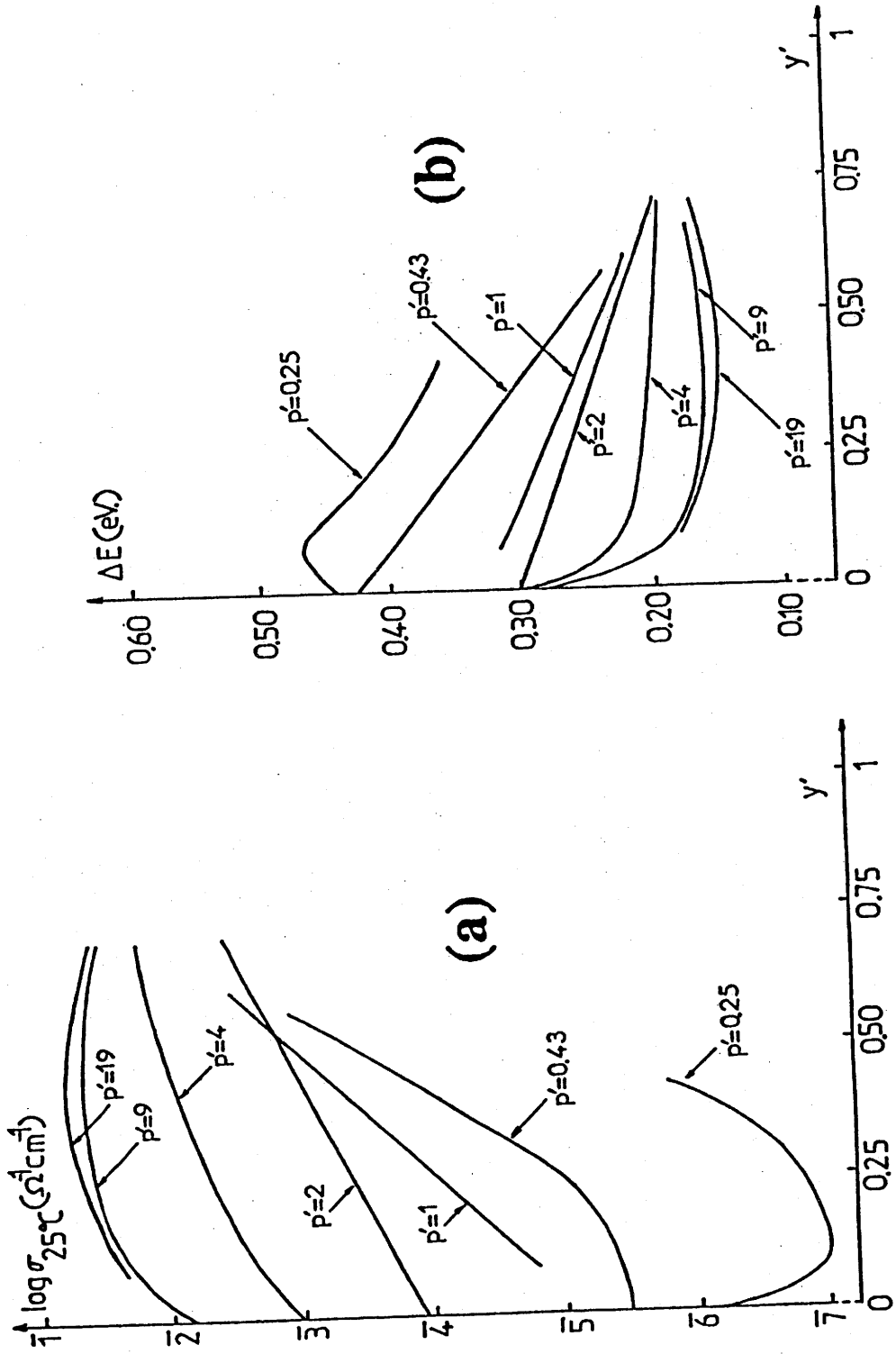


Fig. 1 Variation de $\log \sigma_{25^\circ\text{C}}$ (a) et ΔE (b) en fonction de y pour les verres $(\text{Sb}_2\text{S}_3)_p(\text{Ag}_2\text{S})_{1-y}(\text{AgI})_y$.

conductivités sont plus fortes dans le cas de l'arsenic, pour $p > 4$, on observe le contraire.

Ces résultats peuvent s'expliquer dans le cadre de la théorie d'Anderson-Stuart. La covalence renforcée de la matrice vitreuse dans le cas des verres à l'arsenic doit augmenter le caractère ionique de la liaison S-Ag ou I-Ag par effet de liaison antagoniste. E_b , l'énergie pour vaincre les forces électrostatiques qui retiennent l'ion argent dans son site doit donc être plus faible. Par contre, compte tenu de la taille plus faible des ions As^{3+} , on peut penser que les "fenêtres" sur le chemin de conduction de l'argent seront plus étroites. En conséquence, E_s , l'énergie supplémentaire pour déformer localement la structure de telle sorte que l'ion mobile puisse passer dans le site voisin sans contrainte stérique doit être plus forte. L'énergie d'activation étant la somme de ces deux termes ($E_A = E_b + E_s$), il est probable qu'un phénomène de compensation intervient.

L'allure générale des courbes représentant $\log \sigma_{25^\circ C}$ et ΔE en fonction de y (fig.2 paragraphe 3.2. et fig.1 de ce paragraphe) incite à les extrapoler à $y = 1$. Les valeurs obtenues ($\log \sigma_{25^\circ C} = 8 \times 10^{-2} - 10^{-1} (\Omega.cm)^{-1}$, $\Delta E = 0.17 - 0.19$ eV) caractériseraient AgI vitreux qui n'a jamais été obtenu. Ces valeurs sont environ 100 fois plus faibles que celle estimée, par extrapolation à $25^\circ C$, de AgI- α .

Références

1. H.W.Sun, B.Tanguy, J.M.Reau, J.J.Videau and J.Portier and P. Hagemmuller, J. Solid State Chem., 70 (1987) 141.

3.4 STRUCTURE DES VERRES DU SYSTEME $\text{As}_2\text{S}_3\text{-Ag}_2\text{S-AgI}$

**Infrared absorption investigation of glasses in the system $\text{As}_2\text{S}_3\text{-Ag}_2\text{S-AgI}$.
Correlations between structure and transport properties**

**Liu JUN, Jean-Jacques Videau, Jean Maurice Réau, Bernard Tanguy, Josick Portier
and Paul Hagemuller
Laboratoire de Chimie du Solide, 351 cours de la Libération, 33405 Talence Cedex,
FRANCE**

A structural study by infrared absorption spectroscopy of glasses belonging to the system $\text{As}_2\text{S}_3\text{-Ag}_2\text{S-AgI}$ has been carried out. For high concentration of arsenic sulfide, these glasses are made of AsS_3 pyramids strongly polymerized with some intercalated As(S,I)_3 units. On the contrary, for high silver iodide content, the pyramids are isolated in a Ag(I,S) lattice. The ionic conductivity of silver has been correlated to these different structures.

1. Introduction

Vitreous fast ionic conductors have been previously prepared in the $\text{P}_2\text{S}_5\text{-Ag}_2\text{S-AgI}$ [1], $\text{GeS}_2\text{-Ag}_2\text{S-AgI}$ [2], $\text{As}_2\text{S}_3\text{-Ag}_2\text{S-AgI}$ [3] and $\text{Sb}_2\text{S}_3\text{-Ag}_2\text{S-AgI}$ [4] ternary systems. The ionic conductivity is higher than those of the corresponding oxide glasses as a result of enhanced covalency which weakens the Ag-S bonds [5].

The vitreous domains in the $\text{M}_2\text{S}_3\text{-Ag}_2\text{S-AgI}$ ($\text{M} = \text{As, Sb}$) systems have been significantly widened thanks to hyperquenching technics. Glasses with composition close to Ag_3SI have been isolated, for instance. They show a very high Ag^+ ion conductivity : $\sigma_{25^\circ\text{C}} = 2.10^{-2} (\Omega.\text{cm})^{-1}$ and $\Delta E = 0.16 \text{ eV}$ for the 0.03 $\text{As}_2\text{S}_3\text{-0.47 Ag}_2\text{S-0.50 AgI}$ glass, $\sigma_{25^\circ\text{C}} = 6.10^{-2} (\Omega.\text{cm})^{-1}$ and $\Delta E = 0.15 \text{ eV}$ for the 0.03 $\text{Sb}_2\text{S}_3\text{-0.57 Ag}_2\text{S-0.40 AgI}$ glass [4, 6].

A comparative study of transport properties in the two series of glasses M_2S_3 - Ag_2S - AgI ($M = As, Sb$) in function of the ratio $x = AgI/(AgI + Ag_2S)$ shows clearly that, in both systems, the conductivity and the activation energy extrapolated to the same values when x tends to unity ($\sigma_{25^\circ C} = 8.10^{-2} (\Omega.cm)^{-1}$, $\Delta E = 0.17-0.19$ eV) [6]. Such a property could be assigned to an hypothetical vitreous AgI compound.

It was worthwhile to correlate this behaviour with the structure of the glasses. This paper is devoted to the investigation by infrared absorption of a set of glasses in the As_2S_3 - Ag_2S - AgI system.

2. Infrared absorption studies

2.1 Experimental

The infrared spectra have been recorded on a Fourier transformed spectrometer (FTIR Bruker 113 V) using a mesh metal separator in the $500-50$ cm^{-1} frequency domain. The glasses were first ground and then mixed with polyethylen (10 % weight). The mixture were pressed at 200 kg/cm^2 to form a pellet (thickness 1 mm, diameter 13 mm).

2.2. Results and discussion

Fig. 1 shows the glass domain in the ternary system. By reason of convenience, the formulas of the glass may be expressed as :

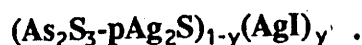


Fig. 2, 3, 4, 5, 6 and 7 show infrared spectra of various samples corresponding to different p values together with those of some significant crystallized phases (AsI_3 , βAgI , β - Ag_2S , Ag_3AsS_3 , $AgAsS_2$) and vitreous As_2S_3 . The set of investigated glasses is shown in Fig. 1.

$p \geq 9$ (Fig. 2)

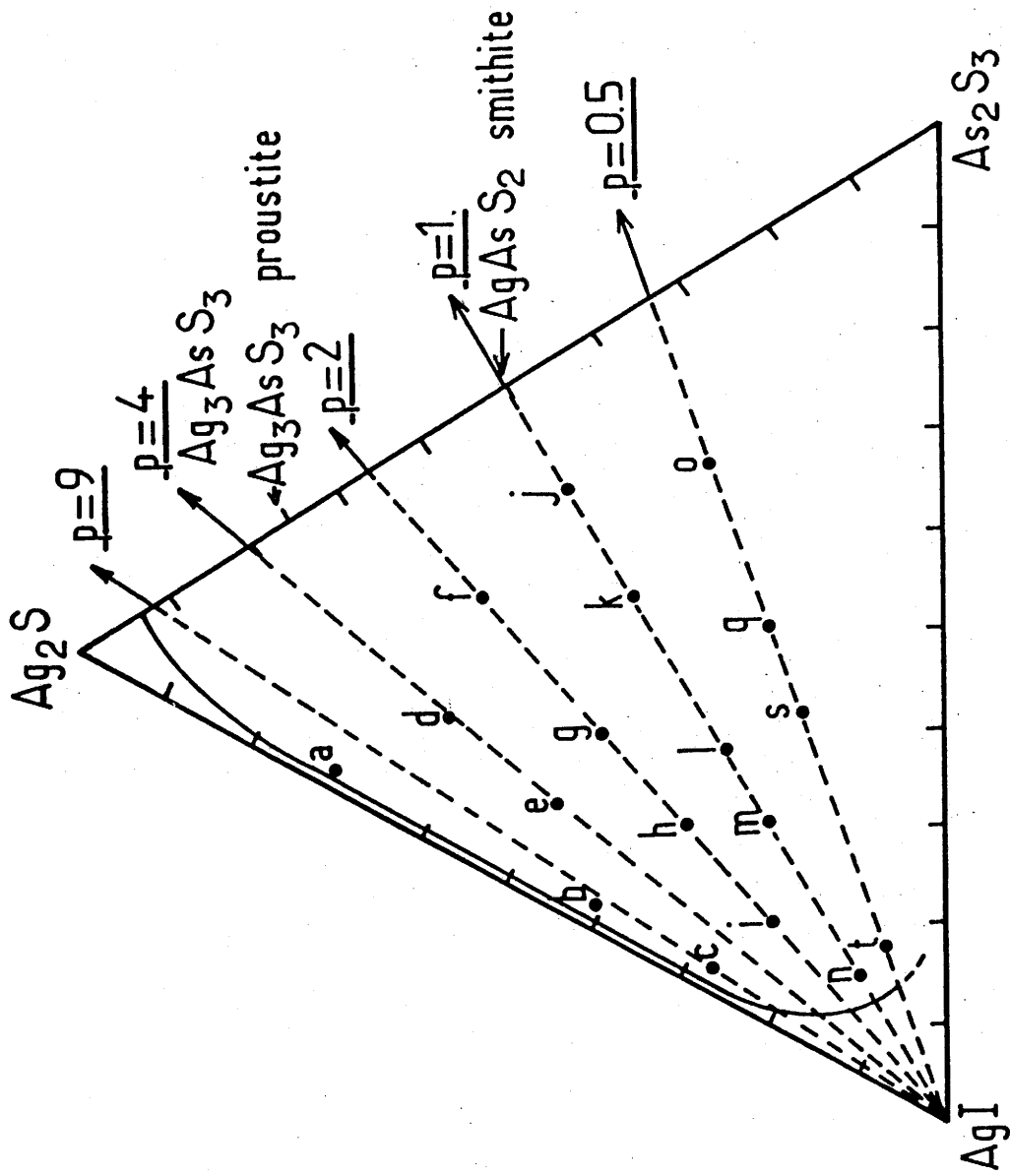


Fig. 1 Chemical composition of the vitreous samples studied by infrared spectroscopy. The continuous line corresponds to the limit of the vitreous domain obtained by hyperquenching of $10^6/\text{s}$ rate.

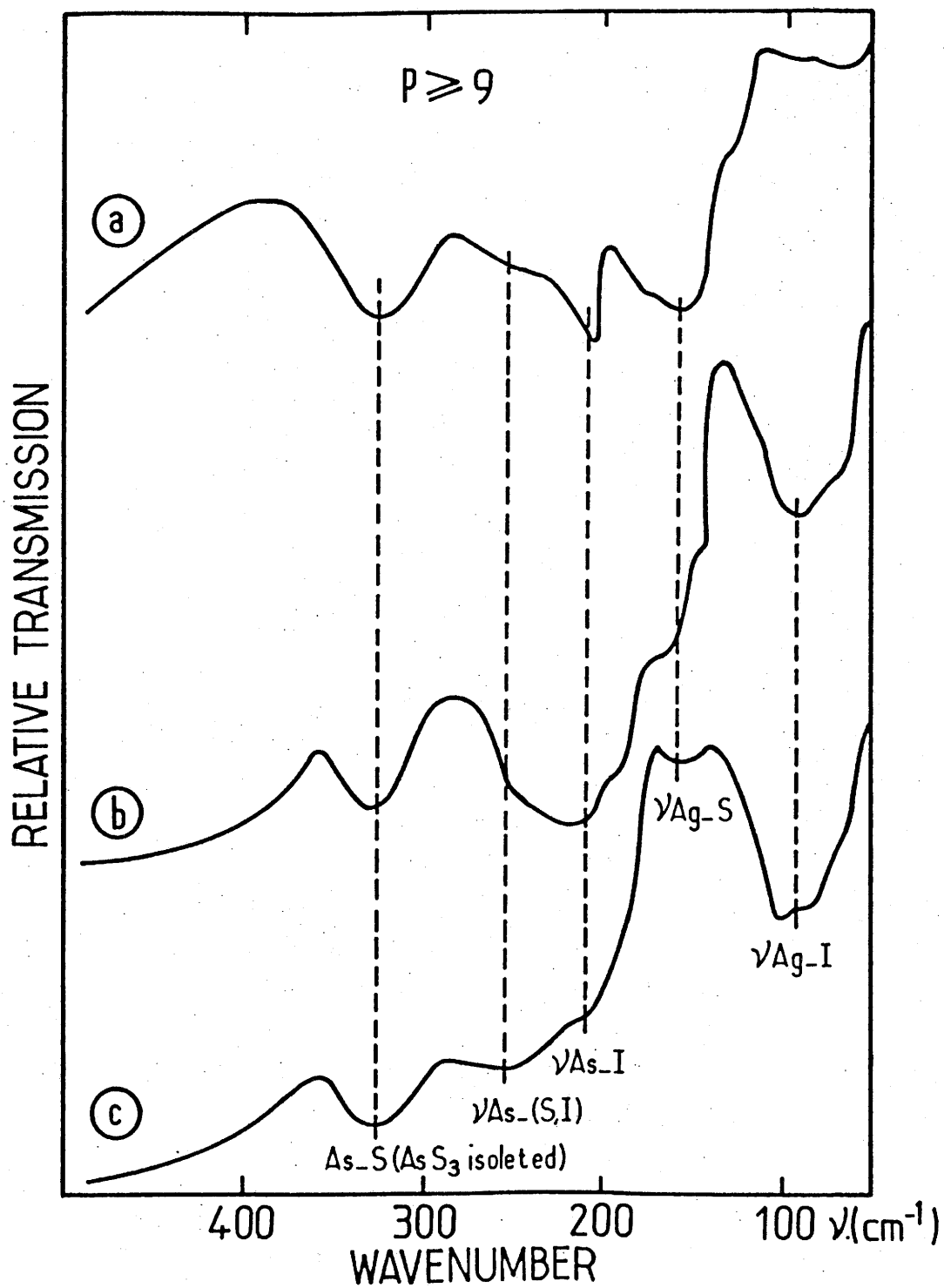


Fig. 2 Infrared absorption spectra of glasses corresponding to $p \geq 9$ (a : $p = 19, y = 0.27$; b : $p = 13, y = 0.57$; c : $p = 9, y = 0.70$).

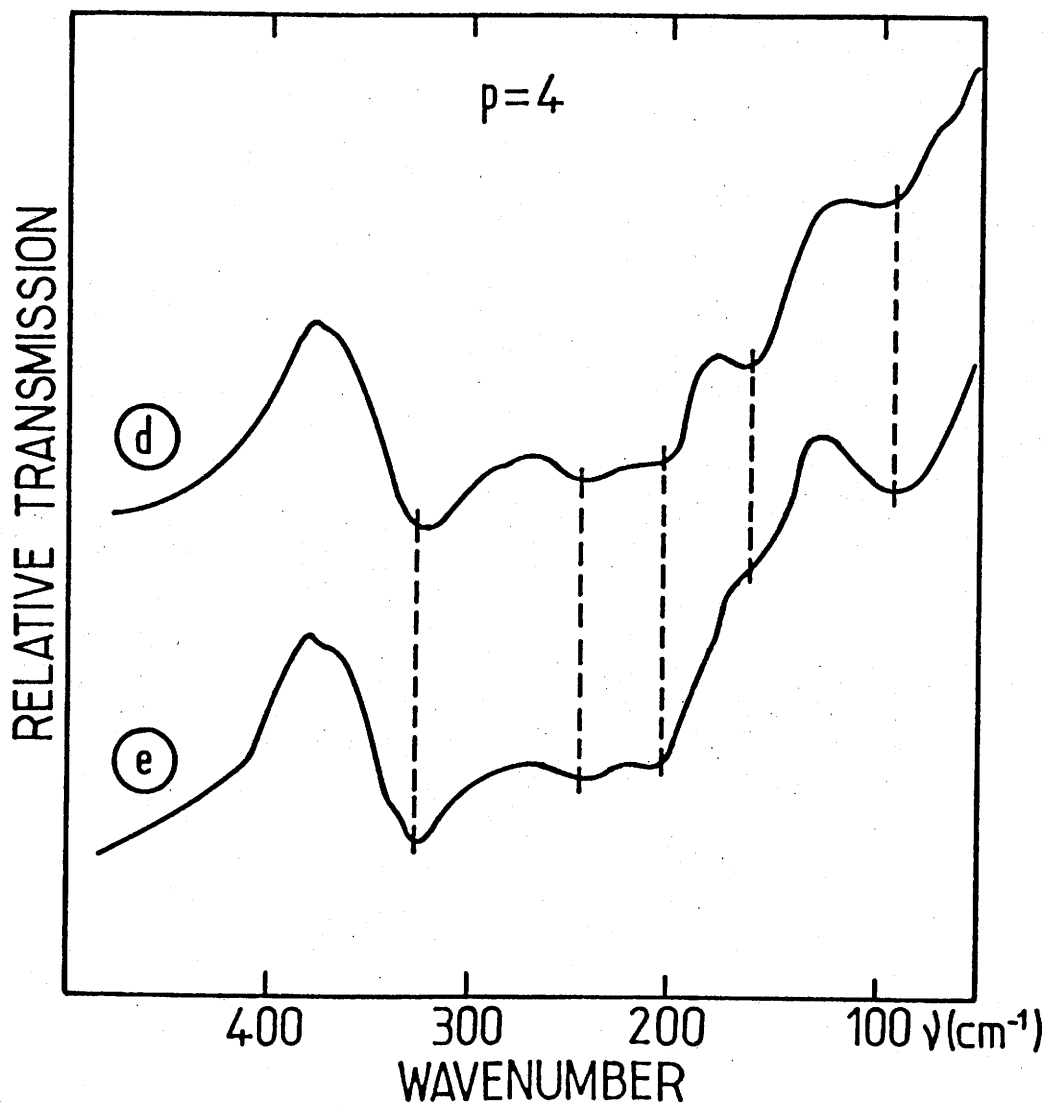


Fig. 3 Infrared absorption spectra of glasses corresponding to $p = 4$ ($f : y = 0.29$; $e : y = 0.45$).

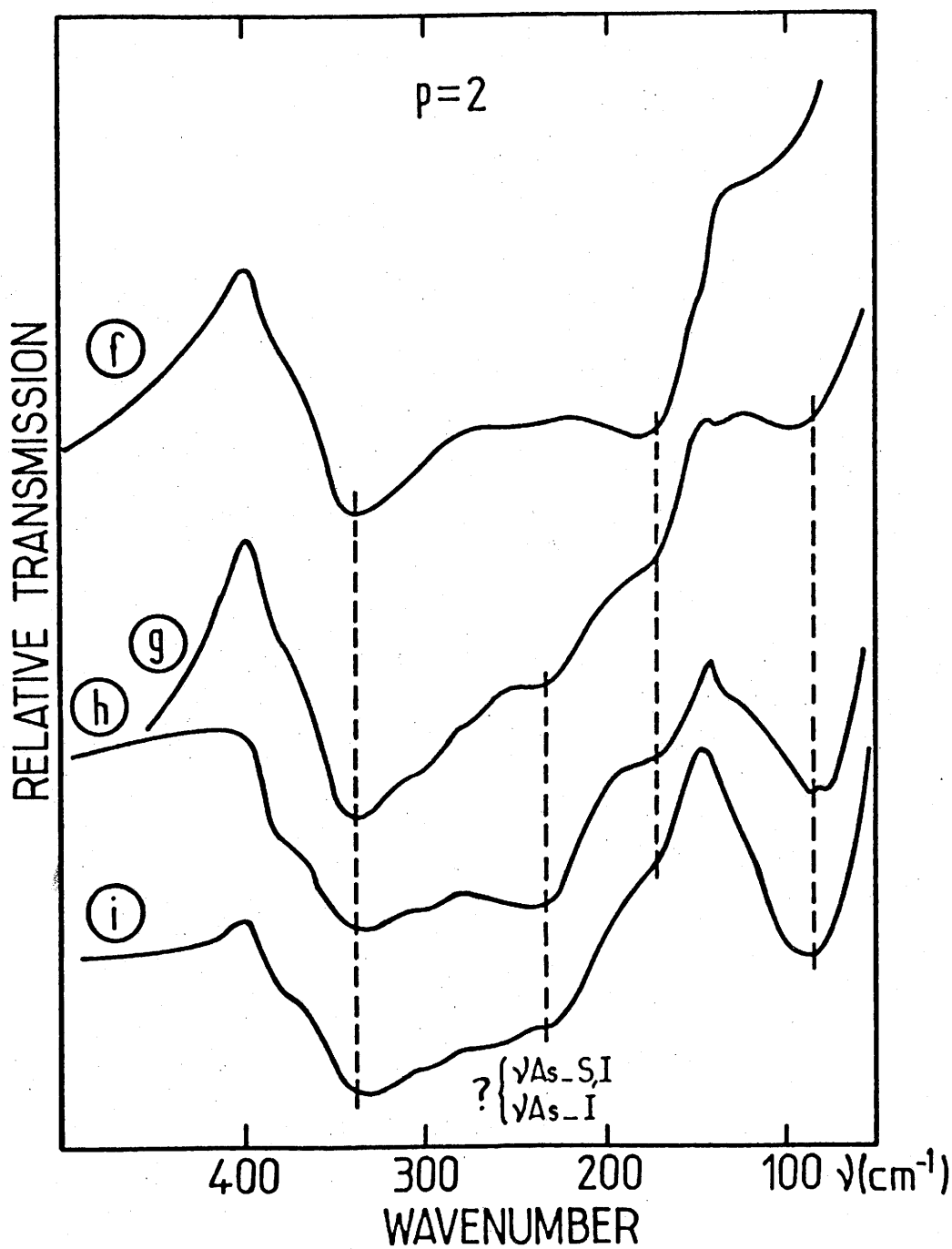


Fig. 4 Infrared absorption spectra of glasses corresponding to $p = 2$ (f : $y = 0.21$; e : $y = 0.40$; h : $y = 0.55$; i : $y = 0.70$).

The a, b and c spectra correspond to increasing y values (low arsenic but high silver concentration). Five set of broad band are observed. The four first high frequency bands are strongly dependent on y (AgI concentration). On the contrary, the last one does not vary with y.

The band located at 330 cm^{-1} could be assigned to the $\nu_{\text{As-S}}$ vibration of isolated AsS_3 triangular based pyramids by comparison with crystallized Ag_3AsS_3 [7].

The band at 205 cm^{-1} could be assigned to $\nu_{\text{As-I}}$ vibrations as in AsI_3 (Fig.7) [8].

A shoulder is observed at about 250 cm^{-1} . As it is situated between the $\nu_{\text{As-S}}$ and $\nu_{\text{As-I}}$ vibration bands it is tempting to attribute it to intermediate $\nu_{\text{As-S,I}}$ vibrations. Such groups have been proposed by T. E. Hopkins who has studied the glasses in the system As-S-I by X-ray diffraction [9]. At the contrary, Koudelka and Pisarcick [10, 11], investigating the same system by Raman spectroscopy, suggested that $\text{S}_2\text{-As-I}$ or S-As-I_2 groups were not present. However, the quenching rate used in this work is much higher than that used by the previous author. Consequently, an increased disorder on anionic sites can be expected.

The band located around 150 cm^{-1} corresponds probably to the $\nu_{\text{Ag-S}}$ vibrations. Its frequency is lower than that observed in $\beta\text{-Ag}_2\text{S}$ (Fig. 7). The same observation has been made for the glasses of the $\text{As}_2\text{S}_3\text{-Ag}_2\text{S}$ system [12]. This behaviour could result from the enhanced ionic character of the Ag-S bond due to the more covalent As-S antagonistic bond.

The lowest frequency band is obviously assigned to $\nu \text{ Ag-I}$ vibrations. It is observed at the same frequency in $\beta\text{-AgI}$ (Fig. 7) [13].

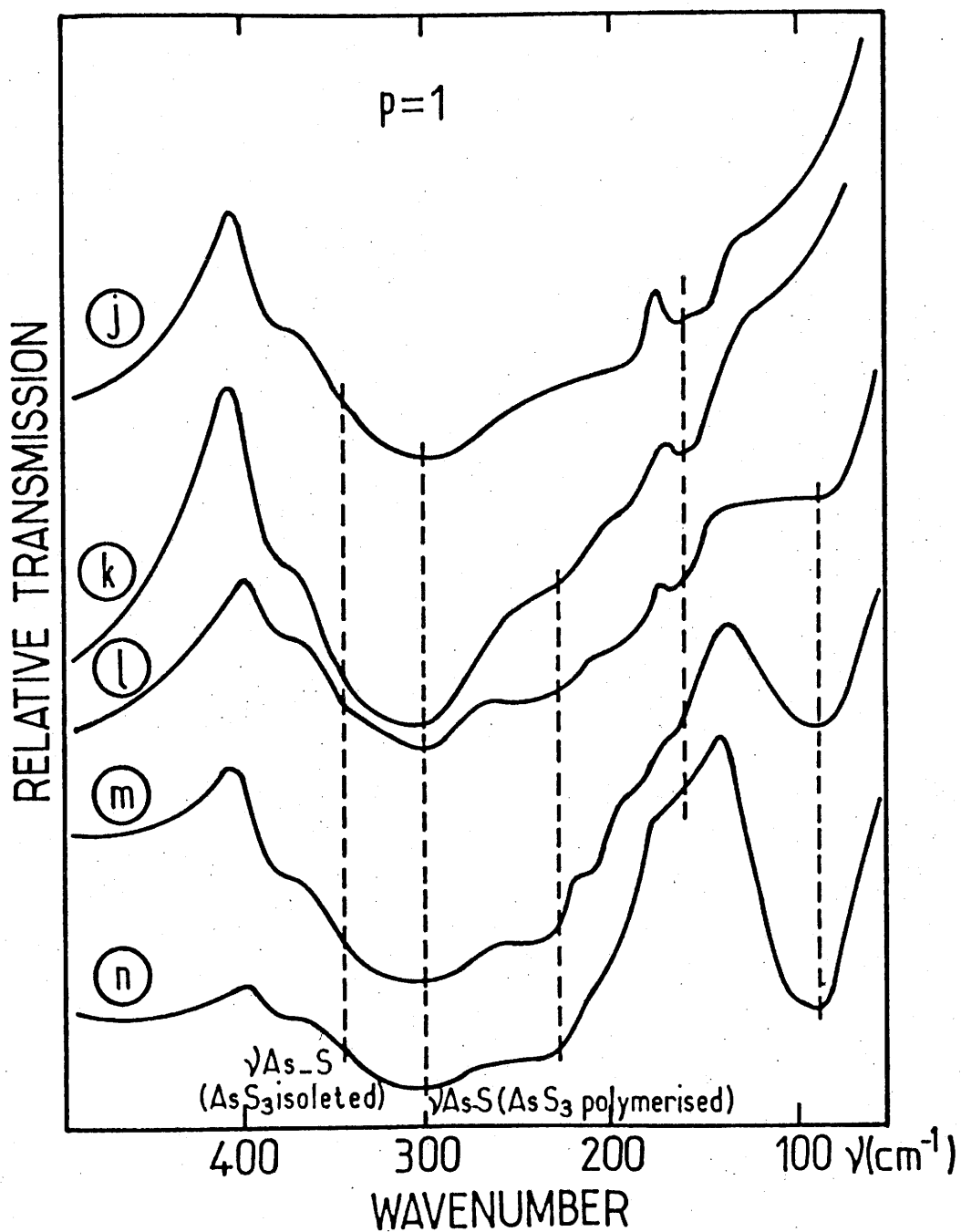


Fig. 5 Infrared absorption spectra of glasses corresponding to $p = 1$ (j : y = 0.15 ; k : y = 0.30 ; l : y = 0.50 ; m : y = 0.60 ; n : y = 0.80).

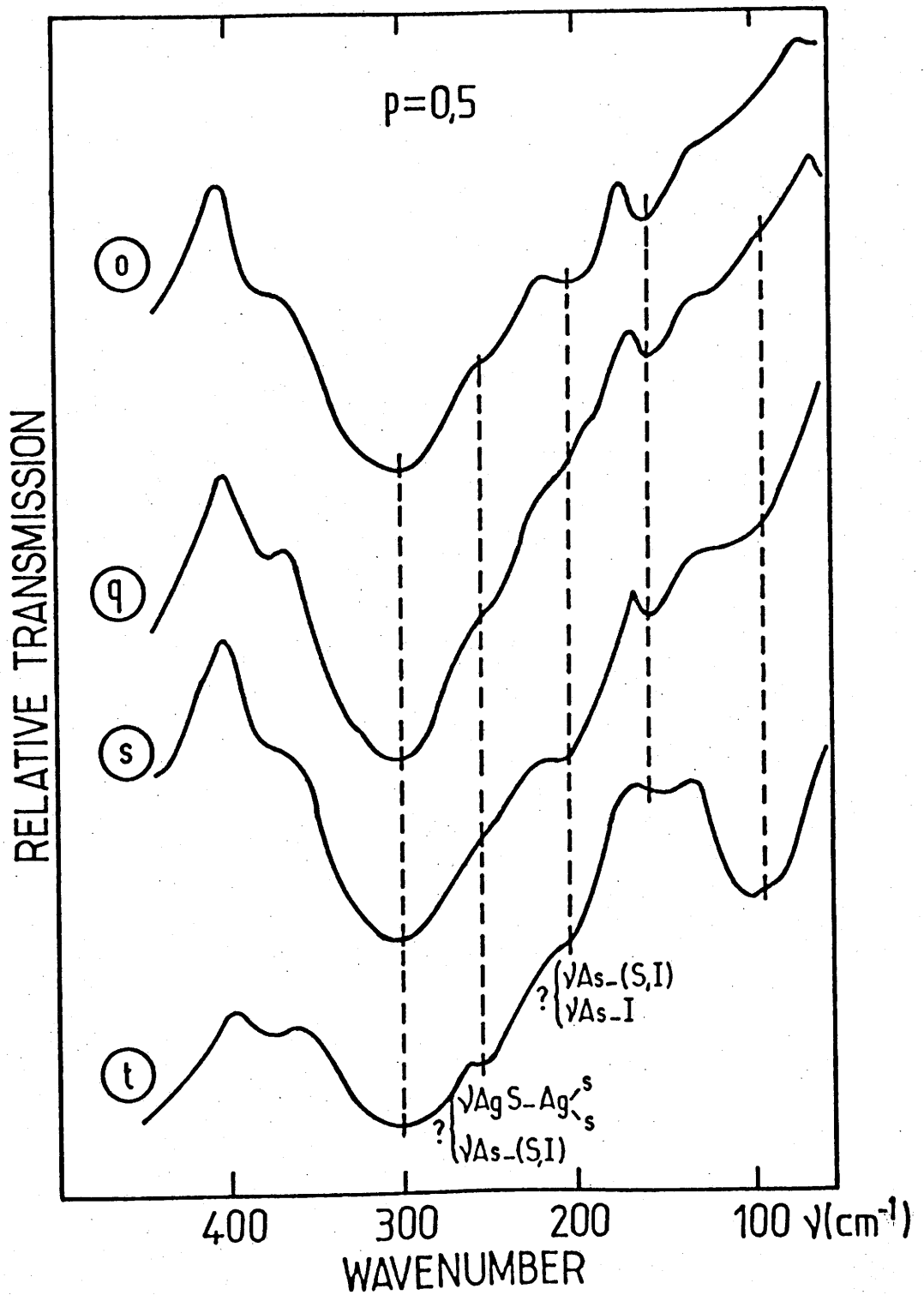


Fig. 6 Infrared absorption spectra of glasses corresponding to $p = 4$ (o : $y = 0.20$; k : $y = 0.39$; s : $y = 0.50$; t : $y = 0.79$).

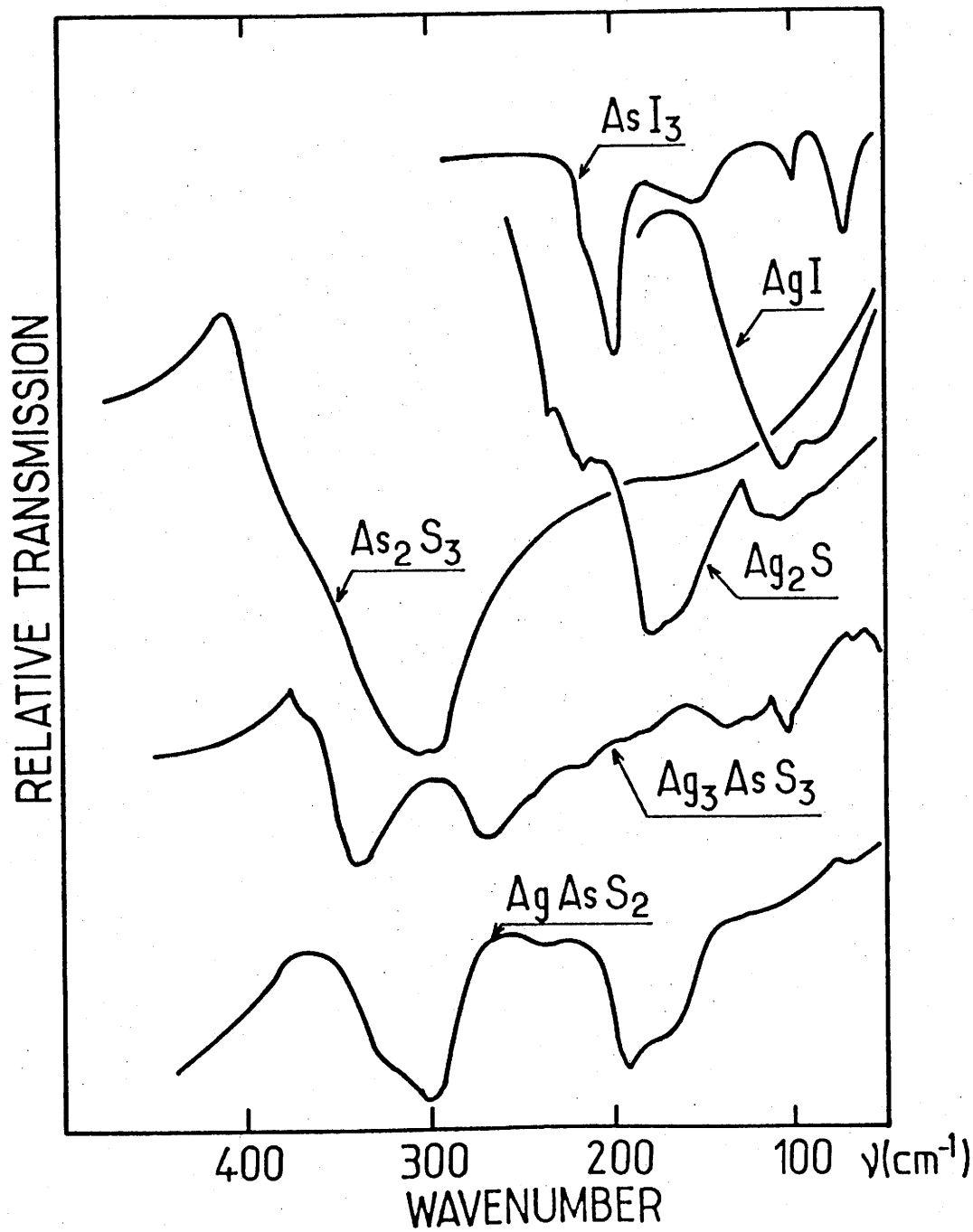


Fig. 7 Infrared absorption spectra of vitreous As_2S_3 and crystalline AsI_3 , AgI , Ag_2S , Ag_3AsS_3 and AgAsS_2 .

p = 4 and p = 2 (Fig. 3 and 4)

The spectra d and e are quite similar. They are rather analogous to those observed for p=9. For p=2, one observes that the weakening of the ν_{A-S} vibration band at 200 cm^{-1} is correlated to the lowering of As_2S_3 content. Moreover, probably for the same reason, only one band close to 220 cm^{-1} appears for the As-(S, I) vibrations.

p = 1 (Fig. 5)

The ν_{A-S} vibration band is shifted towards high frequencies (300 cm^{-1}). It could be interpreted by the polymerization of the corner sharing (As-S₃) groups. However, a shoulder at 330 cm^{-1} is still observed, indicating the presence of some isolated pyramids.

p = 0.5 (Fig. 6)

The four o, q, s, t spectra show a very strong band corresponding to the ν As-S vibrations of polymerized (As-S₃) pyramids as observed in vitreous As_2S_3 (Fig. 7). The 330 cm^{-1} shoulder is no more observed due to a complete polymerization.

The weaker band could be assigned to more complex $\nu_{\text{Ag-S-Ag-S}_2}$ and/or $\nu_{\text{As-(S,I)}}$ at 250 cm^{-1} , $\nu_{\text{As-I}}$ at 200 cm^{-1} and $\nu_{\text{Ag-S}}$ at 170 cm^{-1} .

3. Structure and transport properties

Fig. 8 shows the variation of $\log\sigma_{25^\circ\text{C}}$ versus the atomic ratio

$$r = \frac{\text{Ag}}{\text{As}} = p + \frac{y(1+p)}{2(1-y)}$$

for the glasses of composition $(\text{As}_2\text{S}_3-p\text{Ag}_2\text{S})_{1-y}(\text{AgI})_y$. These results are obviously independent of the nature of the silver salt (sulfide or iodide) added to As_2S_3 for the preparation of the glass.

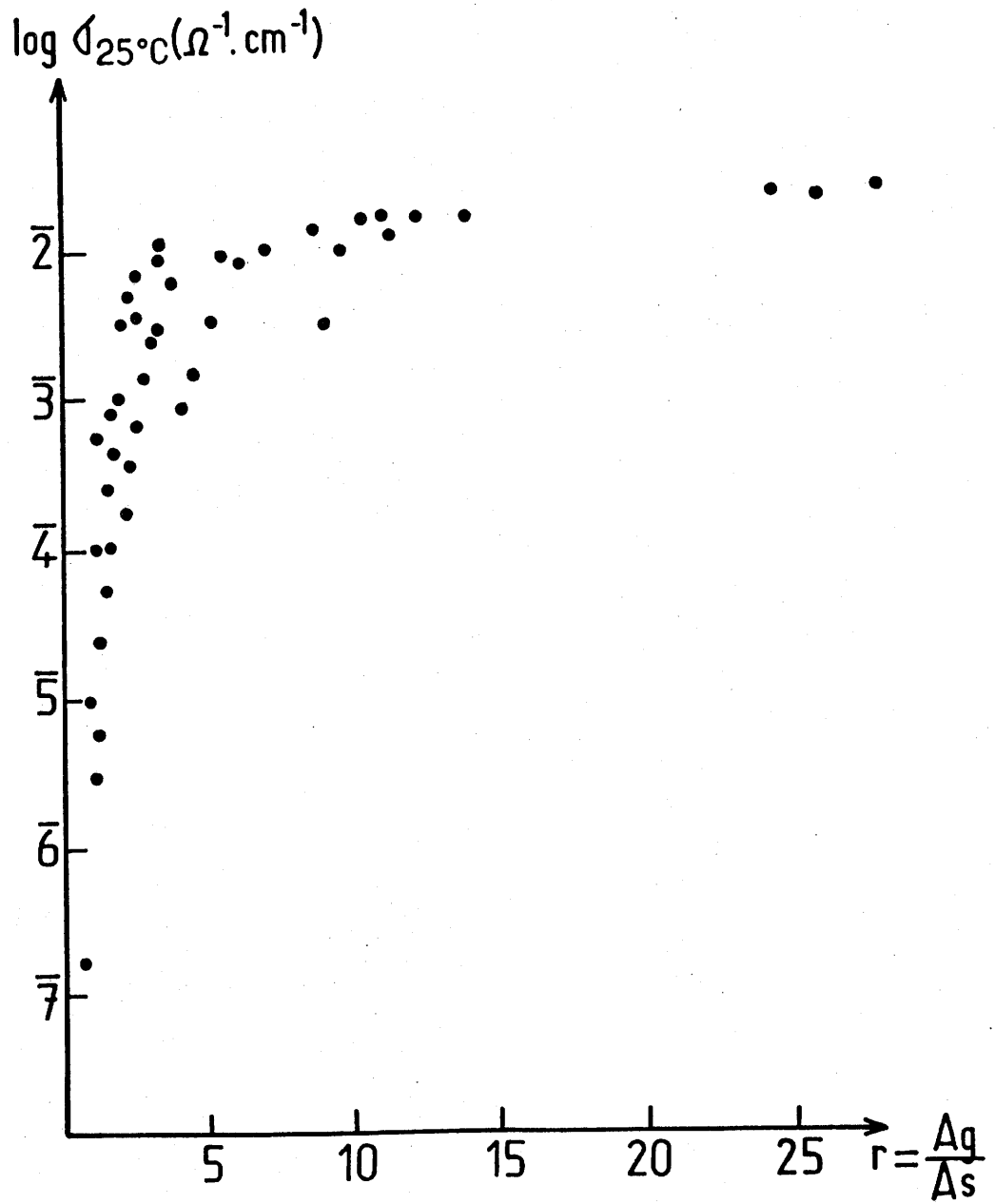


Fig. 8 Variation of $\log \sigma_{25^{\circ}\text{C}}$ vs. $r = \text{Ag}/\text{As}$ ratio for the glasses belonging to the $\text{As}_2\text{S}_3\text{-Ag}_2\text{S-AgI}$ system.

Two different domains are observed : for $r \approx 2$ the conductivity increases sharply with r , for $r > 3$, on the contrary, it increases only smoothly.

The variation of the conductivity in the first domain can be explained by the depolymerization of the arsenic sulfide vitreous lattice as observed by infrared spectroscopy leading to an enhancement of the silver mobility. In the second domain, the lattice is mainly based on silver sulfide, iodide or thioiodide in which As-S_3 entities are dispersed. The Ag^+ mobility is then very high and adding extra silver sulfide or iodide in the vitreous lattice involves merely a slight increase of the conductivity.

Fig. 9 shows the variation of $\log \sigma_{25^\circ\text{C}}$ versus the AgI molar fraction y for some glasses corresponding to given values of r . For $y = 0.50$, the substitution of one S^{2-} by two I^- leads to improved conductivity. This mixed anion effect [14, 15, 16] is more pronounced for the low values of r .

4 Conclusion

The isoconductivity curves have been drawn in Fig. 10. The highest conductivity ($\sigma_{25^\circ\text{C}} = 2.10^{-2} (\Omega.\text{cm})^{-1}$) is very close to that observed in the Sb_2S_3 - Ag_2S - AgI system [4]. Indeed, in both systems, near the AgI - Ag_2S line of the ternary diagrams, the silver thioiodide lattices are similar, the antimony or arsenic sulfide or thioiodide entities playing a limited role for the ionic mobility of silver.

The border limit value of the conductivity is very close to that of β - Ag_3SI itself ($\sigma_{25^\circ\text{C}} \sim 10^{-2} (\Omega.\text{cm})^{-1}$) but relatively lower than that of α - Ag_3SI (extrapolated $\sigma_{25^\circ\text{C}} \sim 0.6 (\Omega.\text{cm})^{-1}$) [17]. It is tempting to explain this observation by a structural similarity between the lattices of glasses and of the ordered low temperature form of silver thioiodide.

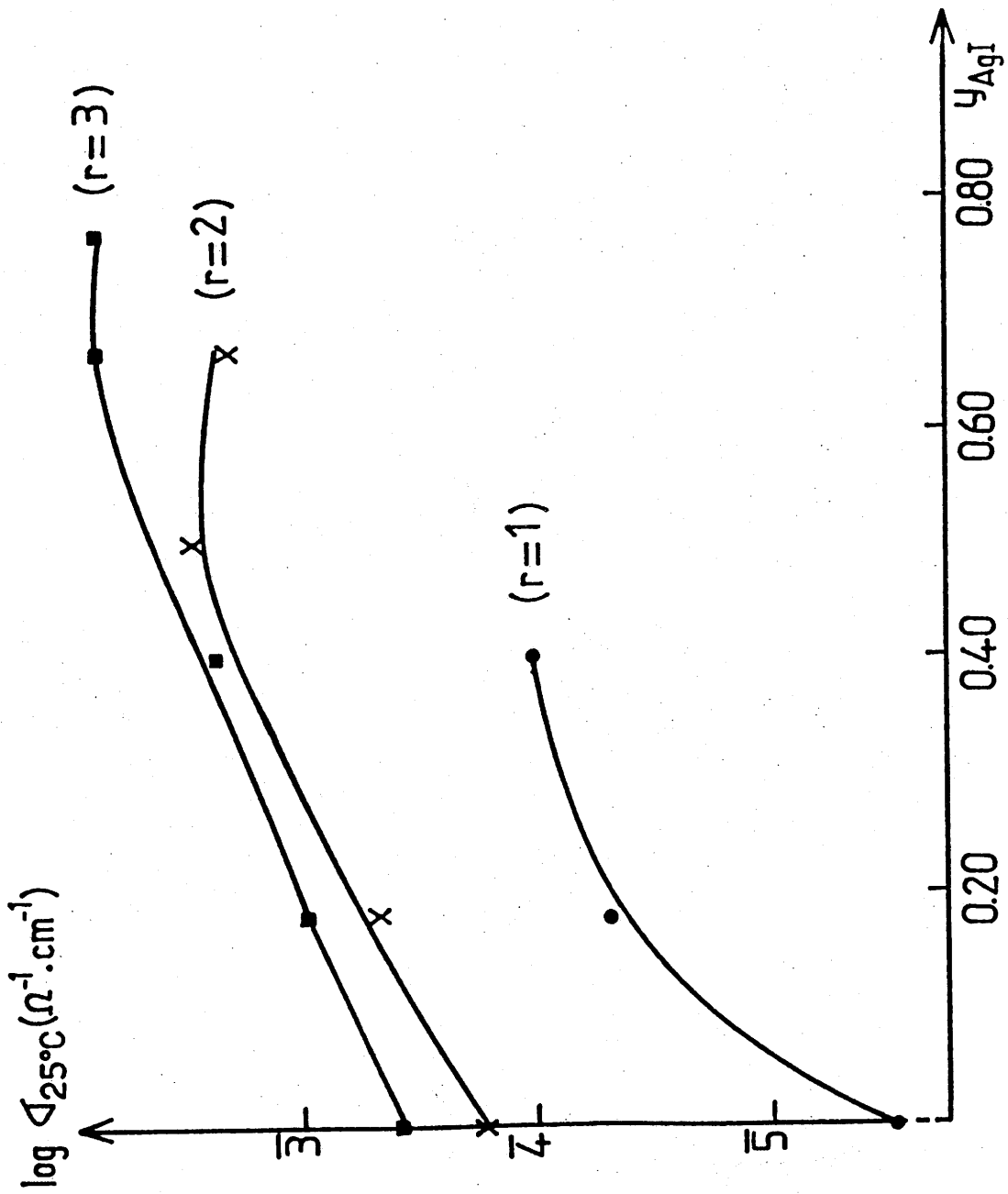


Fig. 9 Variation of $\log \sigma_{25^{\circ}\text{C}}$ vs. AgI molar fraction y for the glasses of the $\text{As}_2\text{S}_3\text{-Ag}_2\text{S-AgI}$ system.

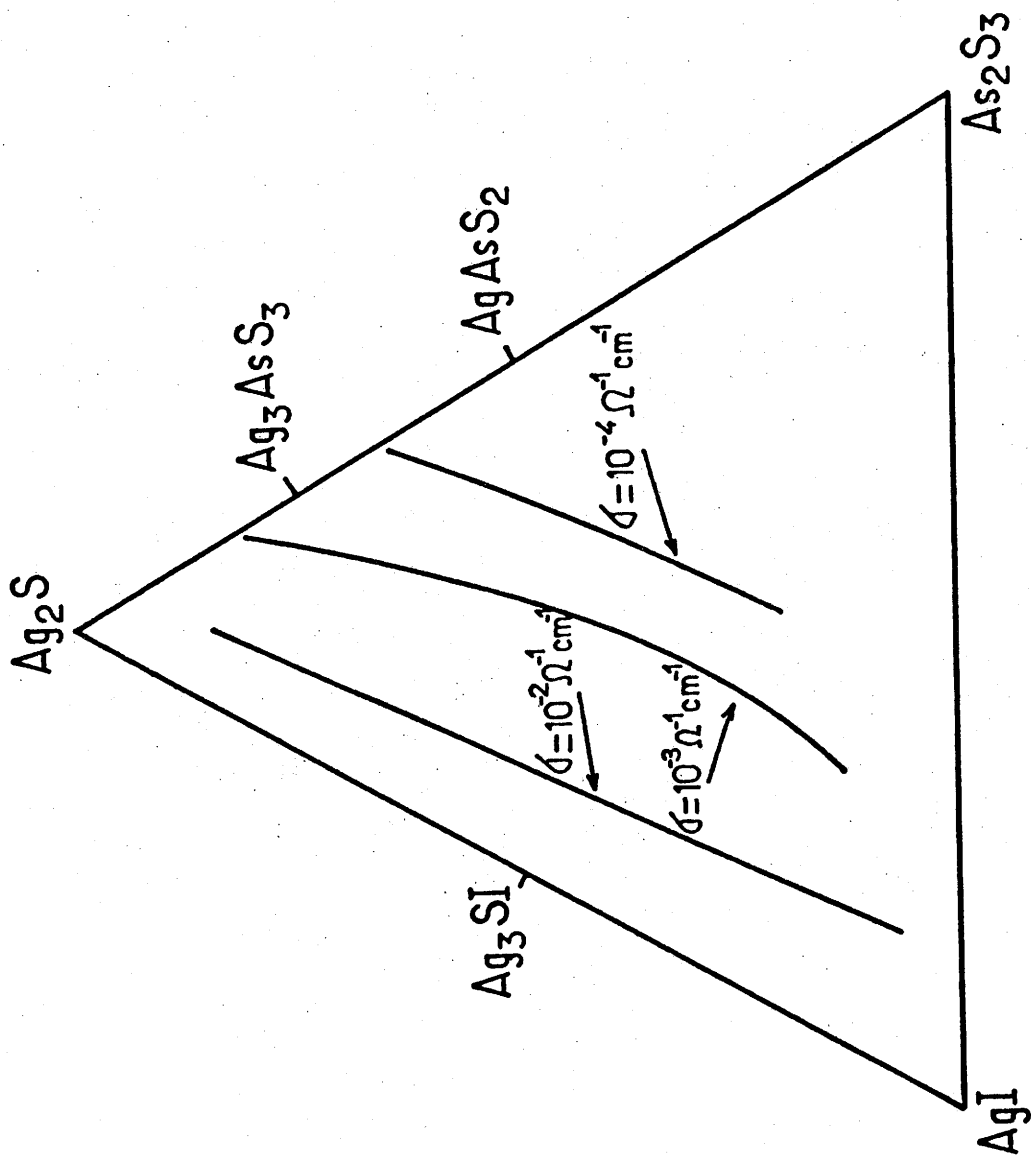


Fig. 10 Isoconductivity curves in the As_2S_3 - Ag_2S - AgI system ($\sigma_{25^\circ\text{C}} = 10^{-2}$, 10^{-3} and $10^{-4} \Omega^{-1} \cdot \text{cm}^{-1}$).

References

1. J.P. Malugani, G. Robert and R. Mercier, *Mat. Res. Bull.* 15 (1980) 715.
2. E. Robinel, B. Carette and M. Ribes, *J. Non-Cryst. Solids* 57 (1983) 49.
3. J.P. Malugani, A. Peida, A. Wasniewski and G. Robert, *C.R.Acad.Sci.Paris*, 289c (1979) 69.
4. Hongwei Sun, B. Tanguy, J.M. Réau, J.J. Videau, J. Portier and P. Hagenmuller, *J. Solid State Chem.*, 70 (1987) 141.
5. T. Minami, Y. Takuma and M. Tanaka, *J. Electrochem. Soc.* , 124 (1977) 1659.
6. J.M. Réau, B. Tanguy, J.J. Videau, J. Portier and P. Hagenmuller, *Proc. 6th Int. Conf. Garmisch Partenkirchen*, Sept. 1987, *Solid State Ionics*, 28-30 (1988) 792-798.
7. H.H. Byer, *Ferroelectrics* 5 (1973) 207
8. T.R. Manley and A. Williams, *Spectrochem. Acta* 21 (1965) 1773
9. T.E. Hopkins, R.A. Pasternak, E.S. Gould and J.R. Herdon, *J. Phys. Chem.* 66 (1962) 733
10. L. Koudelka and M. Pisarcik, *Solid State Comm.* 41 (1) (1982) 195
11. L. Koudelka and M. Pisarcik, *J. Non-Cryst. Solids*, 64 (1984) 87
12. L. Jun, J.J. Videau, B. Tanguy, J.M. Réau and P. Hagenmuller *Mat. Res. Bull.*, 23 (1988) 1315
13. G. L. Bottger and A.L. Geddes, *J. Chem. Phys.*, 46 (1967) 3000
14. H. Tatsumisago, T. Minami and M. Tanaka, *Glastech. Ber.* 56k (1983) 945
15. A. Magistris, G. Chiodelli and M. Duclot, *Solid State Ionics* 9-10 (1983) 611
16. B. Carette, M. Ribes and J.L. Souquet, *Solid State Ionics*, 9-10 (1983) 735
17. B. Reuter and K. Hardel, *Ber. Bunsengesell. f. Phys. Chem.* 70 (1966) 62

3.5 CONCLUSION DU CHAPITRE 3

Des verres de compositions proches de celles du binaire $\text{Ag}_2\text{S-AgI}$ ont été synthétisés.¹ Cependant ni Ag_2S ni AgI n'ont pu être obtenus amorphes pour les vitesses de refroidissement mis en oeuvre. On note que la présence simultanée de soufre et d'iode favorise de façon très importante la formation de verre.

Dans le second chapitre de ce mémoire nous signalions l'hypothèse de la formation de clusters de type $\text{AgI-}\alpha$ avancée par certains auteurs dans le cas de verres à base d'iodure et de phosphate d'argent. Elle se basait sur la variation linéaire de l'énergie d'activation en fonction du taux d'iodure d'argent, la valeur extrapolée à 100% d'iodure conduisant à une valeur voisine de celle de $\text{AgI-}\alpha$. Dans le cas des verres étudiés dans ce chapitre, on observe parfois une telle linéarité. Par exemple, pour la droite As_2S_3 ou $\text{Sb}_2\text{S}_3\text{-Ag}_3\text{SI}$, la variation de l'énergie d'activation en fonction du taux de thio-iodure, observée sur la figure 1, ainsi que la valeur limite proche de celle de $\text{Ag}_3\text{SI-}\beta$ pouvait laisser penser à l'existence d'un phénomène similaire. Cependant l'étude structurale n'apportait pas d'arguments suffisants pour avancer une telle hypothèse.

A ce point de notre étude, il nous a semblé alors intéressant d'étendre nos investigations au phosphate d'argent. En effet, les verres phosphatés se prêtent à des études spectroscopiques approfondies en raison des vibrations P-O et P-S se manifestant à relativement hautes fréquences. En outre il était tentant d'introduire dans ce matériau du sulfure d'argent dont la variété haute température est isotype de celle de AgI afin de tenter d'élucider l'hypothèse des clusters.

1. Dans une expérience récente, nous avons pu obtenir Ag_3SI vitreux en utilisant une méthode de lévitation et fonte au laser à CO_2 mise au point par J. P. Coutures à Orléans

Chapitre 4- VERRES THIO-OXYPHOSPHATES

Table des Matières

Chapitre 4 VERRES THIO-OXYPHOSPHATES	59
4.1 LE SYSTEME $\text{Ag}_2\text{S-AgPO}_3$	59
4.2 Conclusions du chapitre 4.	77

Chapitre 4

VERRES THIO-OXYPHOSPHATES

4.1 LE SYSTEME $\text{Ag}_2\text{S-AgPO}_3$

(Solid State Ionics, accepté pour publication)

Glass formation and conductivity in the $\text{Ag}_2\text{S-AgPO}_3$ system : evidence against cluster pathway mechanisms for high ionic conductivity

LIU JUN, J. PORTIER, B. TANGUY, J-J. VIDEAU

Laboratoire de Chimie du CNRS, 351 cours de la Libération, 33405 Talence, France
and

C. A. ANGELL

Dept. of Chemistry, Purdue University, W. Lafayette, In 47907

The glass forming region in the system $\text{Ag}_2\text{S-AgPO}_3$ has been determined. The studies of electrical conductivity, infrared absorption, thermal expansion and transport number of Ag^+ ions of glasses belonging to this system was carried out. The results of the electrical conductivity and the transport number measurements show that the conduction is essentially ionic in nature and due to silver ions alone. In this system, as in AgI - AgPO_3 , the logarithm of ionic conductivity increases linearly with increasing Ag_2S mole

fraction and extrapolates to the value of the superionic crystalline Ag_2S . However, an explanation similar to the α -AgI cluster pathway model proposed for AgI containing systems is not tenable since IR spectra show that Ag_2S dissolves by an acid-base chemical ordering process to give shorter phosphate chain structures which approach the pyrophosphate stoichiometry at the glass-forming limit.

1.Introduction

The conductivity of vitreous solutions of (AgI + Ag oxyanion) mixtures has been widely investigated in recent years in the search for solid electrolytes with superior properties [1-4]. It has been found that in almost all system studied, the conductivity when plotted in logarithmic form against mole fraction of AgI, extrapolates to the value which the high temperature (cation - disordered) form of AgI would have at the same temperature [1-5]. Since the same behavior is found for other properties such as elastic moduli [6] and density [1-7] it has been widely suggested [5-11] that the high conductivity pathway in these glasses is through microregions possessing the α -AgI structure. The implication, frequently stated explicitly, is that there exist α -AgI-like "clusters", overlapping to various degrees, in the vitreous matrix provided by the oxysalt. Since clustering of one component in a binary solution unambiguously implies positive deviations from random mixing, the cluster postulate leads to the expectation [12-14] that the heat of mixing of AgI and the Ag oxysalt component would be positive. This is not the case according to the results of the only study of this type so far reported, viz., a solution calorimetry study of glasses in the now-classic system AgI-AgPO₃ [15].

In an attempt to clarify this matter we have studied an alternative binary system based on AgPO₃ as glass former in which the second component, like AgI, has a cation disordered highly conducting structure, but whose mode of dissolution

in AgPO_3 is more obvious than for AgI and is also susceptible to confirmation by spectroscopic studies reported herein.

α - Ag_2S in its high temperature disordered form has the same anion lattice structure as has α - AgI and its conductivity is comparable [16]. The solid solubilities of Ag_2S in AgI , and of AgI in Ag_2S , in their high temperature forms, are very high [17]. Ag_2S is more stable than Ag_2O and may be dissolved in liquid AgPO_3 without limit. The solutions prove to be glass-forming up to 35 mole % of added Ag_2S .

We report here some of the glass properties. We show that the conductivity, as in the case of AgPO_3 - AgI glasses, extrapolates to the value expected for the disordered crystalline α - Ag_2S at the same temperature, but that in this case the explanation cannot possibly lie in the cluster-type microstructure commonly proposed to explain similar behavior in AgI -containing glasses.

2. Experimental

2.1. Preparation of the glasses

The starting materials were Ag_2S (purity 99.9% ALDRICH Co.) and AgPO_3 which was prepared from AgNO_3 and NaPO_3 by a wet method as described elsewhere [11]. Two grams batches were melted in evacuated, sealed silica glass ampoule, at 500°C to 900°C during 24h, followed by quenching in water. The glassy state was confirmed by X-ray diffraction. The colour of the glasses varies from red to dark red as the Ag_2S content increases and become black on prolonged exposure to light.

2.2. Calorimetric and volumetric characterization

The glass transition temperature were determined by differential scanning calorimetry, using a Setaram Model DSC 92 instrument. The coefficients of linear

thermal expansion of the glasses were obtained using a differential dilatometer (402 ED Netzsch).

2.3. Electrical conducting measurements

The conductivity measurements have been performed by complex impedance method using a Solartron 1170 frequency response analyser. The pellets were cylindrical (8 mm diameter, 1-2 mm thickness). On both sides the gold electrodes were deposited by evaporation. The used frequency range was 10^{-2} - 10^4 Hz, the measurements were carried out between 20°C and T_g of the vitreous sample under argon atmosphere.

2.4. Transport numbers

The transport number of Ag^+ has been measured by the EMF method [18] which distinguishes between cationic and electronic processes.

2.5. Chemical durability

Chemical durability of the glass $0.2 Ag_2S-0.8 AgPO_3$ was measured in distilled water and in solutions of various pH. The glass sample was immersed in the solution for one day and then weighed. The presence of Ag^+ ions in the solution was checked and the absence of crystalline products was confirmed by X-ray diffraction pattern.

2.6. Spectroscopic studies of glass structure

Infrared absorption spectra in the range $700-1400\text{ cm}^{-1}$ have been obtained using a double beam PERKIN ELMER 983 Spectrometer and KBr pellet samples. Pellets of thickness 1 mm and diameter 13 mm were obtained by pressing a ground mixture of 1 part glass 60 parts KBr at 200 Kg/cm^2

3. Results

In the $xAg_2S - (1-x)AgPO_3$ binary system, the glass domain is observed in the range of $x = 0$ to $x = 0.35$ as shown by the range of glass transition temperatures in

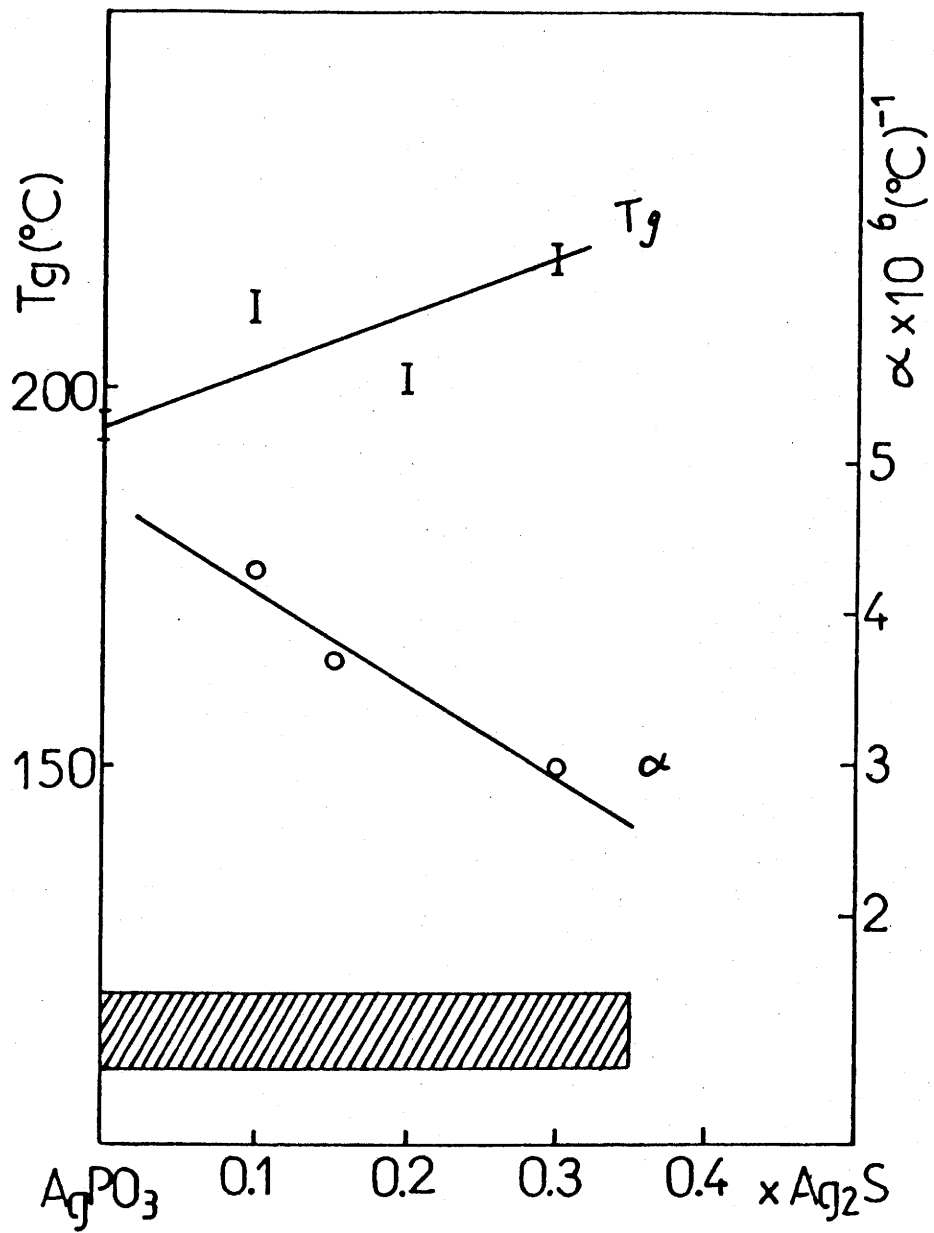


Fig.1 Vitreous domain in $x\text{Ag}_2\text{S}-(1-x)\text{AgPO}_3$ system;(I) glass transition temperature (T_g) and (O) expansion coefficient (at 25°C).

fig. 1. This figure also contains some values of the glass state expansivities which fall in the usual range of 10^6 K^{-1} .

Fig.2 shows the variation of the logarithm of the conductivity with the reciprocal absolute temperature for various compositions in $x \text{ Ag}_2\text{S}-(1-x) \text{ AgPO}_3$ system. The conductivity can be described by the well known Arrhenius law, $\sigma = \sigma_0 \exp^{-E_a/RT}$, for all the samples in the 293 K-T_g temperature range. It is possible that, as in the AgI-AgPO_3 system [14, 18] some curvatures may appear at lower temperature beyond the range of our measurements.

Fig.3 shows the conductivity at room temperature, the activation energy and preexponent versus the percentage of Ag_2S . Data are collected in Tab.I. The conductivity increases and the activation energy decreases with increasing Ag_2S content, as observed frequently in other binary system [1-4]. It is of special interest to note that, as in the case of $\text{AgPO}_3\text{-AgI}$, both $\sigma_{25^\circ\text{C}}$ and E_a extrapolate to the value for the pure Ag compound, high temperature disordered form, extrapolated itself at room temperature.

The transport number of Ag^+ ions has been measured by emf method. It shows that the ionic mobility is the main process (Tab. II).

Infrared spectra of some glasses are shown in Fig.4. The spectrum (a) corresponds to AgPO_3 , (b) to $0.7\text{AgPO}_3\text{-}0.3 \text{ AgI}$, and (c) to $0.7\text{AgPO}_3\text{-}0.3\text{Ag}_2\text{S}$. The attributions of the vibrations has been done following R.F. Bartholomew in phosphate glasses [20].

The glasses containing AgI has a similar spectrum of that of AgPO_3 itself showing that the $(\text{PO}_4)_n$ infinite chains are not modified by introducing silver iodide, which thus acts as a plasticising agent as in polymer-diluent systems. By contrast, the spectrum of the glass containing silver sulfide is greatly modified. In particular the

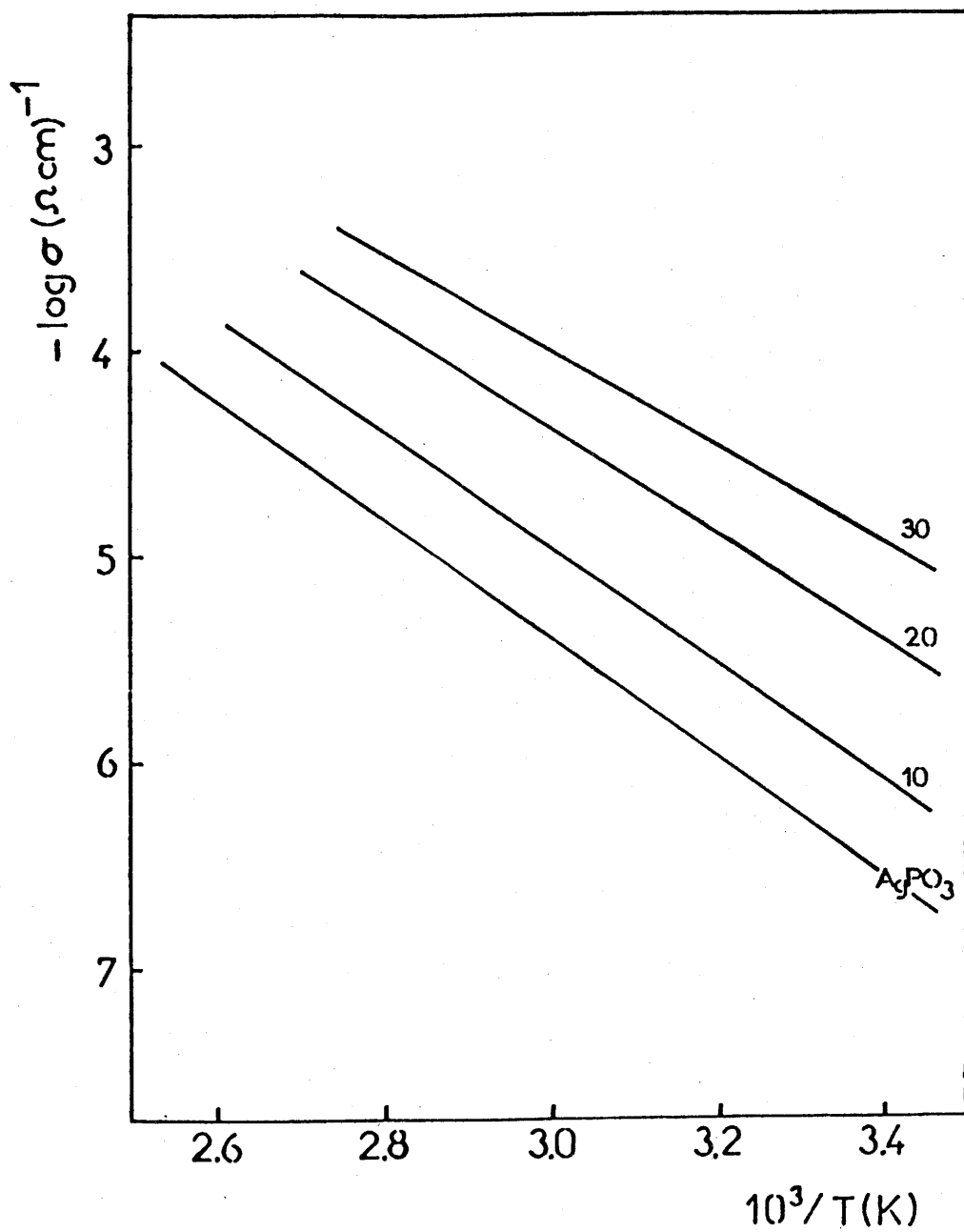


Fig.2 Arrhenius plot of conductivity for $x\text{Ag}_2\text{S}-(1-x)\text{AgPO}_3$ glasses.

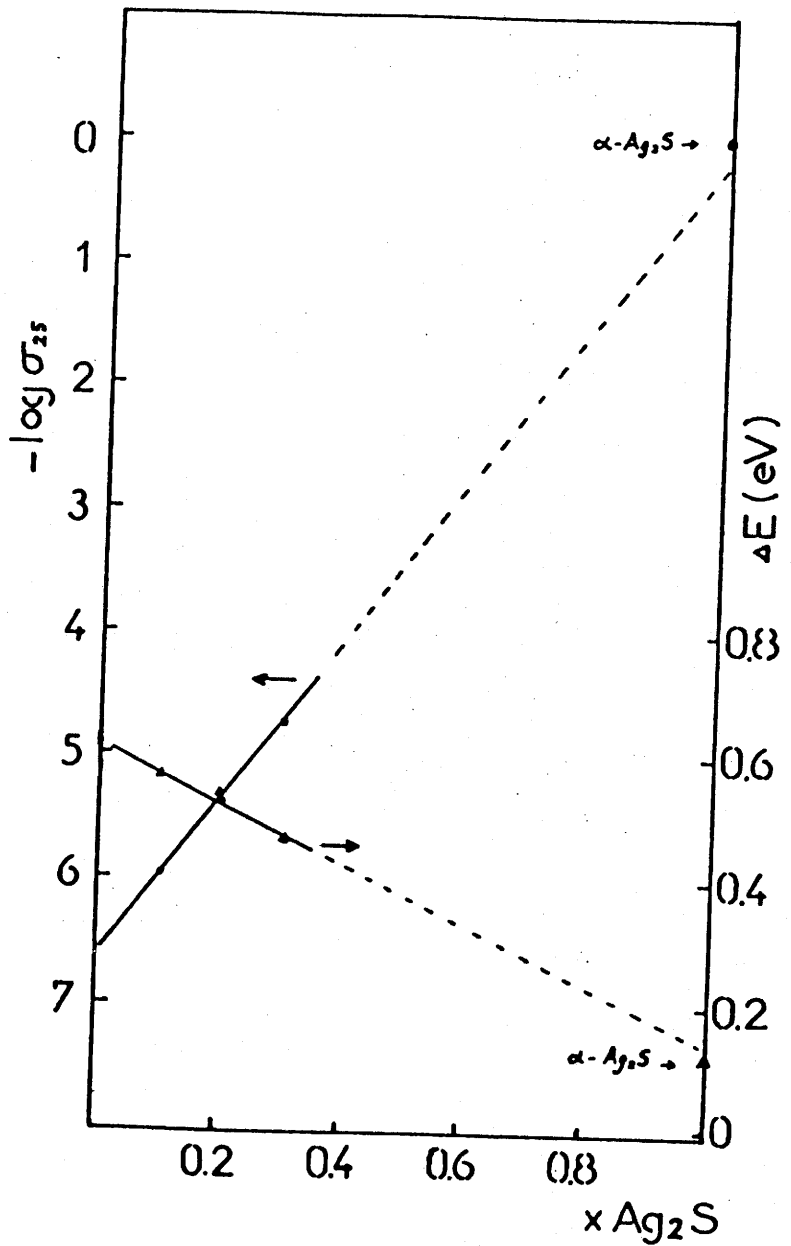


Fig.3 Variation of conductivity at 25°C and activation energy of the $x\text{Ag}_2\text{S}-(1-x)\text{AgPO}_3$ glasses. Note extrapolations to values for supercooled crystalline Ag_2S in high temperature superionic form.

Table I. Values of conductivity at 25°C, activation energy and pre-exponential term of the Ag₂S-AgPO₃ glasses.

n°	composition mole	$\sigma_{25^\circ\text{C}}$ ($\Omega^{-1}\cdot\text{cm}^{-1}$)	E σ (eV)	log σ_0
1	0.10Ag ₂ S-0.90AgPO ₃	1.05 10 ⁻⁶	0.562	3.55
2	0.20Ag ₂ S-0.80AgPO ₃	4.79 10 ⁻⁶	0.515	3.41
3	0.30Ag ₂ S-0.70AgPO ₃	1.45 10 ⁻⁵	0.467	3.08

Table II Transport numbers of Ag⁺ ions in Ag₂S + AgPO₃ glasses

n°	Composition(mole)	E _o (mv)	E _t (mv)	t=E _o /E _t
1	0.10Ag ₂ S-0.90AgPO ₃	627	687	0.91
2	0.15Ag ₂ S-0.85AgPO ₃	655	687	0.953
3	0.30Ag ₂ S-0.70AgPO ₃	659	687	0.959
4	0.35Ag ₂ S-0.65AgPO ₃	661	687	0.962

Table III Chemical durability of 0.20 Ag₂S-0.80 AgPO₃ glass

pH	Time(hrs)	AgCl	ΔW%	X-ray
3	24	no	+0.04	glassy
7	24	no	-0.26	glassy
11	24	no	-0.07	glassy

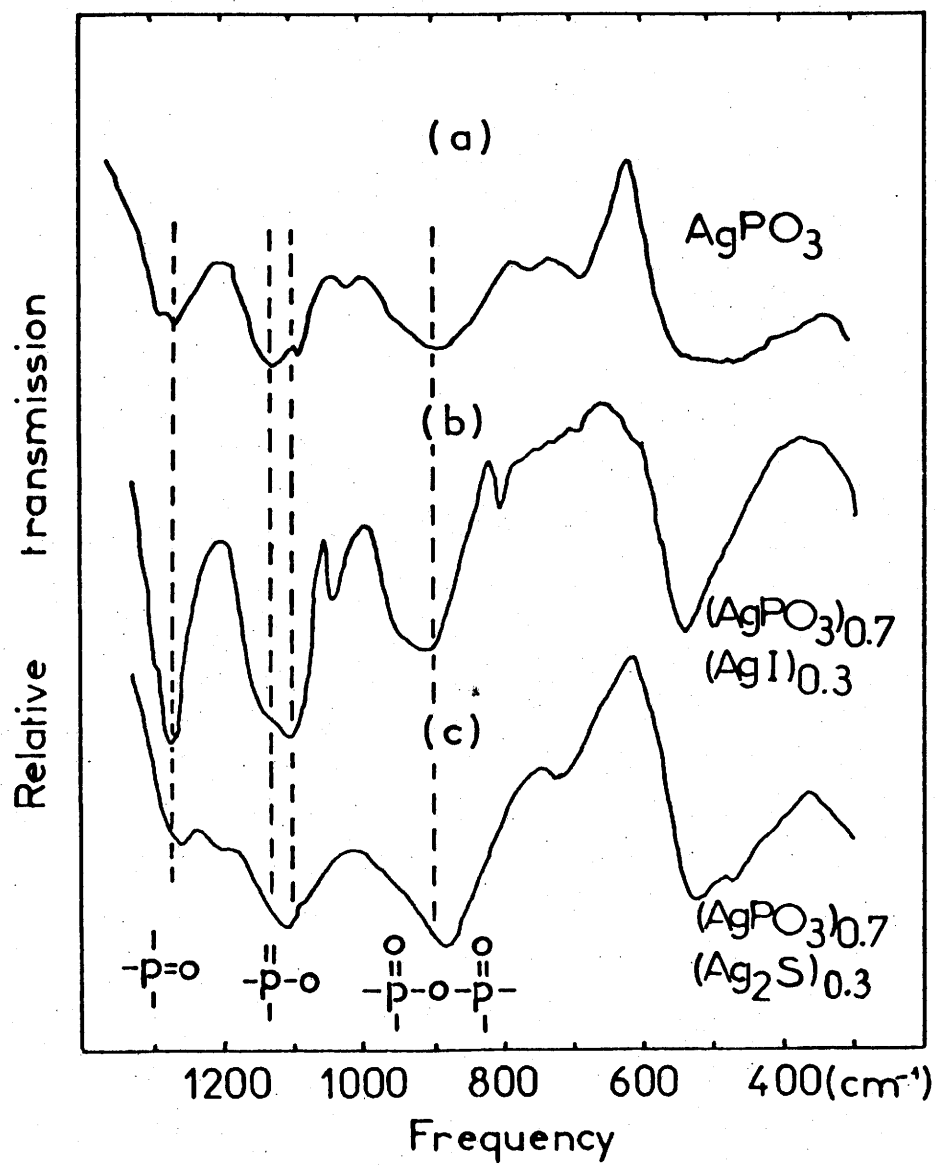


Fig.4 Infrared spectra of the glasses : (a) AgPO_3 ; (b) $0.3 \text{ AgI}-\text{AgPO}_3^{0.7}$; (c) $0.3 \text{ Ag}_2\text{S}-0.7 \text{ AgPO}_3$.

band at 1270 cm^{-1} corresponding to the P=O vibrations decreased strongly in intensity.

By contrast with AgI-rich glasses, the sulfide-metaphosphate glasses are very resistant to attack by water in a wide pH range. Data are summarized in table 3.

4. Discussion

Fig. 3 shows that the present system conforms to a simple pattern of linear composition dependence of the logarithm of the conductivity which has been observed in many [1-3, 5] though not all [3] previous studies of fast ion conducting systems. In particular Minami and Tanaka[7] showed that anywhere in the ternary system AgX-Ag₂O-P₂O₅, the conductivity could be expressed by the simple expression :

$$\log \sigma_{25^\circ\text{C}} = a.M_a + b.M_b + c.M_c \quad (1)$$

where a, b and c are constant and M_a, M_b and M_c are the mole fractions of AgX, Ag₂O and P₂O₅ respectively. A similar relationship was demonstrated by Martin and Schiraldi [5] to hold for the system AgI-Ag₂O-As₂O₃ when the composition was correctly scaled. In each case involving AgI, the constant a was found to be the conductivity of crystalline α -AgI (cation disordered phase) extrapolated to 25°C through the α - β phase transition at 146°C. A common explanation has been given in terms of microclusters of α -AgI-like structures in the glassy matrix which increase in number and degree of overlap with increasing AgI content [5-11].

It is helpful in discussing the equivalent finding for the present system (see Fig.3) to recognize that the system AgPO-Ag₂S is a cut across the ternary system Ag₂S-Ag₂O-P₂O₅ which maintains a total of one mole of components at all compositions as illustrated in Fig. 5. The glass-forming extreme of the pseudo binary

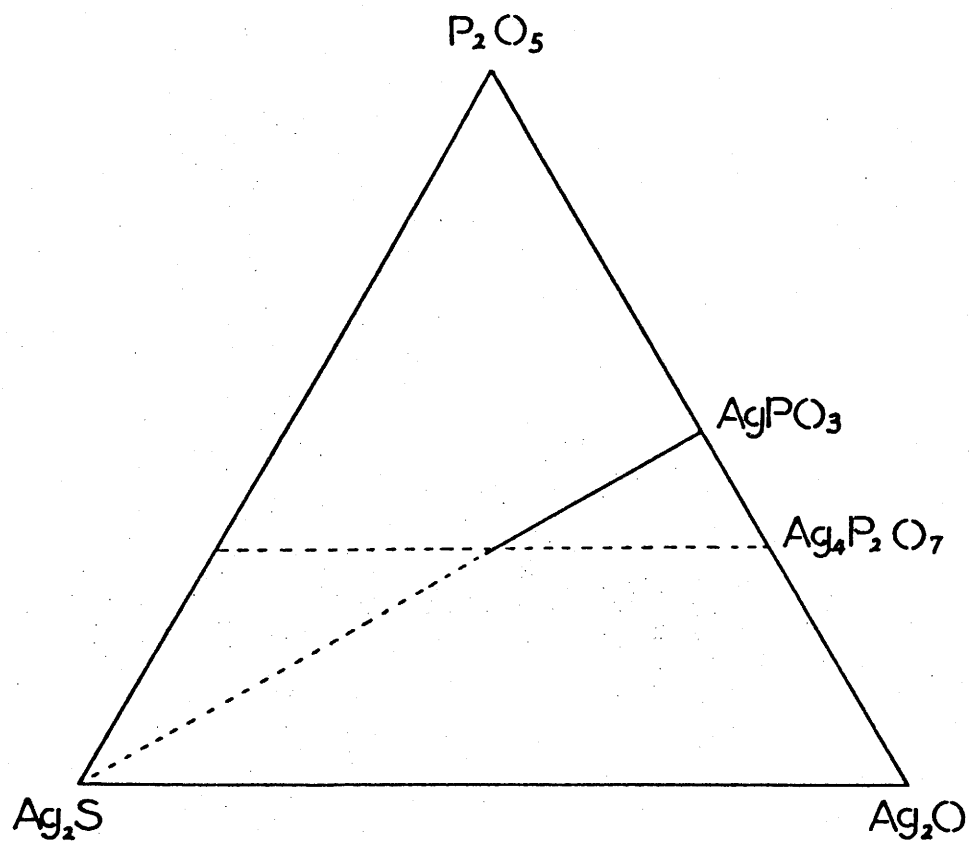


Fig.5 Location of present pseudo-binary system in the ternary system $\text{Ag}_2\text{S}-\text{Ag}_2\text{O}-\text{P}_2\text{O}_5$.

$\text{AgPO}_3\text{-Ag}_2\text{S}$ at 35 % Ag_2S is then found to fall almost on the pyrophosphate-pyrothiophosphate join of the ternary system.

The linear variation of $\log \sigma$ seen in Fig.3 then suggests that an additive relation like Equ. (1) will also apply to the system $\text{Ag}_2\text{S-Ag}_2\text{O-P}_2\text{O}_5$, with the constant a now corresponding to the conductivity of the high temperature cation-disordered $\alpha\text{-Ag}_2\text{S}$ phase. The question provoked by this observation is whether or not it is also plausible to seek an explanation in terms of microclusters of $\alpha\text{-Ag}_2\text{S}$. The following arguments from chemical reasoning, using acid-base reaction considerations, and from the interpretation of the infrared spectra of Fig.4, will suggest an answer in the negative.

The reaction between Ag_2O and P_2O_5 is of the classical Lewis acid - Lewis base type in which the oxygen bridged polymeric P_2O_5 structure is broken down by the addition of the basic species O^{2-} to give first island anions, then linear chains (sometimes rings) and finally the isolated ions pyrophosphate $\text{P}_2\text{O}_7^{4-}$, and orthophosphate PO_4^{3-} . The thermodynamics of such process have been studied in detail by Richardson and coworkers [21] for phosphates and by Willis and Hennessy [22] for the $\text{Ag}_2\text{O-B}_2\text{O}_3$ system. The mixing enthalpy minimum in the $\text{M}_2\text{O-P}_2\text{O}_5$ systems occurs at the orthophosphate stoichiometry [21]. The energy released can be viewed as a reflection of the energetic stability of the "chemical short range order", CSRO [23] induced on mixing of the components. The corresponding free energy change, expressed as an activity change, can quantitatively be related to the results of small angle neutron scattering experiments through the Bhatia-Thornton theory [24]. CSRO is the opposite of the phenomenon of "clustering" of one component in a

two [or multi] component system. Clustering can only occur when the enthalpy of mixing of that component in the others is positive [12, 13, 24]

In the present system S^{2-} is also a Lewis base though a weaker base than O^{2-} . Since, in $AgPO_3$, the acid-base process culminating in formation of PO_4^{3-} is only partly completed, it must be expected that the process of P-O-P bond breaking which leads towards the orthophosphate stoichiometry, will continue when the weaker base S^{2-} is added to the Ag metaphosphate. A continued release of energy, implying chemical ordering rather than clustering into Ag_2S -like groups, is therefore to be expected in the observed glassforming range of the present system. The acid-base process just discussed, will occur by the replacement of chain-end oxygens by sulfur, such that phosphorus-to-phosphorus links will always be via oxygens. The final stoichiometry at the end of the $AgPO_3$ - Ag_2S glass forming range, corresponds to $(O_3P-O-PO_2S)^{4-}$. That spectroscopic observations are consistent with these structural changes that may be seen from the following considerations.

The band near at 900 cm^{-1} is recognised as corresponding to the P-O-P stretching vibrations [26]. In both the 70 $AgPO_3$ -30 AgI and 70 $AgPO_3$ -30 Ag_2S glasses this band remains essentially as in $AgPO_3$, which is consistent with the idea that P-O-P linkages remain an important structural feature. The band at 1270 cm^{-1} is attributed to the P=O vibration [27]. This band is a clear feature in the spectrum of all metaphosphate chain structures in which the double-bonded oxygen has a well defined existence, but is missing from the spectrum of PO_4^{3-} in which all oxygens are equivalent. The pyrophosphate anion $P_2O_7^{4-}$ is the last state in which the double bond exists before the symmetric PO_4^{3-} is reached, and in pyrophosphate much of

1. Such positive deviations from ideal mixing are equivalently detected by an excess neutron scattering over that for a random or ideal mixture. The absence of such an excess has been noted in recent neutron scattering studies of the AgI - Ag_2O - B_2O_3 system [25]

the double bond electron density has already been redistributed to the other chain-end oxygen[28]. The diminished intensity of the 1270 cm^{-1} band in the $70\text{ AgPO}_3 \cdot 30\text{ Ag}_2\text{S}$ glass which contrasts with continued strength in the corresponding iodide glass, is therefore consistent with the drastic shortening of the phosphate chains with sulfide additions that our reaction models requires. In the species $(\text{O}_3\text{P-O-PO}_2\text{S})^{4-}$ one out of four P-O links has been replaced by a P-S link. Some diminution in intensity and frequency shift of the $\sim 1000\text{ cm}^{-1}$ band in Fig. 4(c) compared to the intensity in Fig. 4(a) and (b) would therefore be expected, as seen. A corresponding build-up in intensity at a lower frequency characteristic of P-S stretching band is not to be expected because the electronegativity difference between phosphorus and sulphur is too small to generate an important fluctuating dipole to couple to the incident IR beam.

It may be concluded that in the present pseudobinary system the solutions form with an increase in chemical short range order. Therefore the fact that the conductivity of the glasses containing a constant one mole of components extrapolates approximatively to the conductivity of the supercooled crystal form of one of the component ($\alpha\text{-Ag}_2\text{S}$) evidently tells us nothing useful about the microstructural arrangement of the ions of that component. The observations on AgI-containing systems, for which thermodynamic evidence for chemical short range ordering also exists [14], should be reconsidered in this light.

Acknowledgments

One of us (C. A. Angell) is indebted to the University of Bordeaux for financial support as Professeur Associé during some of this work. The Purdue component was supported by the U.S. department of Energy under Grant No. DE-F402-84ER45

References

- [1] T.Minami, K. Imazawa and M.Tanaka, *J. Non-Cryst. Solids.*, 42, 469 (1980).
- [2] T. Minami, H.Nambu and Masami Tanaka,*J.American Ceramic Soc.* 60,9-10, 467 (1977).
- [3] J.L. Souquet, *Solid State Ionics* 5 (1983) 77.
Ann. Rev. Mat. Sci. 11 (1981) 211.
- [4] R.J. Grant, M.D. Ingram, L.D.S. Turner and C.A. Vincent, *J. Phys. Chem.*, 82 (1978) 2838
- [5] S.W. Martin and Schiraldi *J. Phys. Chem.*, 89, (1985) 2071.
- [6] L.M. Torell and L. Borjesson, *Phys. Lett.* 107A (1985) 190.
- [7] T. Minami and M.Tanaka, *Rev. Chim. Miné.*, 16, 283 (1979).
- [8] M. Tachez, R. Mercier, J. P. Malugani and A. J. Dianoux, *Solid State Ionics*, 20, 93-98 (1986).
- [9] G.Robert, J.P.Malugani and A.Saida, *Solid State Ionics* 3/4, 311-315 (1981).
- [10] M. Tachez, J. P. Malugani, R. Mercier and P.Chieux, *Solid State Ionics* 18/19 (1986) 372.
- [11] J. P. Malugani, A. Wasniewski, M.Doreau, G. Robert and A. Al Rikabi, *Mat.Res.Bull.*,13, 427-433 (1978).
- [12] M.L. Saboungi, J.J. Marr and M. Blander, *J. Chem. Phys.* 68 (1978) 1375.
- [13] J.L. Holm and O.J. Kleppa, *Inorg. Chem.* 8 (1969) 207
- [14] C. Liu and C.A. Angell, *J. Non-Cryst. Solids* 83 (1986) 162.
- [15] M. el Kettai, J.P. Malugani, R. Mercier and M. Tachez, *Solid State Ionics* 20 (1986) 87
- [16] J. S. Kasper in "Solid electrolytes", P. Hagenmuller and W.Van Gool ed., 221, Academic Press, New York (1978).

- [17] R. Blacknick and H.A. Dreisbach, *J. Solid State Chem.* **60** (1985) 115
- [18] T. Takahashi, S. Ikada and O. Yamamoto, *J. Electrochem. Soc.*, **119** (1972) 477
- [19] M. D. Ingram, C.A. Vincent and A.R. Wandless, *J. Non-Cryst. Solids* **53** (1982) 73.
- [20] R. F. Bartholomew, *J. Non-Crystalline Solids*, **7**, 221, 1972
- [21] T.R. Meadowcraft and F.D. Richardson, *Trans. Faraday Soc.* **59** (1963) 1564; **61** (1965) 54.
- [22] X. Willis and Y. Henessy, *Trans. Faraday Soc.* **49** (1953) 1333
- [23] H. Ruppertsburg and H. Egger, *J. Chem. Phys.* **63** (1975) 4095
- [24] A.B. Bhatia and D.E. Thornton, *Phys. Rev. B* **2** (1979) 30004
- [25] L. Börjesson and L.M. Torell, private communication.
- [26] D.E. Corbridge and E.J. Lowe, *J. Chem. Soc.* (1954) 493
- [27] K. P. Muller, *Glasstechn. Ber.*, **42**, 83 (1969)
- [28] A. Mitchell, *Trans. Faraday Soc.* **62** (1966) 3470.

4.2 Conclusions du chapitre 4

Nous avons montré au paragraphe précédent que dans les verres $\text{AgPO}_3\text{-Ag}_2\text{S}$ il n'existait pas de microdomaines de type $\text{Ag}_2\text{S-}\alpha$.

Dans une publication récente relative à l'étude par diffraction de neutrons des verres de composition $(\text{AgI})_x(\text{Ag}_2\text{O}+\text{B}_2\text{O}_3)_{1-x}$, Bøjesson et al. ont mis en évidence un domaine ordonné. Ce phénomène est attribué soit à la formation de microdomaines de AgI soit à des lacunes dans le réseau bore-oxygène [1]. Une telle anomalie a été observée lors de l'étude des verres $\text{AgPO}_3\text{-AgI}$ par diffraction et diffusion des neutrons [2].

L'existence de microdomaines au sein de ce type de verre n'est donc pas prouvée. Néanmoins, il nous semble que la présence de tels microdomaines n'est pas nécessaire pour expliquer la superconductivité de ces matériaux.

Nous proposons ici une autre explication permettant d'interpréter les propriétés de transport ionique dans ce type de verres.

La haute conductivité des cristaux tels que $\text{AgI-}\alpha$, $\text{Ag}_2\text{S-}\alpha$, les solutions solides de ces deux derniers composés et RbAg_4I_5 est due pour l'essentiel à la faible coordinence de l'ion argent (2, 3 et 4). Lorsqu'on introduit de l'iodure d'argent dans le métaphosphate, l'iodure se répartirait dans l'espace inter-chaîne qui s'adapterait facilement aux ions étrangers, les chaînes étant faiblement liées entre elles (Fig. 1). Pour de faibles quantités d'iodure, on peut imaginer que les ions Ag^+ ont une faible coordinence. Elle serait par exemple constituée d'une part d'un iode et d'autre part d'un, deux ou 3 oxygène des ions phosphates (2, 3 ou 4 par exemple). On retrouve là

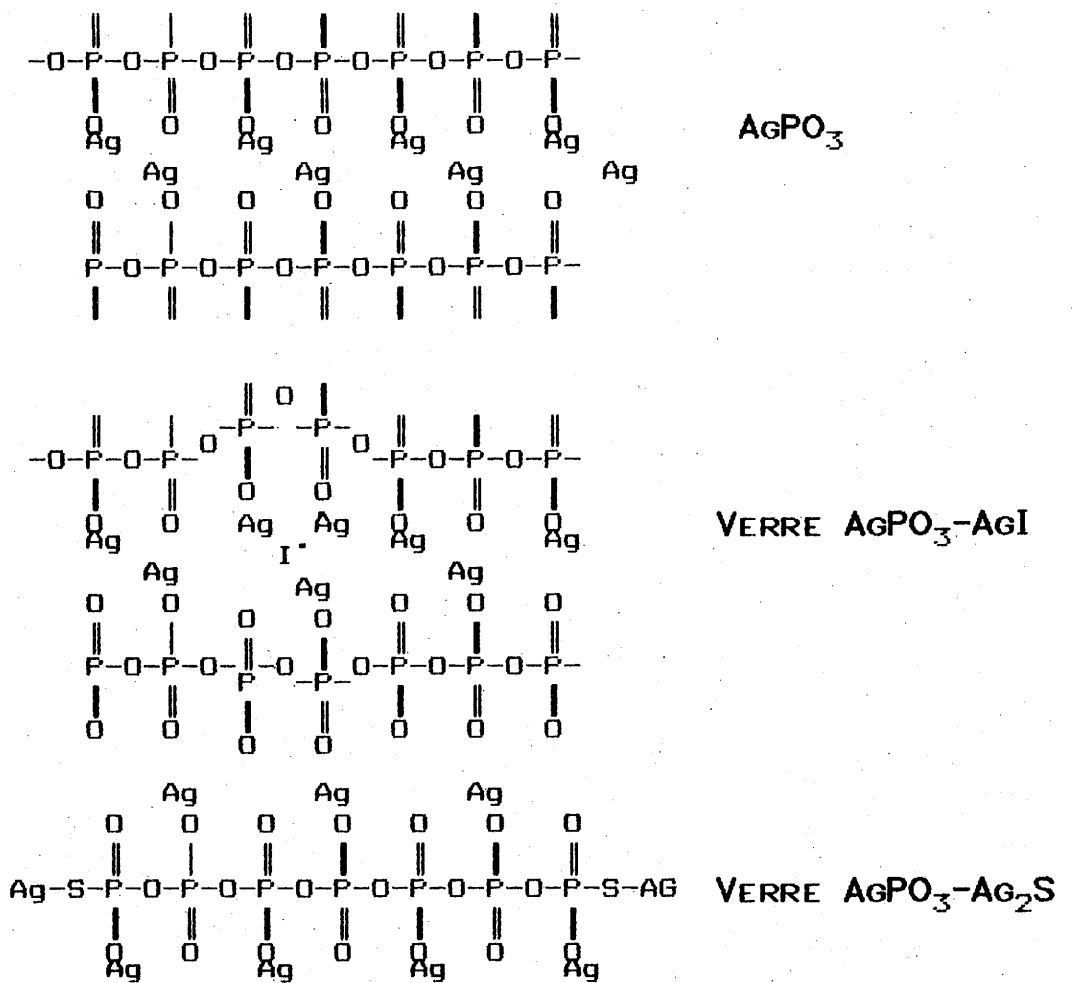


Fig. 1 Représentation schématique des réseaux de AgPO_3 , des verres $\text{AgPO}_3\text{-AgI}$ et $\text{AgPO}_3\text{-Ag}_2\text{S}$

une situation structurale analogue à celle des superconducteurs ioniques cristallisés précédemment cités.

On distingue alors deux types d'ions argent. Les premiers sont fortement liés aux chaînes phosphates (site P). Les seconds, situés au voisinage de l'iode sont plus mobiles (site I). La conductivité ionique implique que les ions argent passent d'un site de type P à un autre site de type P vacant, d'un site de type P à un site de type I vacant ou d'un site de type I à un site de type P vacant, les sauts I-I étant peu probables compte tenu de la dilution. En utilisant le modèle de Anderson-Stuart un ion argent devra vaincre une énergie E_{bp} pour un saut P-P et E_{bi} pour un saut I-P. A ces deux énergies s'ajoutent les contraintes du réseau E_{sp} et E_{si} . E_{bi} sera du même ordre de grandeur que l'énergie correspondante dans $AgI-\alpha$ puisque l'argent est essentiellement lié à l'iode. E_{si} est également voisin de l'énergie correspondante dans le cristal compte tenu de la faible coordinence signalée précédemment. L'énergie d'activation moyenne sera alors :

$$E_a = (1-x) E_{bp} + x E_{bi} + (1-x)x E_{sp} + x E_{si}$$

où x et $1-x$ sont les fractions molaires de phosphate et d'iodure d'argent. On retrouve la variation linéaire observée par Minnami [3] :

$$\Delta E_{verre} = (1-x)\Delta E_{AgPO_3} + x \Delta E_{AgI}$$

Le même type de raisonnement peut être appliqué dans le cas des verres obtenus entre le phosphate et le sulfure d'argent bien que les structures des verres soit très différentes (Fig.1). Cependant les ions argent terminaux seront liés au soufre et en faible coordinence comme dans la variété haute température du

sulfure. Les ions liés aux oxygène des chaînes raccourcies seront dans une situation énergétique et stérique voisine de celle rencontrée dans le métaphosphate du moins pour des valeurs de x faibles. Il n'est donc pas étonnant de retrouver la variation linéaire :

$$\Delta E_{\text{verre}} = (1-x)\Delta E_{\text{AgPO}_3} + x \Delta E_{\text{Ag}_2\text{S}}$$

Référence

- [1] L. Börjesson, L.M. Torell, U. Dahlborg and W.S. Howells, Phys. Rev. B, 39, 5, 3404 (1989).
- [2] R. Mercier, communication personnelle.
- [3] T.Minami, K. Imazawa and M.Tanaka, J. Non-Cryst. Solids., 42, 469 (1980).

**Chapitre 5 REMPLACEMENT DE L'ARGENT DANS LES VERRES
SULFURES ET PHOSPHATES**

Table des Matières

Chapitre 5 REMPLACEMENT DE L'ARGENT DANS LES VERRES	
SULFURES ET PHOSPHATES	82
5.1 INTRODUCTION	82
5.2 INCORPORATION ELECTROCHIMIQUE DU CUIVRE	
DANS UN VERRE CONDUCTEUR IONIQUE DE L'ION	
ARGENT	83
5.3 LE SYSTEME $TiI-AgPO_3$	90
5.4 LE SYSTEME $Ti_2S-AgPO_3$	100
5.5 CONCLUSIONS DU CHAPITRE 5	108

Chapitre 5

REMPACEMENT DE L'ARGENT DANS LES VERRES SULFURES ET PHOSPHATES

5.1 INTRODUCTION

Notre précédent travail concerne les verres obtenus avec deux types de formateurs As_2S_3 (ou Sb_2S_3) et AgPO_3 dans lesquels nous avons introduit l'iodure et le sulfure d'argent.

On pouvait penser obtenir des verres structurellement proches par réaction des mêmes formateurs avec d'autres sulfures et iodures.

Dans un premier temps, le choix de CuI et de Cu_2S s'est imposé. En effet, l'analogie des ions Cu^+ et Ag^+ est bien connue. Cependant la dismutation aisée des ions cuivreux en ions cuivriques et cuivre métallique rend la préparation des verres difficile surtout si des températures élevées sont nécessaires. Nous avons donc cherché à substituer le cuivre à l'argent par voie électrochimique.

Les ions Ag^+ et Tl^+ présentent également de grandes analogies cristallographiques. Il était tentant de substituer l'argent par cet ion, introduit soit sous forme d'iodure soit sous forme de sulfure, dans les verres à base de métaphosphate d'argent.

5.2 INCORPORATION ELECTROCHIMIQUE DU CUIVRE DANS UN VERRE CONDUCTEUR IONIQUE DE L'ION ARGENT

published in Materials letters, 6, 8/9 (1988)

ELECTROCHEMICAL INCORPORATION OF COPPER INTO A Ag^+ IONIC CONDUCTING GLASS

Liu Jun, Michel Lahaye, Josik Portier and Bernard Tanguy

Laboratoire de Chimie du Solide du CNRS, Université de Bordeaux I, 351 Cours de la Libération, 33405 Talence Cedex, France

Abstract: Silver ions in a glass with the composition $0.67 \text{AgI}-0.33 \text{Sb}_2\text{S}_3$ have been partially exchanged for copper by an electrochemical method. The concentration profile of copper has been measured as a function of the depth with an electron microprobe X-ray analyser. An ESR study has shown that only cuprous ions exist in the sample. The conductivity of the copper-silver glass has been compared with that of the initial sample.

1. Introduction

The incorporation of copper into a glass has been investigated by many authors. The most common method consists in heating the glass in copper salts. Sakka et al.[1] investigated the Cu-Ag ion-exchange of an aluminosilicate glass which contained 20 mol% Na_2O by heating the glass in a CuCl melt. Chakravorty et al [2] indicated that copper enters the glass as Cu^+ ions but is partially changed into Cu^{2+} ions in the glass. Because Cu^+ glass is difficult to obtain by melting the cuprous-containing compound at high temperature, it seems necessary to make ion-exchange at low temperature.

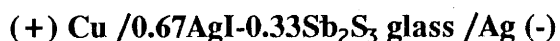
In a previous paper, Sun et al.[3] studied glasses prepared by the hyperquenching method in the system $\text{Sb}_2\text{S}_3\text{-AgI-Ag}_2\text{S}$. This type of glasses has potential applications in selective ion electrode [4] or ISFET devices. It is possible to prepare such glasses containing Cd^{2+} , Hg^{2+} , Pb^{2+} and Tl^+ ions. However, attempts to prepare the corresponding Cu^+ glasses failed because of the

dismutation of CuI at high temperature into Cu metal and Cu^{2+} . Consequently, we chose to substitute silver with copper by a low-temperature electrochemical method.

2. Experimental

A glass of composition 0.67 AgI-0.33 Sb_2S_3 has been prepared. The starting materials were silver iodide (purity 99%; ALDRICH Co.) and Sb_2S_3 (purity 99%; VENTRON Co.). The mixture of AgI and Sb_2S_3 was well homogenized and pressed into pellet and then heated at about 700°C in a silica tube under premier vacuum and the melt was quenched in water. The amorphous character of the sample was controlled by X-ray diffraction.

The Cu+ exchange experiment was performed using the following electrolysis cell:



A stainless-steel holder was used to make a good contact between the Ag and Cu electrodes and metal leads. The current was provided by a potentiostat instrument (PRT 20-2, SOLEA Co.).

The voltage was set at about 1 V in agreement with the electrochemical stability of the glass [3]. Because of the weak density of current, the experiment was performed during 500h.

The concentration profiles of Cu in the glass were measured with a Cameca electron microprobe X-ray analyser. The accelerating voltage was 25KV. The specimen was coated with carbon to eliminate electrical charges. The observed current was set to only 6nA to avoid sample damage. The electron beam was scanning a square of $25\mu\text{m}^2$ across the ion-exchanged sample. 200 points were measured along the sample thickness ($1000\mu\text{m}$).

It should be noted that the Cu concentration estimated by this method is the total amount of copper element incorporated into the glass and no information is available for determining whether Cu is present as Cu^+ ion or Cu^{2+} ion.

The conductivity measurements were done by the complex impedance method using a Solartron 1170 frequency response analyser. The pellets of the glass were cylindrical, with 8mm diameter and 1mm thickness. Gold electrodes were deposited by vacuum evaporation on both sides. The frequency range was from 0.1 Hz to 100KHz. The temperature was kept constant at 25°C.

ESR spectra were recorded at room temperature on a Bruker ER 200tt spectrometer (X-band) with KHz modulation.

3. Results

3.1 Distribution of Cu and Ag in the glass

Fig 1 and Fig 2 show the respective concentration profiles of Ag and Cu in the glass after ion-exchange by electrolysis. The sawtooth shape of the curves arises from the texture of the sample, which is a pellet made of glass powder. The concentration of Ag seems unchanged. The atomic percentage of Cu decreases from the Cu electrode to the Ag one. The reason is that the migration of cuprous ions is very slow at room temperature.

3.2 ESR analysis

No ESR signal is observed for the g values corresponding to Cu^{2+} ($3d^9$). This result demonstrates that only cuprous ions ($3d^{10}$) are present in the glass.

3.3 Conductivity measurements

Electrical ionic transport measurements indicate the conductivity of the sample containing Cu^+ ions is lower than the starting glass. The comparison is reported in table 1.

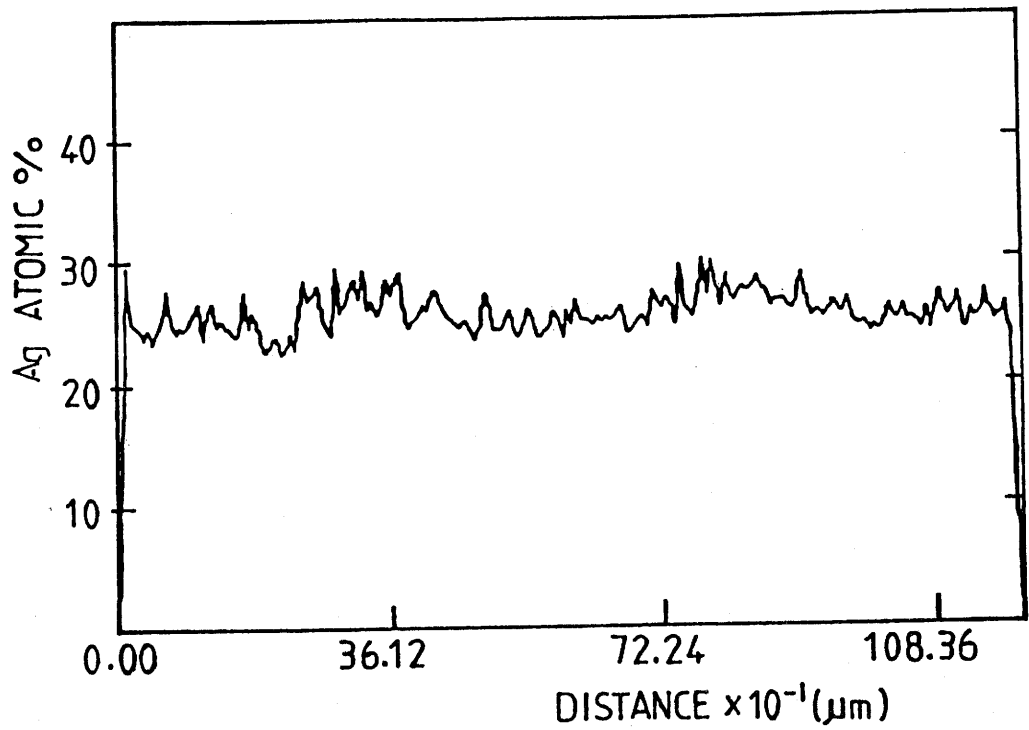


Fig.1 The concentration profile of silver as a function of depth obtained with electron microprobe X-ray analysis.

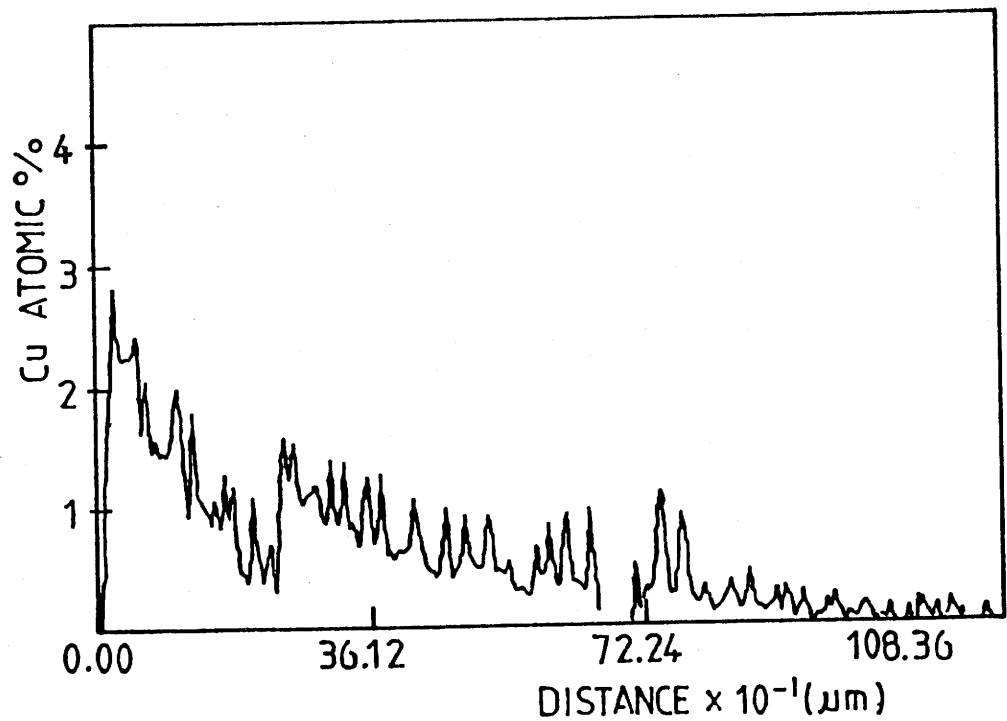


Fig.2 The concentration profile of copper as a function of depth obtained with electron microprobe X-rays analysis.

Table 1 Conductivity of the 0.67AgI-0.33Sb₂S₃ glass at 25°C

before ion-exchange	after incorporation of Cu
$1.10 \times 10^{-3} \text{ } (\Omega^{-1}\text{cm}^{-1})$ [3]	$6.38 \times 10^{-4} \text{ } (\Omega^{-1}\text{cm}^{-1})$

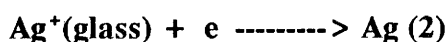
4. Discussion

Fig.2 shows a stepwise profile of the copper concentration which decreases as the distance from the copper electrode increases. A zero concentration is observed near the silver electrode. This stepwise concentration profile is known to occur when the ion exchange is carried out under an applied electric field [4,5]. As shown by ESR experiment, the concentration of Cu^{2+} ions in the sample is negligible and the following process is assumed for the Cu-Ag ion-exchange reaction :

at the copper electrode,



and at the silver electrode,



By integrating the curve in Fig.1 and Fig.2, the average silver and copper atomic percentages were calculated as 25.28% and 0.65% . From the left part of Fig 1 , where the concentration of copper is near zero, the silver content in the starting material can be estimated at about 26 atom%. This means a loss of silver in the glass of about 0.72 atom% which is very close to the value of the copper atom percentage in the glass and demonstrates that one silver atom is replaced by one copper atom.

The conductivity of cuprous ionic conducting materials is usually significantly lower than that of corresponding silver compounds. For example, the ratio $\sigma_{\text{Cu}}/\sigma_{\text{Ag}}$ in CuI and AgI is about 10^{-4} . It is reasonable to expect the same difference of the mobility in glass system. However, it should be noted that in the present study copper ions replace only about 2.5% of silver ions. This is

the reason why the conductivity of the sample after ionic exchange is almost unchanged.

5. Conclusion

We have shown the possibility of partial replacement of Ag^+ by Cu^+ using an electrochemical method. This process that is unusual in glassy systems can be performed in the case of chalcogenide glasses thank to their high ionic conductivity.

Acknowledgement The authors would like to thank Dr. J.M. Dance for the ESR experiment, Mrs. N. Charlassier for electrical measurements, Dr. F. Menil and Dr. J.M. Reau for the helpful discussion.

References

- [1] S. Sakka, K. Kamiya and K. Kato, *J. Non-Crystalline Solids* 52(1982) 77.
- [2] D. Chakrovorty, A. Shuttleworth and P.H. Gaskell, *J. Mater. Sci.* 10 (1975) 799.
- [3] H.W. Sun, B. Tanguy, J.M. Reau, J.J. Videau, J. Portier and P. Hagenmuller, *J. Solid State Chem.* 70 (1987) 141.
- [4] N. Tohge and M. Tanaka, *J. Non-Cryst. Solids* 80(1986) 550.
- [5] R.F. Bartholomew and H.M. Garfinkel, in: *Glass: Science and Technology* vol.5, eds., D.R. Uhlmann and N.J. Kreidl (Academic Press, New York, 1980).
- [6] H. Ohta, *J. Non-Cryst. Solids* 24(1977) 61.

5.3 LE SYSTEME TII-AgPO₃

LETTER TO "MATERIAL SCIENCE and ENGINEERING"

Structure and properties of new glasses in the system TII - AgPO₃

LIU JUN, B. TANGUY, J. J. VIDEAU, J. PORTIER

Laboratoire de Chimie du Solide, 351 cours de la Libération, Talence, France
and C.A. ANGELL

Department of Chemistry, Purdue University, West Lafayette, IN 47907, USA

ABSTRACT

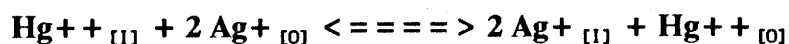
New glasses have been prepared in the x TII - $(1-x)$ AgPO₃ system. Conductivity measurements and structural studies by infrared spectroscopy show results comparable with those for x AgI- $(1-x)$ AgPO₃ glasses. Ag⁺ ions surrounded by halide ions are mobile and provide the main contribution to the ionic conductivity in the glasses.

1. INTRODUCTION

Glasses with general formula x MX_{*n*} - $(1-x)$ AgPO₃ ($M = \text{Ag, Na, K, Pb, Hg, Cd}$; $X = \text{Cl, Br, I}$) have been recently investigated [1-4]. Both M cations and X halides influence the silver conduction in the glasses. In the case of $M = \text{Ag}$ and $X = \text{I}$, Malugani et al. [1] concluded that the high silver ion conductivity is due to the formation of microscopic "AgI clusters" dispersed within the vitreous network provided by the $(\text{PO}_3)_n^{n-}$ chains. The structure of the "clusters" would mimic the α -AgI high temperature superionic conducting phase. This interpretation has recently been contested on the basis of thermodynamic [6] and crystallographic arguments [7].

Glasses in which $M = \text{Na, K, Cd or Pb}$, possess high conductivities comparable to that observed for AgPO₃ - AgI glasses [2,4]. The authors conclude that this is made possible by an exchange between Ag⁺ and M cations which again generates

the silver halide clusters which are the seat of the high conductivity by previous hypothesis. This interpretation is in agreement with the theory of hard and soft acids and bases [9]. According to Pearson [9] a hard acid will coordinate preferentially with the hardest base available, while the soft acid Ag^+ and soft base I^- would form AgI rather than MI_n in the cases of $\text{M} = \text{Na}, \text{K}$, (and also of the Pb cation which is an intermediate acid). For Hg^{++} (soft acid), the conductivity should depend on the extent of the exchange equilibrium :



where the subscript I indicates an iodide environment and O an oxygen environment .

In the present paper we explore the extent to which this interesting phenomenology can arise when the counter cation is also a soft acid, in our case Tl^+ . Thus we report conductivity measurements and IR spectra in $x \text{TlI} - (1-x) \text{AgPO}_3$ glasses.

2. EXPERIMENTAL

TlI (Ultrapure, Ventron GMBH) and AgPO_3 prepared by a wet method from AgNO_3 and NaPO_3 as described elsewhere [3] have been used for the preparation of glasses. About 2g batches were melted in an evacuated sealed silica glass ampoule at 700°C for 10 hrs. The melted mixture was then quenched to room temperature by immersion in water. Complete vitrification was confirmed by X-ray diffraction.

The glass transition temperatures T_g were measured by differential scanning calorimetry (Setaram DSC 92) using a heating rate of $10^\circ\text{C}/\text{min}$. The electrical conductivities were obtained by complex impedance analysis using a Solartron

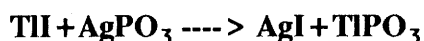
1170 frequency response analyser in the range of 10KHz to 500mHz. The samples were disks of bulk glasses (cylinder 8mm diameter, 1-2mm thickness) on both sides of which gold electrodes were deposited by evaporation. All measurements were carried out under an argon atmosphere between 20°C and a high temperature limit set by T_g.

Infrared absorption spectra in the range 200-2000cm⁻¹ have been obtained using a double beam PERKIN ELMER 983 Spectrometer and disc pellets of thickness 1mm and diameter 13 mm obtained by pressing a ground mixture of 1 part glass with 60 parts KBr at 200Kg/cm².

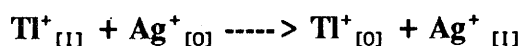
3.RESULTS AND DISCUSSION

The vitreous domain is observed in the range of x=0 to x=0.35 in the xTII-(1-x)AgPO₃ pseudo binary system. The glasses are transparent and yellowish colored.

The glass transition temperature T_g decreases with increasing TII concentration (Fig.1). As observed by Malugani et al. for PbX₂ (X=I,Br,Cl)-AgPO₃ [1] glasses, T_g decreases more sharply than in the case of AgI based glasses. It is interesting to note that, at the limit of the vitreous domain, the formation of crystalline AgI is observed from the X-ray diffraction pattern. This observation shows that the combination TII+AgPO₃ is not the stable join in the quaternary system TII+AgI+TIPO₃+AgPO₃ and that the metathetical reaction



occurs in this system. This usually would imply that, in the melt, the exchange process :



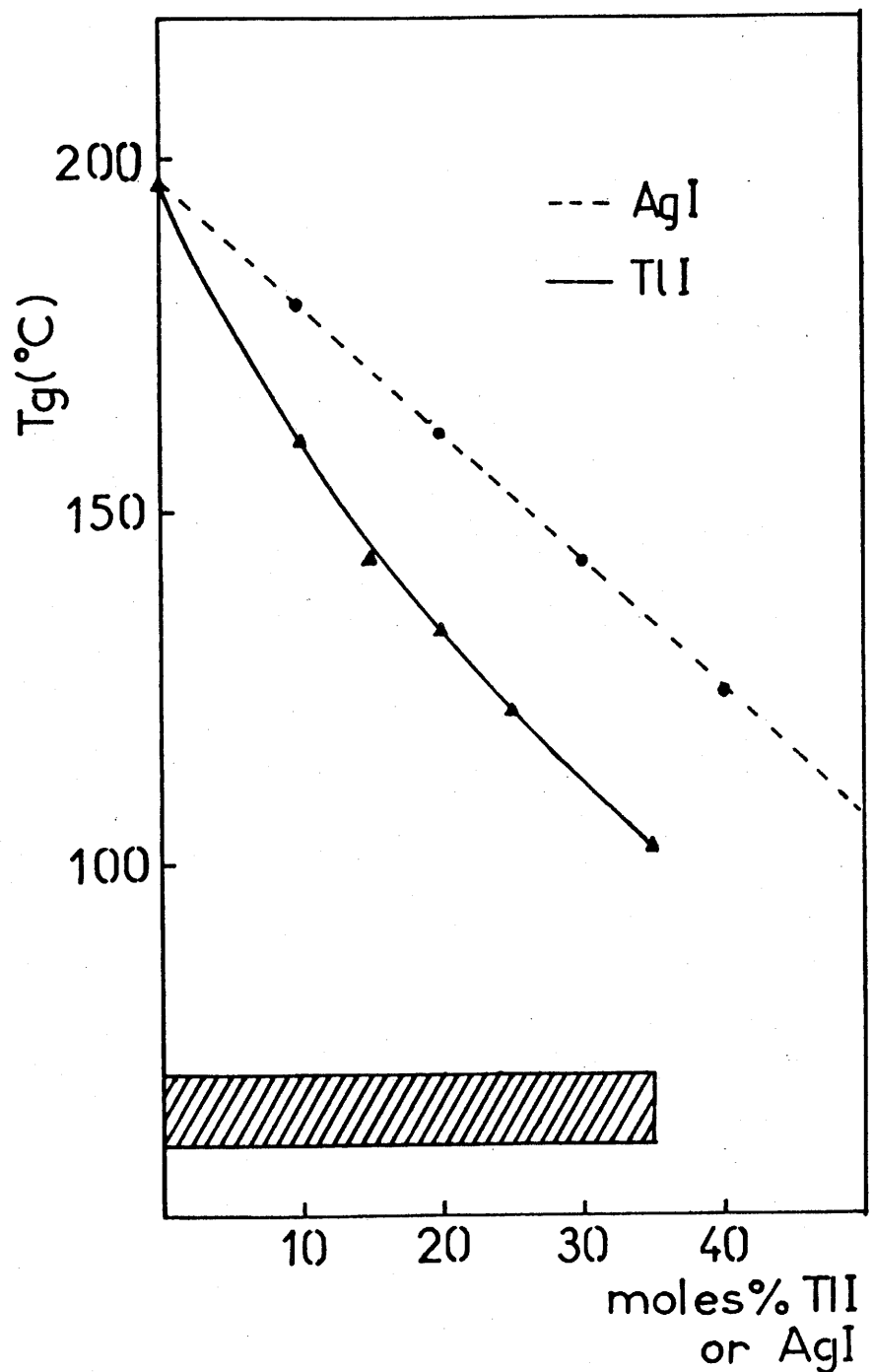


Fig.1 Vitreous domain (hatched area) and variation of T_g with iodide concentration in x TlI-(1-x)AgPO₃ (solid line) and x AgI-(1-x)AgPO₃ (dotted line).

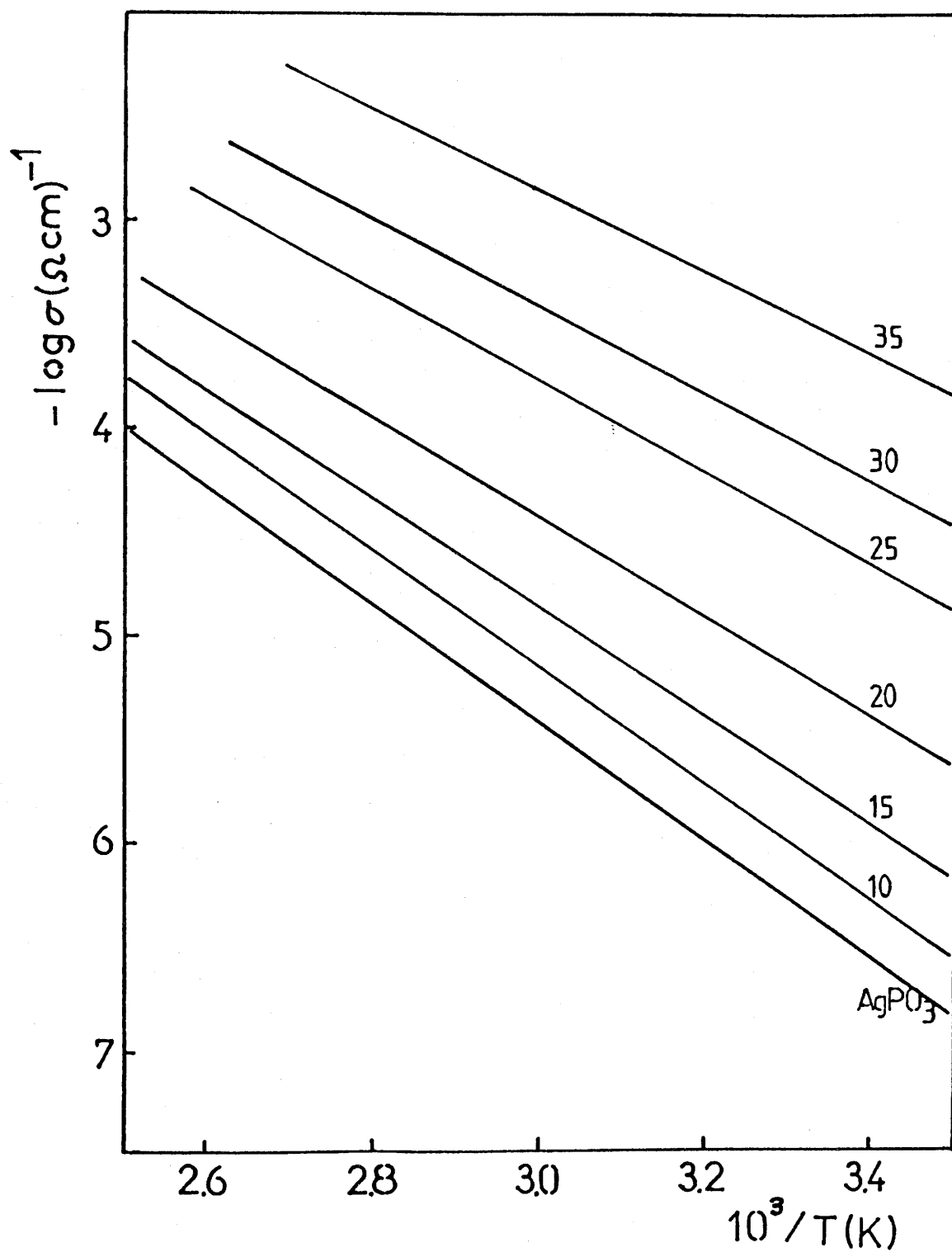


Fig.2 Arrhenius plots of conductivities of TII-AgPO₃ glasses (composition in mole % TII).

is energetically favored. This fact implies that Ag^+ is a softer acid than Tl^+ , and therefore suggest that the conductivity will mimic that of the metathetical systems studied earlier[1].

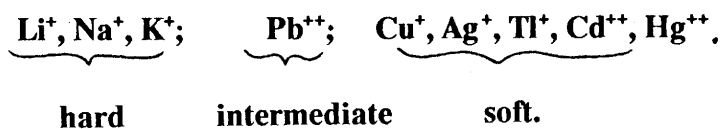
In the glass-forming domain, the total conductivity obeys Arrhenius law $\sigma = \sigma_0 \exp^{-E\sigma/kT}$ in the temperature range 20°C to T_g (Fig.2). The conductivity at room temperature (Fig.3) and activation energy (Fig.4) are strongly dependent on the composition. The values of σ_{25} and E are very close to those of the corresponding AgI containing glasses [1]. As anticipated above, this fact implies that the ionic conductivity is mainly due to the Ag^+ ions, moving in a predominantly I- environment.

Consistent with this observation and with the visible transparency, the ion-or - electron transport number measured by the emf method is unity within experimental error.

The IR spectra of the $x \text{TlI} - (1-x)\text{AgPO}_3$ glasses are very similar to those of $x \text{AgI} - (1-x)\text{AgPO}_3$ glasses (Fig.5) of the same composition showing that neither cation strongly perturbs the polymer anion structure in the glasses.

4.CONCLUSION

The following Lewis acid series has been proposed by Pearson [9] on the basis of solution observations :



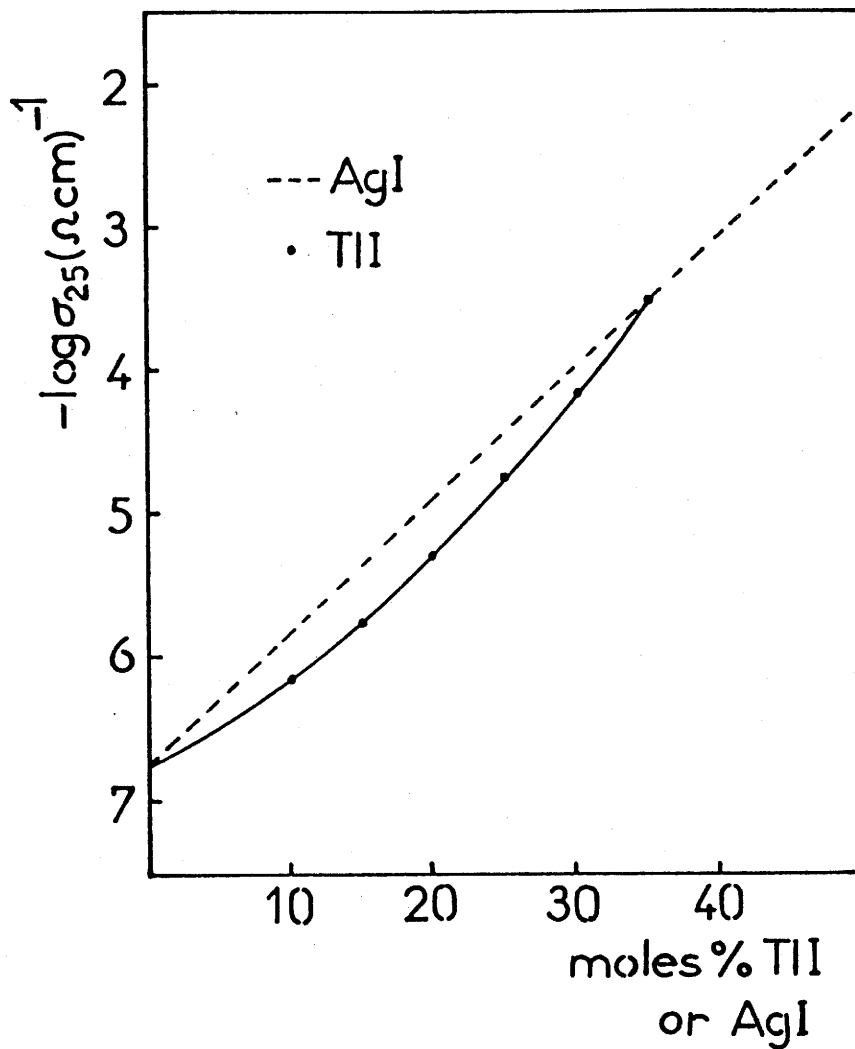


Fig.3 Variation of the logarithm of the conductivities with % TlI of TlI-AgPO₃ glasses (solid line) compared with corresponding behavior of AgI-AgPO₃ glasses.

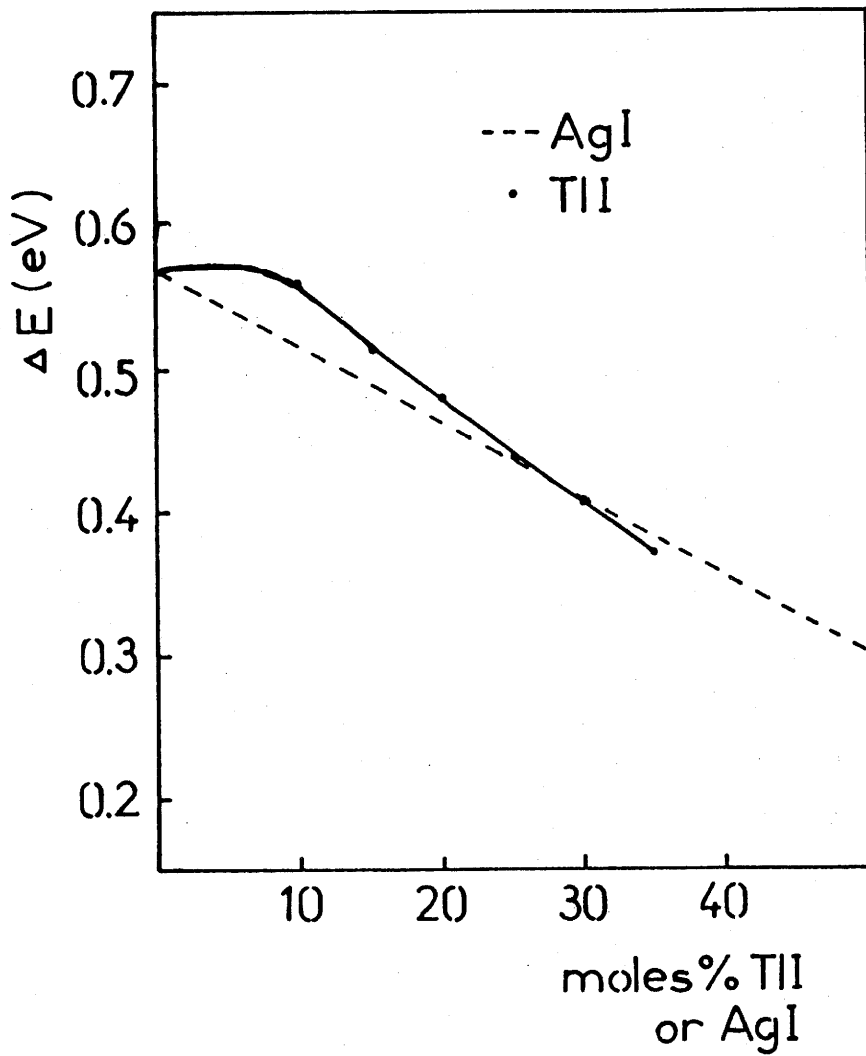


Fig.4 Variation of the activation energy for TII-AgPO₃ glasses versus % TII, compared with that for AgI-AgPO₃ glasses.

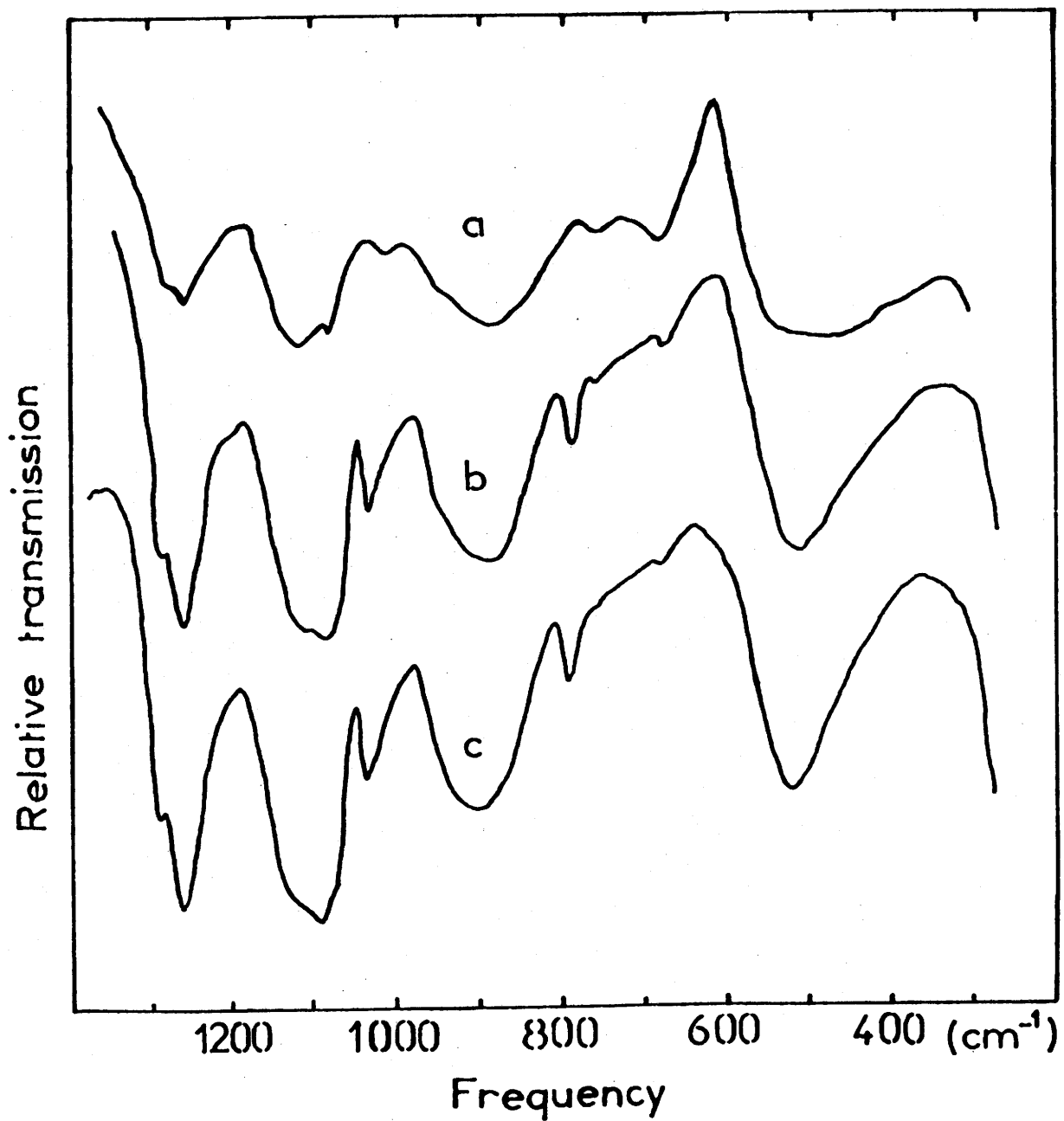
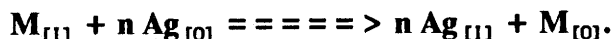
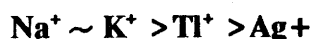


Fig.5 Infrared spectra of the glasses a) AgPO₃, b) 0.3 AgI-0.7 AgPO₃, c) 0.3 TlI-0.7 AgPO₃.

This ordering is in general agreement with the exchange of Ag^+ and M^{n+} in the systems $x\text{MI}_n - (1-x)\text{AgPO}_3$, implied by the conductivity result for the ionic liquids, according to the processes :



From conductivities of the corresponding phosphate glasses, it is possible to deduce the following hardness sequences :



for monovalent ions and



for divalent cations. Note that when Cd^{++} is considered as a soft acid in Pearson's classification, it behaves like Pb^+ (intermediate acid) in the phosphate glasses.

REFERENCES

- [1] J.P.Malugani, R.Mercier and M.Tachez, *Solid State Ionics* 21(1986) 131.
- [2] J.P.Malugani, A.Wasniewski, M.Doreau, G.Robert and R.Mercier, *Mat.Res.Bull.*, vol.13 (1978) 1009.
- [3] J.P.Malugani, A.Wasniewski, M.Doreau, G.Robert and A.Al Rikabi, *Mat.Res.Bull.*, vol.13, (1978) 427.
- [4] M.Doreau, J.P.Malugani and G.Robert, *Electrochimica Acta*, Vol.26, No.6, 711 (1981).
- [5] T. Minami, *J.Non-Cryst. Solids*, 56 (1983) 15.
- [6] C.A.Angell, "Phenomenology of fast ion conducting glasses : facts and confusions" in "Solid Electrolytes" ed. Takahashi.
- [7] A. Musimi, G. Piccaluga and G. Pinna, *J. Chem. Phys.* 89, (1988) 1074
- [8] J.C.Reggiani, J.P.Malugani and J.Bernard, *J.Chim.Phys.*, 75 (1978) 846.
- [9] R.G.Pearson, *J.American Chem.Soc.* vol.85 (1963) 3533.

5.4 LE SYSTEME $Tl_2S-AgPO_3$

GLASS FORMATION, STRUCTURE, CONDUCTIVITY IN THE $Tl_2S-AgPO_3$ SYSTEM. COMPARISON WITH $Ag_2S-AgPO_3$ AND $TlI-AgPO_3$ GLASSY SYSTEMS

Materials Science and Engineering (to be published)

Liu Jun, J. Portier, B. Tanguy, J.J. Videau and P. Hagenmuller

Laboratoire de Chimie du Solide du C. N. R. S.
Université de Bordeaux I
351, cours de la Libération, 33405 Talence Cédex, France

ABSTRACT

New glasses have been prepared in the $Tl_2S-AgPO_3$ system. Conductivity measurement and structural studies by infrared spectroscopy have been made. As observed in the $Ag_2S-AgPO_3$ glasses, the introduction of thallium sulfide leads to a shortening of the $(PO_4)_n$ chains. The silver ionic conductivity decreases with increasing Tl_2S mole fraction when it increases in the case of Ag_2S or TlI based glasses.

Introduction

Glasses based on $AgPO_3$ have been widely investigated. Vitreous solution with halides (AgI , NaI , KI , TlI , PbI_2 , CdI_2 , HgI_2) and sulfide (Ag_2S) have been studied [1-4]. In the case of AgI based glasses, it has been widely suggested that two types of silver ions exist. The first one is bonded to $(PO_4)_n$ chains like in silver metaphosphate when the second type form microregions possessing the $\alpha-AgI$ structure and leading to the high conductivity [1,2]. This explanation has been controversially discussed on the base of an x-ray diffraction analysis [9]. In the case of other halides except HgI_2 , the same behaviour is observed due to an exchange between silver primarily connected to the phosphate chains and the other cation according to the hardness of the Lewis acids [4].

In the case of $\text{Ag}_2\text{S-AgPO}_3$ glasses, silver sulfide dissolves by an acid-base chemical ordering process to give shorter phosphate chain structures which approach the pyrophosphate stoichiometry at the glassforming limit[3].

It was interesting to extend these previous studies to thallium sulfide. In this case, perhaps, the shortening of phosphate chains and the exchange between silver-thallium could occur in the same time.

Experimental

The starting materials were Tl_2S (purity 99.9%, Ventron GMBH) and AgPO_3 which was prepared from AgNO_3 and NaPO_3 by a wet method as described elsewhere [5]. About two grams batches were melted in evacuated, sealed silica glass ampoules, at 700°C during 24h, followed by quenching in water. The glassy state was confirmed by X-ray diffraction. The color of the glasses varies from green yellow to brown as the Tl_2S content increases.

The glass transition temperatures were determined by differential scanning calorimetry, using a Setaram Model DSC92 instrument.

The conductivity measurements have been performed by complex impedance method using a Solartron 1170 frequency response analyzer. The pellets were cylindrical (8mm diameter, 1-2mm thickness). On both sides gold electrodes were deposited by evaporation. The measurements were carried out under an argon atmosphere in the frequency range 10^{-2} - 10^4 Hz and temperature range 20°C - T_g .

Infrared absorption spectra in the range 200 - 1400cm^{-1} were obtained using a double beam Perkin Elmer 983 Spectrometer and KBr pellet samples. Pellets of thickness 1mm and diameter 13mm were obtained by pressing a ground mixture of 1 part glass and 60 parts KBr at 200kg/cm^2 .

Results and discussion

In the $x \text{ Tl}_2\text{S}-(1-x) \text{ AgPO}_3$ binary system, the glassforming domain is observed in the range of $x=0$ to $x=0.20$ (Fig. 1). Fig.1 also shows the glass transition temperatures T_g variation. It decreases as Tl_2S content increases as observed for TII based glasses. This behaviour is probably due to the low fusion temperatures of thallium sulfide and iodide.

Fig. 2 and Fig.3 give the results of electrical measurements. The conductivity decreases and the activation energy increases as the content of Tl_2S increases.

Infrared spectra of AgPO_3 (a) , $0.8\text{AgPO}_3 \cdot 0.2 \text{ Tl}_2\text{S}$ (b) and $0.2\text{Ag}_2\text{S} \cdot 0.8\text{AgPO}_3$ (c) glasses are shown on the figure 4. The attributions of the vibrations has been done following R.F. Bartholomew [7].

The glass containing thallium sulfide has a different spectrum of that of AgPO_3 itself showing that the $(\text{PO}_4)_n$ infinite chains are changed by introducing thallium sulfide. In particular the band corresponding to the $\text{P}=\text{O}$ vibrations decreased strongly. It could be interpreted by the partial replacement of oxygen by sulphur and by a shortening of the $(\text{PO}_4)_n$ chains. In addition the band located at 880 cm^{-1} (P-O-P vibrations) is shifted towards high frequencies. It is well-known that this behaviour is also connected to the depolymerisation of the phosphate chain leading to an increase of the covalency of the P-O-P bonds. A new band appears at 620 cm^{-1} ; it could be assigned to the P-S at the extremity of the short chains [8].

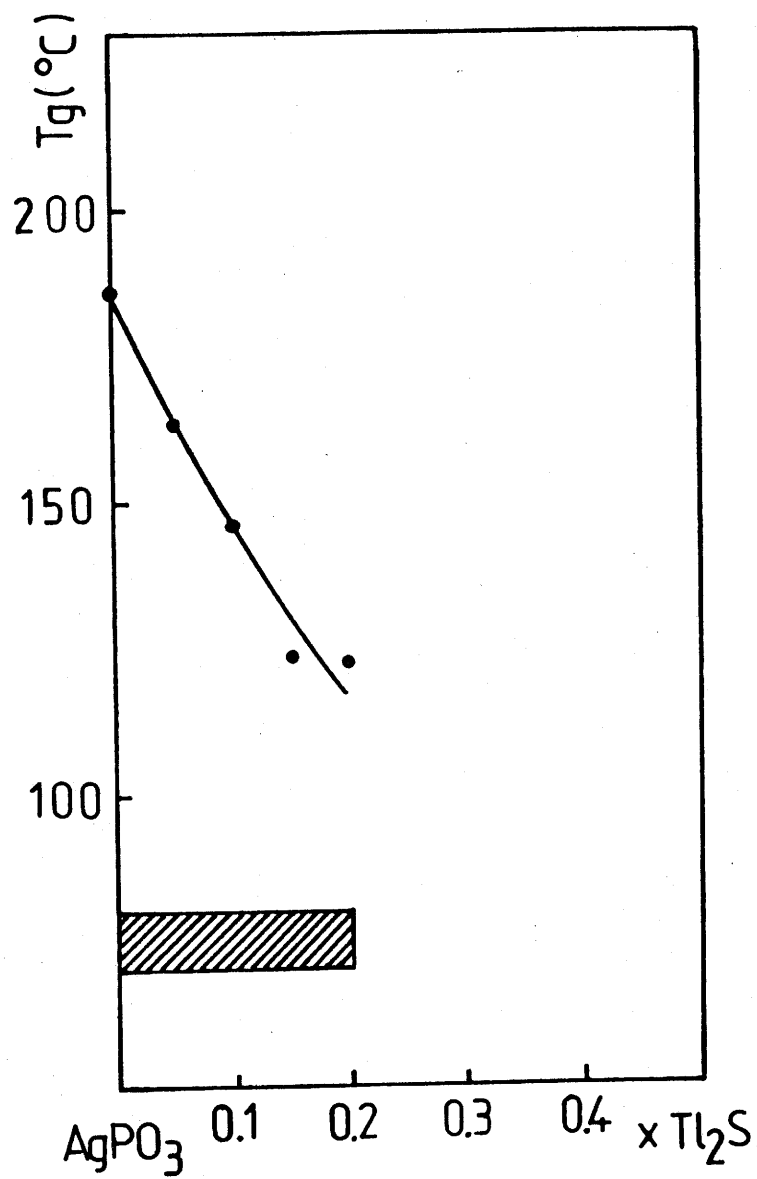


Fig.1: Vitreous domain (hatched area) and variation of T_g (solid line) with Tl_2S concentration in $x Tl_2S-(1-x)AgPO_3$ system.

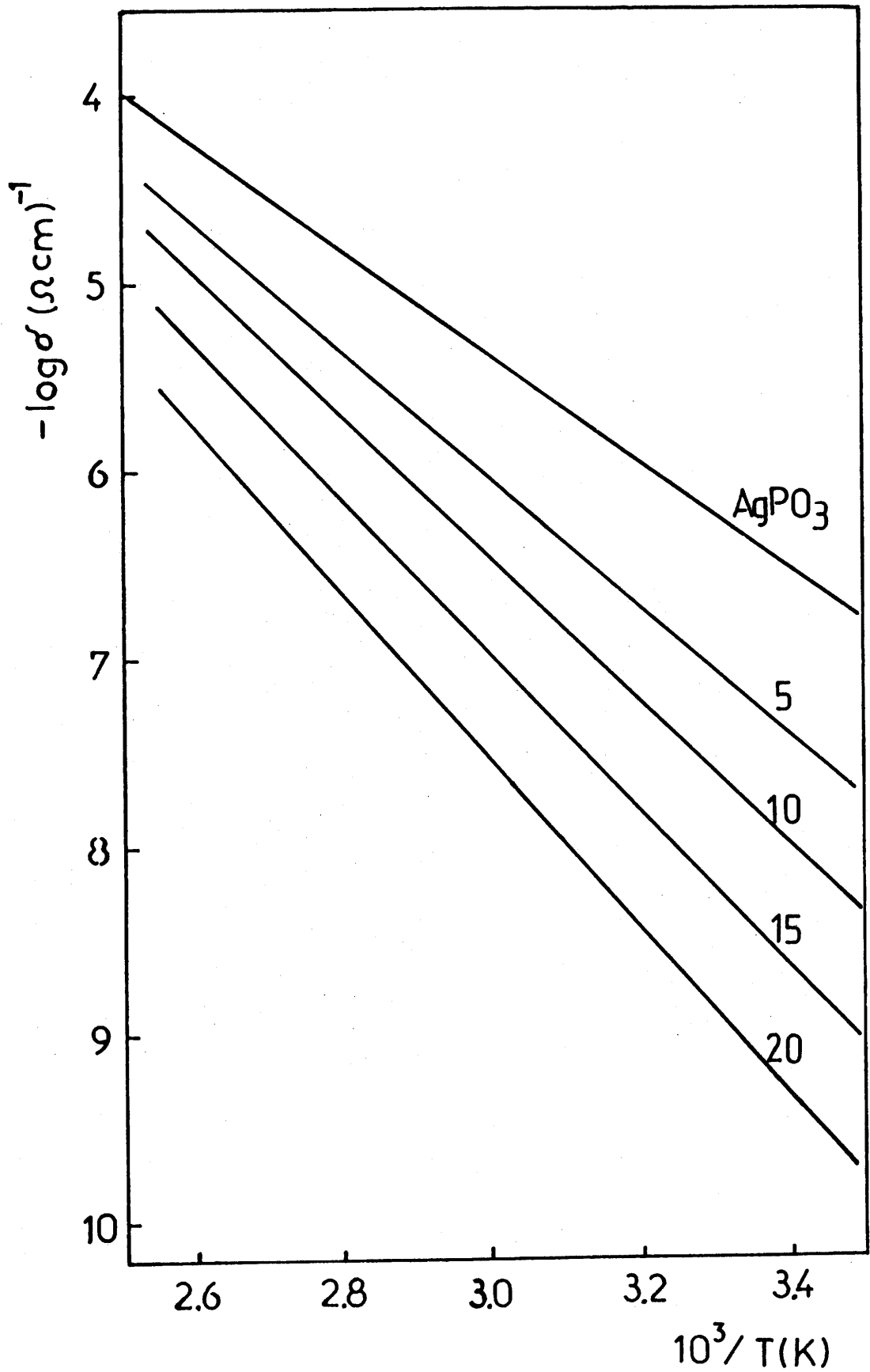


Fig.2: Arrhenius plots of conductivities of Tl₂S-AgPO₃ glasses (composition in mole % Tl₂S).

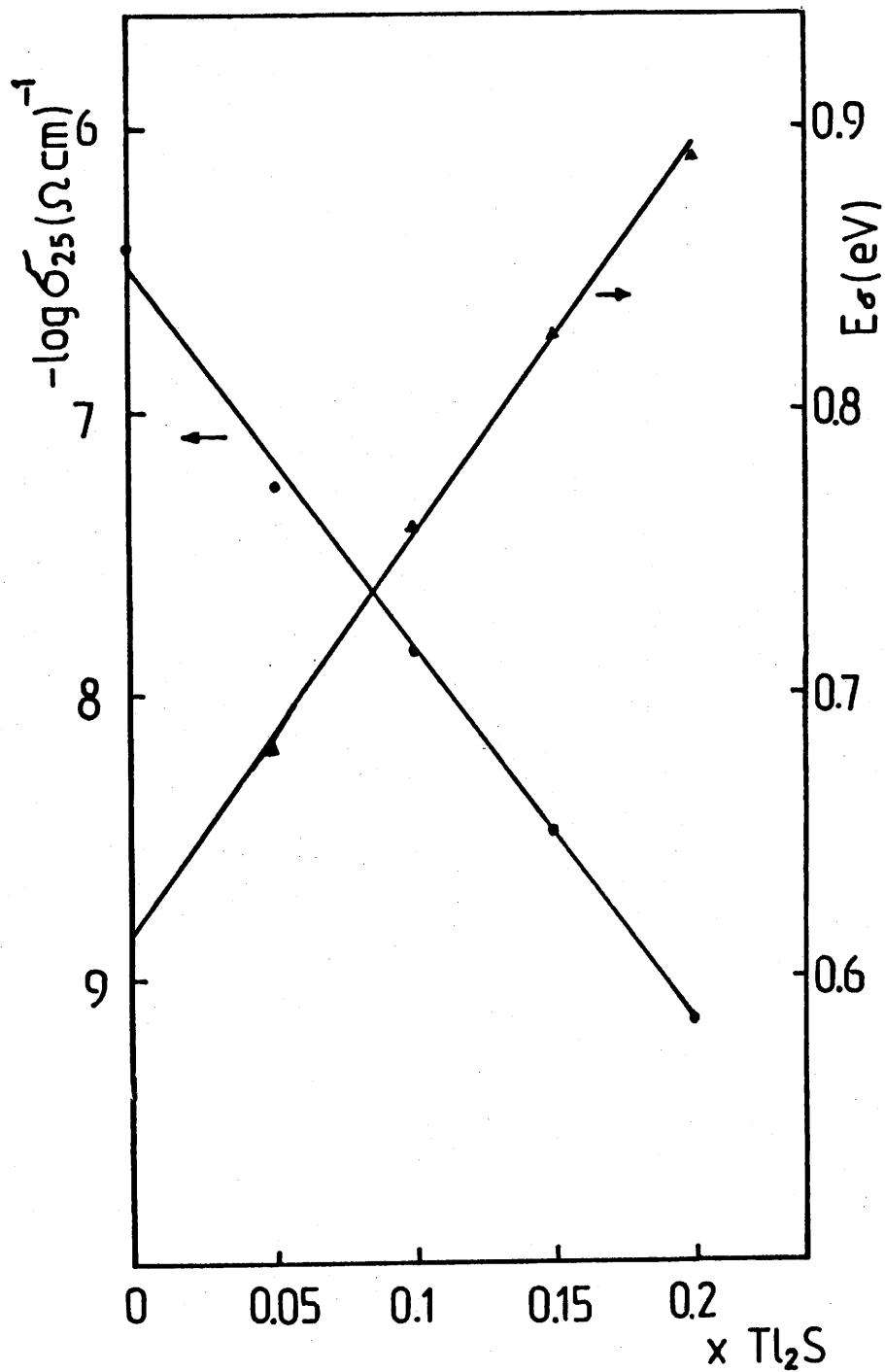


Fig.3: Variation of the logarithm of the conductivities at 25°C and the activation energy for Tl₂S-AgPO₃ glasses versus % Tl₂S

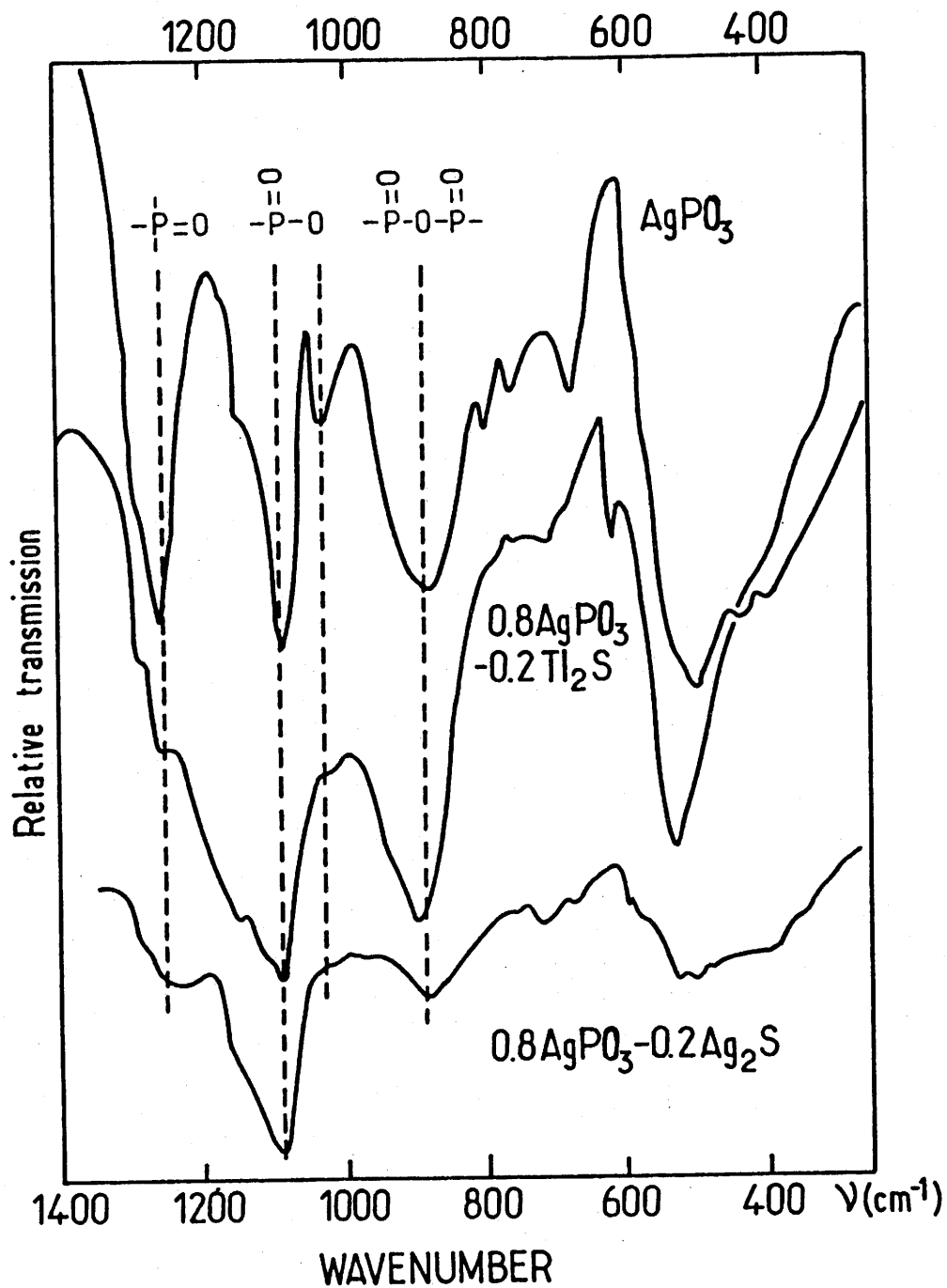


Fig.4: Infrared spectra of the glasses a) AgPO_3 ,
 b) $0.2\text{Tl}_2\text{S} - 0.8\text{AgPO}_3$, c) $0.2\text{Ag}_2\text{S} - 0.8\text{AgPO}_3$.

Conclusion

In the case of glasses formed in the TlI-AgPO₃ system, we observed that the ionic conductivity increases with the thallium concentration. It is very close to that of AgI corresponding glasses [5]. This behaviour support the formation of AgI from exchange reaction between Tl⁺ and Ag⁺ iodide inserting in between the PO₄ infinite chains. On the contrary, in the case of Tl₂S-AgPO₃ glasses, the ionic conductivity decreases with the thallium concentration. This difference is due to a different structure. The introduction of sulfide leads to a shortening of phosphate chains. Silver and thallium ions are bonded to -O⁻ or -S⁻ belonging to these chains. The diminution of conductivity is then due to the lowering of silver ions concentration and to the weak mobility of Tl⁺ ions.

References

- [1] J.P.Malugani, A.Wasniewski, M.Doreau, G.Robert and R.Mercier, *Mat. Res. Bull.*, Vol.13 (1978) 1009.
- [2] J.P.Malugani, R.Mercier and M.Tachez, *Solid State Ionics*, 21(1986)131.
- [3] Liu Jun, J.Portier, B.Tanguy, J.J.Videau and C.A.Angell *Solid State Ionics* (1989) (in press).
- [4] Liu Jun, B.Tanguy, J.J.Videau, J.Portier and C.A.Angell (to be submitted).
- [5] J.P.Malugani, A.Wasniewski, M.Doreau, G.Robert and A.Al Rikabi, *Mat. Res. Bull.*, Vol.13, (1978) 427.
- [6] R.G. Pearson, *J. Am. Chem. Soc.*, 85, 3533 (1963).
- [7] R. F. Bartholomew, *J.Non-Crystalline Solids*, 7, 221, 1972.
- [8] G. Tridot et P. Tribodet, *L'industrie Chimique* 369 (1965).
- [9] A. Musini, G. Piccaluga and G. Pinna, *J. Non-Cryst. Solids*, 106 (1988) 70-72.

5.5 CONCLUSIONS DU CHAPITRE 5

Nous avons montré que l'argent pouvait être remplacé partiellement par le cuivre dans les verres chalcobalogénés par une méthode électrochimique. Il est tentant d'étendre ce travail aux verres phosphates. Ce sera l'objet de nos prochains travaux.

Le thallium peut se substituer à l'argent dans les verres iodophosphatés. Nous avons également montré qu'il existait des verres entre le métaphosphate d'argent et le sulfure de thallium. Ce résultat semble montrer que les verres thiooxyphosphatés, préparés pour la première fois lors de notre étude dans le cas de l'argent et du thallium, doivent exister pour d'autres cations. Il n'est pas interdit de penser que dans cette nouvelle famille de verres, on puisse découvrir de nouveaux superconducteurs ioniques du lithium par exemple.

Chapitre 6 APPLICATIONS ELECTROCHIMIQUES DES VERRES
CONDUCTEURS DE L'ION ARGENT

Table des Matières

Chapitre 6 APPLICATIONS ELECTROCHIMIQUES DES VERRES

CONDUCTEURS DE L'ION ARGENT	110
6.1 INTRODUCTION	110
6.2 APPLICATIONS ELECTROCHIMIQUES DES VERRES	
CONDUCTEURS IONIQUES DE L'ION ARGENT	110

Chapitre 6

APPLICATIONS ELECTROCHIMIQUES DES VERRES CONDUCTEURS DE L'ION ARGENT

6.1 INTRODUCTION

Compte tenu des performances exceptionnelles des matériaux décrits précédemment, il était tentant de les utiliser dans des dispositifs électrochimiques. C'est l'objet de ce chapitre.

6.2 APPLICATIONS ELECTROCHIMIQUES DES VERRES CONDUCTEURS IONIQUES DE L'ION ARGENT

Material Science and Engineering (To be published)

Application of silver conducting glasses to solid state batteries and sensors.

Liu Jun, J. Portier, B.Tanguy, J.J. Videau, Laboratoire de Chimie du Solide, 351 cours de la Libération, 33405 Talence France.
and J. Salardenne, LEMME, 351 cours de la Libération, 33405 Talence France.

Abstract :

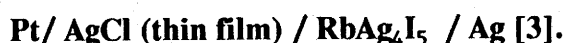
The possible applications of fast silver ion conducting glasses in electrochemical devices have been tested. A silver-iodine battery using a silver ionic conducting glass ($\text{AgPO}_3\text{-Ag}_2\text{S-AgI}$) has been studied. The interaction of some gases (O_2 , Cl_2 , H_2S) with the electrochemical chains $\text{Pt/Sb}_2\text{S}_3\text{-AgI(glass)/Ag}$ and $\text{Pt/AgCl(thin film)/Sb}_2\text{S}_3\text{-AgI(glass)/Ag}$ have been investigated.

1. Introduction

Among the potential or actual applications of solid electrolytes, solid state batteries and chemical sensors are the most promising. These two applications need fast ionic conductors in order to minimize the internal resistance of the batteries or the impedance of the sensors.

In some solid phases, silver ions possess a very high mobility, as evidenced by the room temperature ionic conductivity of RbAg_4I_5 is $\sigma = 0.3 \Omega^{-1} \cdot \text{cm}^{-1}$. Saito and Kashihara suggested the use of this material in a silver iodine battery [1]. Compared to lithium batteries, they possess a much lower OCV ($E = 0.68 \text{ V}$ for Ag/I_2 system versus $E = 2.6 \text{ V}$ for Li/TiS_2 [2]) but a higher rate of discharge.

In the case of chemical sensors, Hötzel and Weppner have studied a chlorine gas sensor based on the following galvanic chain :



We have recently studied new glasses obtained by reaction of a glass former (As_2S_3 , Sb_2S_3 , AgPO_3) with AgI and Ag_2S mixtures [4, 5, 6]. In these electrolytes silver ions possess a very high mobility. The conductivity at room temperature can reach $10^{-1} - 10^{-2} \Omega^{-1} \cdot \text{cm}^{-1}$.

It was tempting to use these glasses in batteries and chemical sensors. Although the conductivity of the glasses is 10-100 times lower than that of RbAg_4I_5 , they possess some advantages. Indeed the silver rubidium iodide decomposes at 18°C and is not very stable towards moisture and iodine. In addition the thioiodide glasses are much easier to shape.

2. Silver-iodine batteries

2.1. Experimental

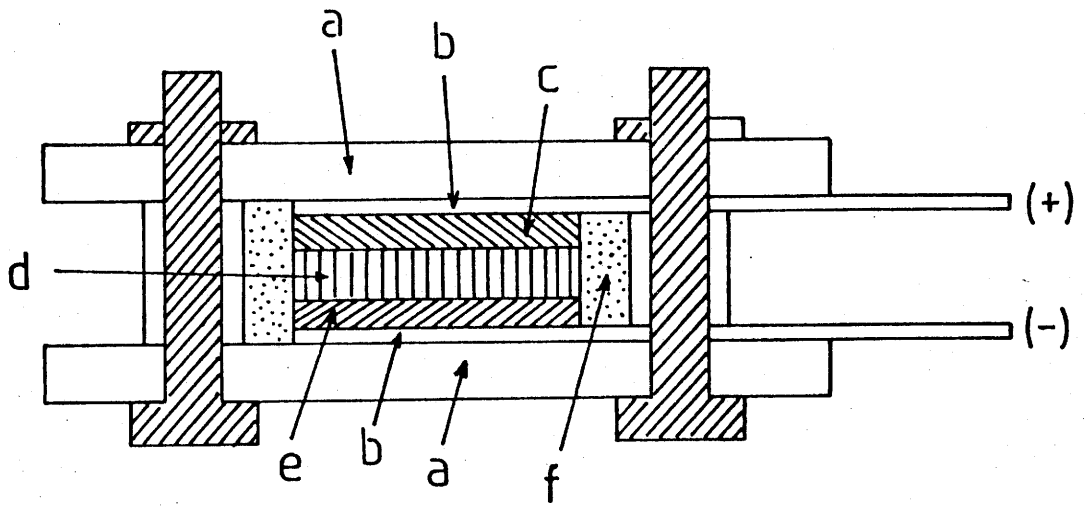
The electrolyte was a glass of composition $0.12 \text{ Ag}_2\text{S}-0.44\text{AgI}-0.44\text{AgPO}_3$ prepared as described elsewhere [6]. The galvanic chain was as follows :
 $\text{Ag} + \text{electrolyte} / \text{electrolyte} / \text{electrolyte} + \text{phenothiazine} + \text{I}_2 + \text{C}$. The anode was made of 70 w% of glass and 30 w% of silver powder. The composition of the cathode was 24 w% carbon, 16 w% phenothiazine, and 60 w% iodine. Carbon was added to the cathode to insure electronic conductivity. The charge transfer complex iodine - phenothiazine was used in place of pure iodine to disperse the iodine atoms in order to avoid the formation of an ionic and electronic insulating film of $\beta\text{-AgI}$ [1]. Anode, electrolyte and cathode were pressed together at 5 t/cm^2 . The surface of the obtained pellet was coated by epoxy resin and then introduced into a teflon cell (Fig.1).

2.2. Results

A discharge curve is displayed in Fig.2. It corresponds to a load resistance of $47 \text{ k}\Omega$ and a current density of $10 \mu\text{A/cm}^2$. In a previous work, Sun Hongwei studied a comparable galvanic chain ($\text{Ag}/\text{electrolyte}/\text{I}_2 + \text{C}$) [7]. The discharge voltage for a $2 \mu\text{A/cm}^2$ discharge current density was 0.66 V. In our case the plateau of the discharge curve corresponds to a lower voltage (0.63 V) due to the use of the charge transfer complex. However, the yield of the battery is about 2.5 times higher. This result can also be compared to that obtained by Saito and Kashihara [1]. In comparable discharge conditions, the lifetime of the battery using the glass electrolyte (500 h) is slightly longer than that working with RbAg_4I_5 (400 h).

3. Chemical gas sensors

3.1. Introduction



- a. Insulator
- b. Nickel lead
- c. Cathode
- d. Electrolyte
- e. Anode
- f. Epoxy resin

Fig. 1 Cross section of the battery test cell.

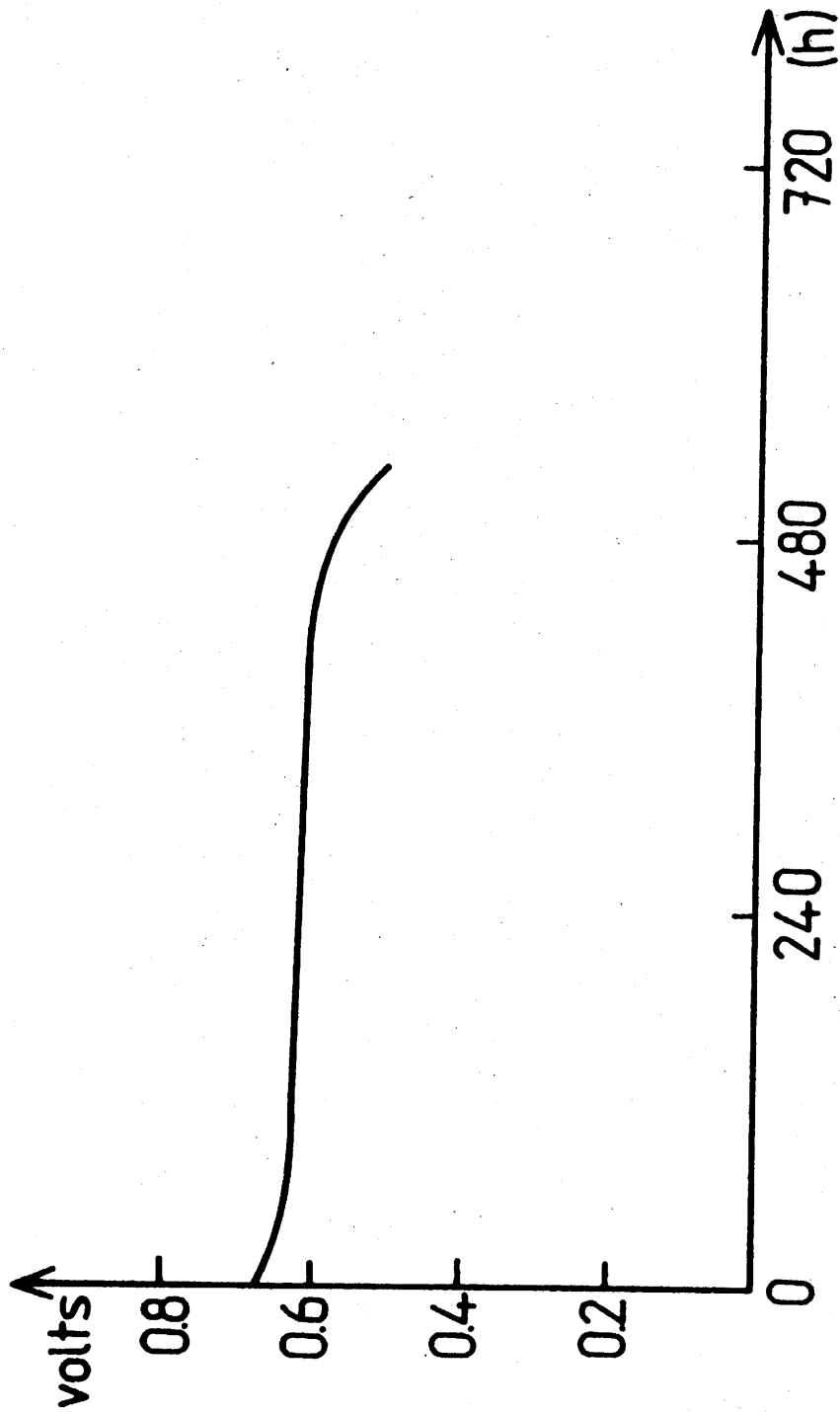


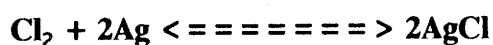
Fig. 2 Discharge curve of the battery ($T = 25^{\circ}\text{C}$, current density = $10 \mu\text{A}/\text{cm}^2$)

Gas chemical sensors are becoming increasingly important in many fields : power consumption, raw material savings, industrial process improvements, pollution control, etc. . However for many applications, the main drawback of potentiometric sensors is their high working temperature. A great deal of current research is aimed at lowering this temperature [3-8-9]. Oxygen sensor working at room temperature or slightly above have been studied [10]. Sensors are also being developed industrially for other gases (i.e. Cl₂, SO₂, SO₃) [11, 12]. Auxiliary layer were recently used to analyze gases which have no suitable ionic conductor materials [3, 13].

An electrochemical sensor is essentially a galvanic cell which is used to monitor the concentration of species present in another phase. Nernst's law is the basic concept used to explain their behaviour. For example, in this paper, the galvanic cell used to test Cl₂ gas was :



Ag metal and silver ionic conducting glass form a reference electrode. The silver ionic conducting glass is the electrolyte. AgCl is the auxiliary layer and Pt is the measurement electrode. The electrode reaction is :



According Nernst's law, the e.m.f. obeys equation :

$$E = E_0 + \frac{RT}{nF} (\ln P_{\text{Cl}_2})$$

where R is the gas constant (8.32 J .mol⁻¹.K⁻¹), F is Faraday's constant (96500 C), n = 2 is the number of electrons involved in the electrode reaction and T is the absolute temperature of the cell. E₀, the standard potential can be calculated from ΔG⁰, the Gibbs energy of formation of AgCl.

3.2.Experimental

Cl_2 gas is obtained from UCAR (research purity). The gas line used for this study is shown in Fig.3.

The sensor device is depicted in Fig. 4. $\text{AgI-Sb}_2\text{S}_3$ glass was used as the solid electrolyte. Measurement electrode was made by a sputtered AgCl film coated with a Pt film obtained also by sputtering. A pellet of silver powder was co-pressed with the electrolyte as the reference electrode. The sensor was then sealed by an epoxy resin to avoid any reaction of the reference electrode with the gas atmosphere. Sputtered Pt electrode and gold leads were used. An Al_2O_3 ceramic substrate was used. The carrier-gas was argon or air.

The sensor EMF was measured for various gas concentration with a high input impedance ($10^{14}\Omega$) multimeter (KEYTHLEY 16).

3.3. Results

3.3.1 Response to O_2 and H_2S gas

Oxygen response was first tested in the simple galvanic cell : $\text{Ag} / \text{Ag} + \text{conducting glass} / \text{Pt}$. A variation of the EMF was observed due to the formation of Ag_2O film on the surface of the electrolyte. The experimental curve is shown in Fig. 5 (a). For high oxygen concentration the EMF varies linearly with the logarithm of the oxygen partial pressure. However at low oxygen pressure the slope of the lines changes. This behaviour is probably due to a kinetic adsorption effect. Indeed, at room temperature the response time became long.

The sensitivity to H_2S has been tested (Fig. 5). In air, when the partial pressure of H_2S is lower than 10^{-2} atm (Fig. 5b), the EMF value corresponds to the response at $P_{\text{O}_2} = 0.21$ atm which is the partial pressure of oxygen in air (Fig. 5a). When H_2S is mixed with argon (Fig. 5a), with $P_{\text{H}_2\text{S}} < 10^{-2}$ atm, the EMF approaches the value corresponding to that of P_{O_2} at the same pressure in an argon mixture

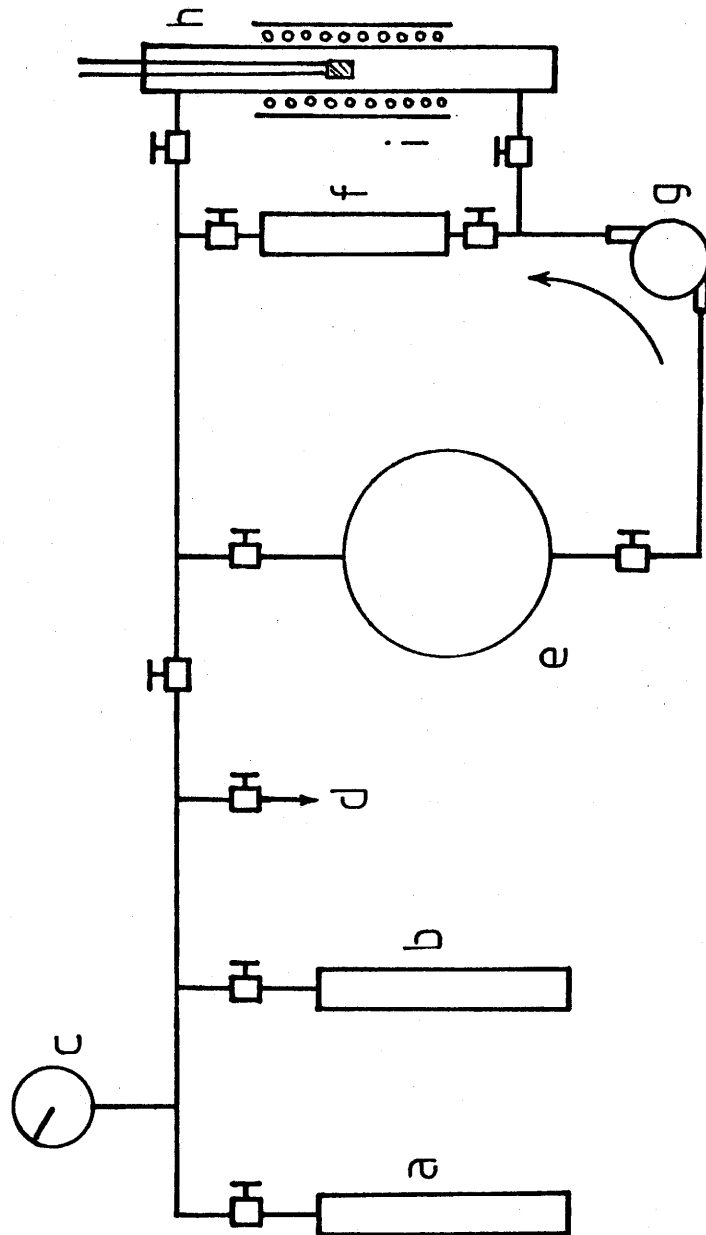


Fig. 3 Gas line used for testing the sensors : a) gas tank (high pressure), b) gas tank (low pressure), c) manometer, d) vacuum pump, e) mixture chamber, f) mixing gas device, g) cycling pump, h) test chamber, i) heater.

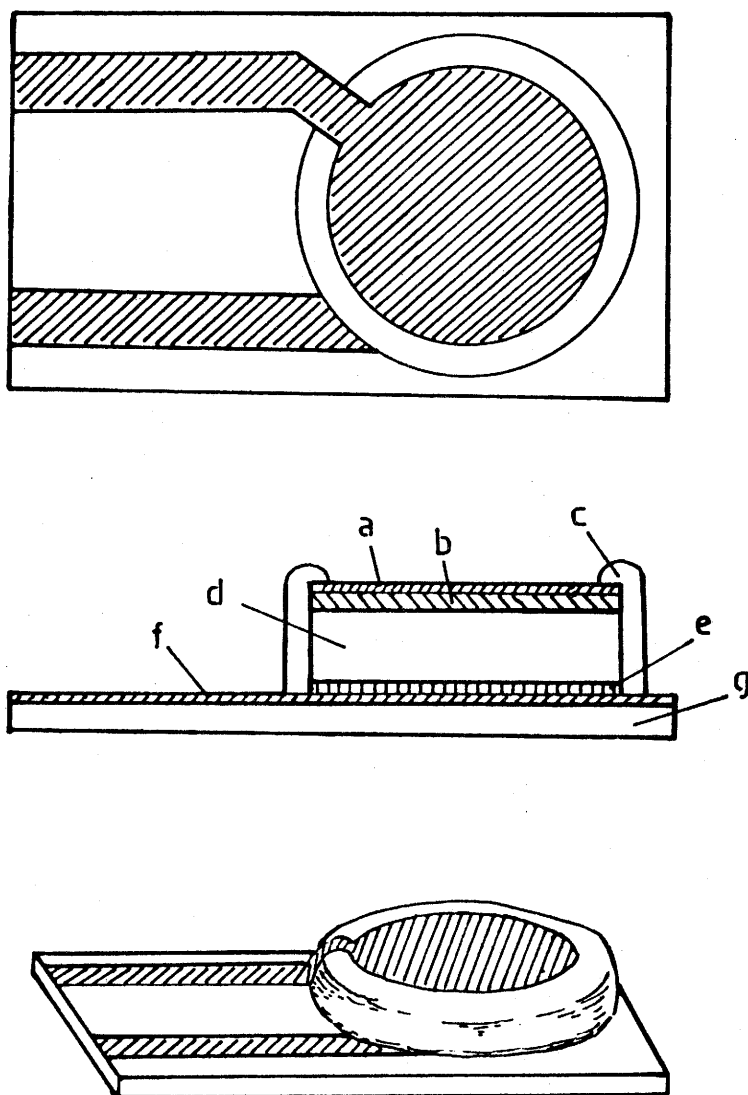


Fig. 4 Schematic diagram of the investigated cell : a) sputtered Pt thin film, b) sputtered AgCl thin film, c) epoxy resin coating, d) Ag⁺ conducting glass electrolyte, e) Ag reference electrode, f) Gold lead, g) Al₂O₃ ceramic substrate.

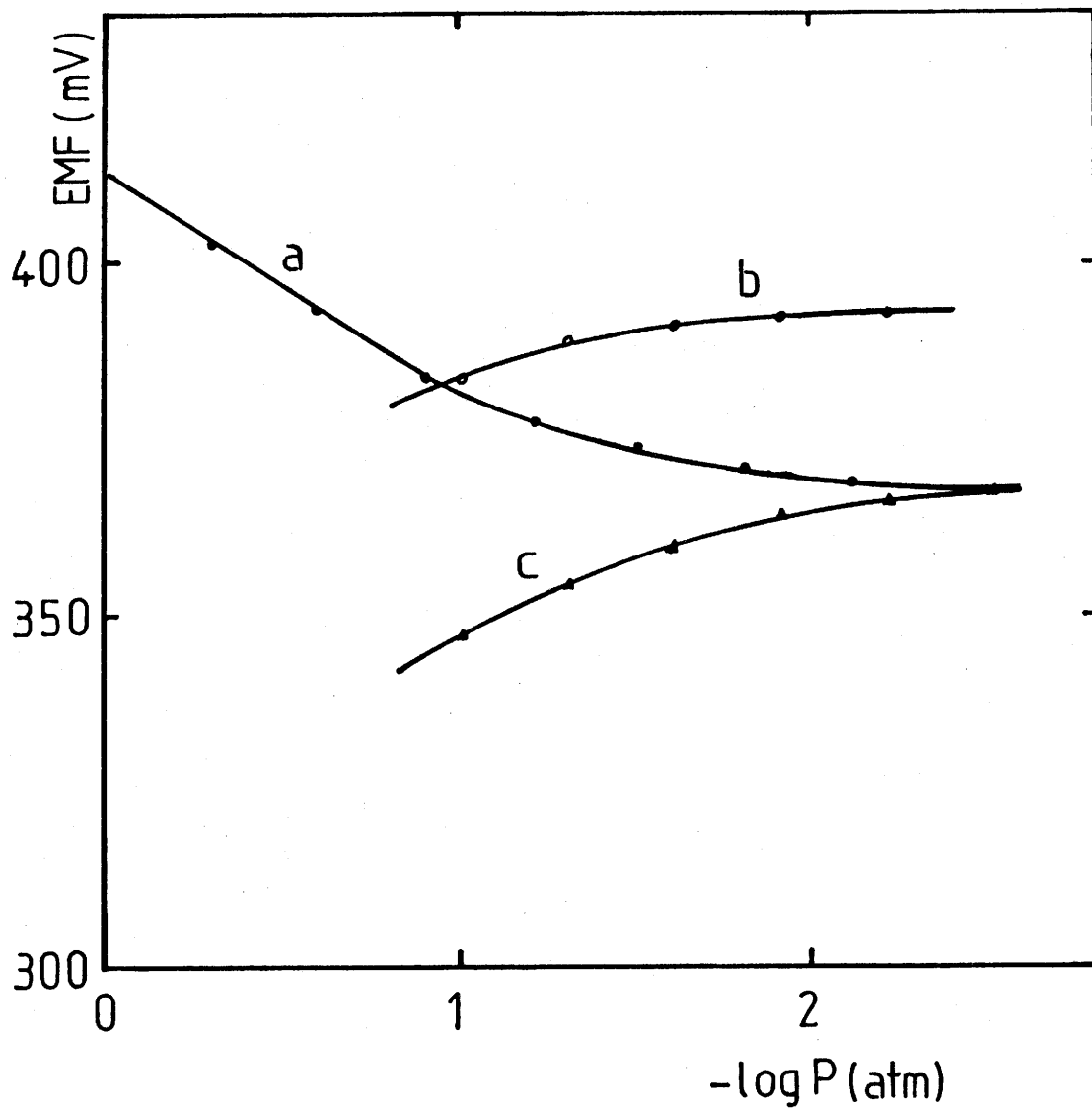


Fig. 5 Sensor Ag/Ag+(glass)/Pt response : a) oxygen-argon at 93°C, b) H₂S-air at 92°C, c) H₂S-argon at 81°C.

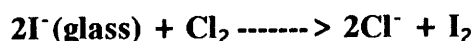
(Fig. 3a). These results show that this device can not be used to detect traces of H₂S in air.

3.3.2. Response to chlorine

The chlorine response of the AgCl sensitive layer (1000 Å thick) coated galvanic cell is given in Fig. 6c. In the pressure range of 1-10⁻⁴ atm, a linear variation is observed. At lower pressure, the linear relationship is no longer obeyed due to a kinetical slow absorption.

Even in the linear domain, the EMF is lower than the potential expected from Nerst's law indicating an extra chemical reaction between the electrolyte and chlorine due to the permeability of the silver chloride film. Consequently, another test was undertaken with a sensor coated with a thick AgCl film (1µm). The results are shown in Fig. 6b. The experimental data approach the theoretical values. In a limited case, a sensor using a pure AgCl layer as electrolyte was tested. For high Cl₂ pressure, the response is very near the theoretical value (Fig. 6a) while for chlorine partial pressure lower than 10⁻¹ atm, the EMF deviates because of the poor ionic conductivity of silver chloride at room temperature.

These results show that the conducting glass which contains I⁻ ions may react with Cl₂. The reaction may proceed as shown below :



As the sensor EMF depends on the activity of the gas at the electrolyte surface (i.e. at the "triple contact" gas/electrolyte/electronic conductor), the potential is lower than that calculated with Nernst's law from Gibbs energy of formation of AgCl.

With thick AgCl film, the response time is less than 3 minutes for a chlorine partial pressure of 5x10⁻⁴ atm (Fig.7). At lower pressure the response time become longer and the EMF variation is no longer linear.

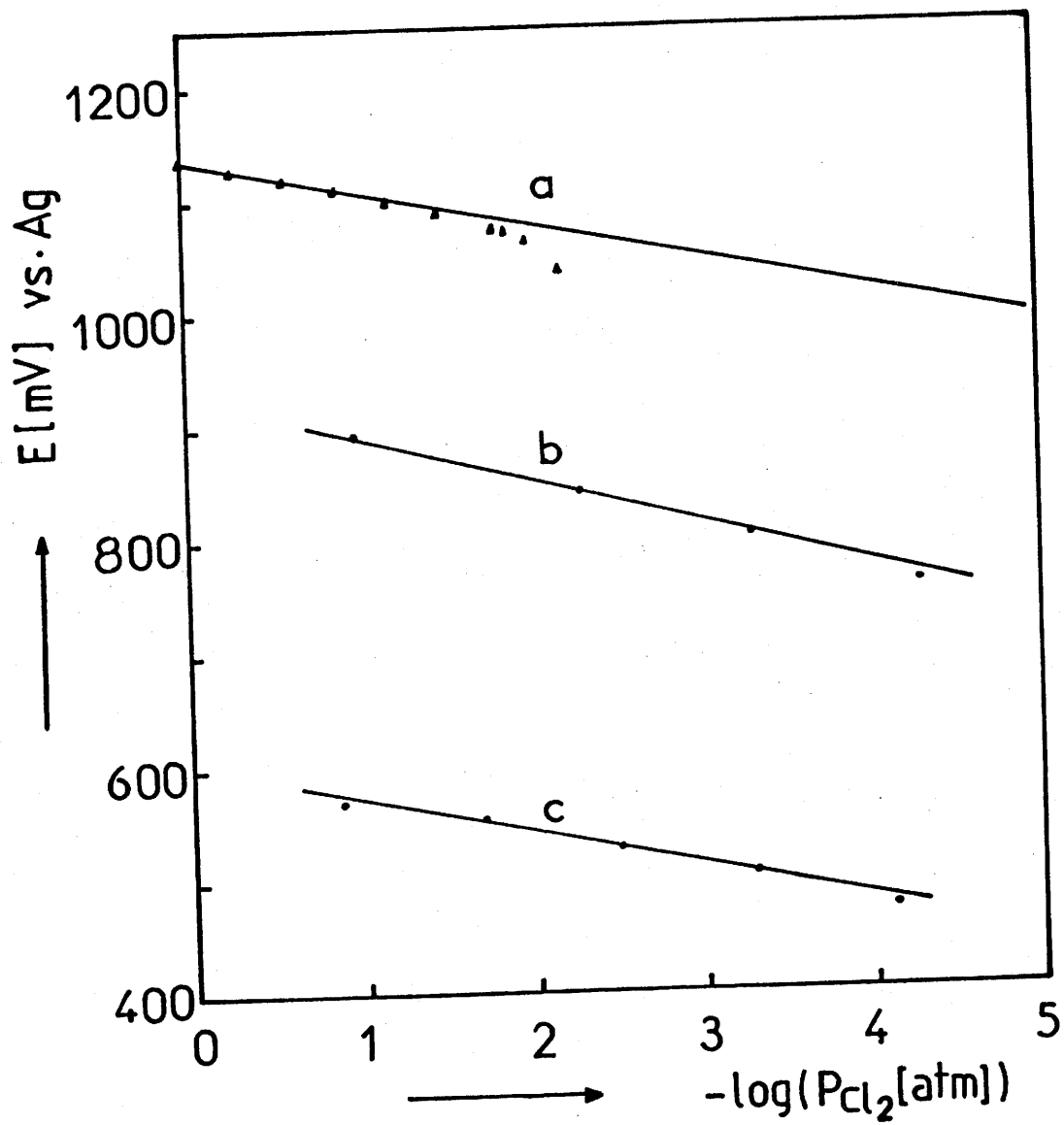


Fig. 6 Variation of EMF versus chlorine partial pressure ($T = 25^\circ\text{C}$) a) pure AgCl sensor, b) sensor coated with AgCl thick film, c) sensor coated with AgCl thin film.

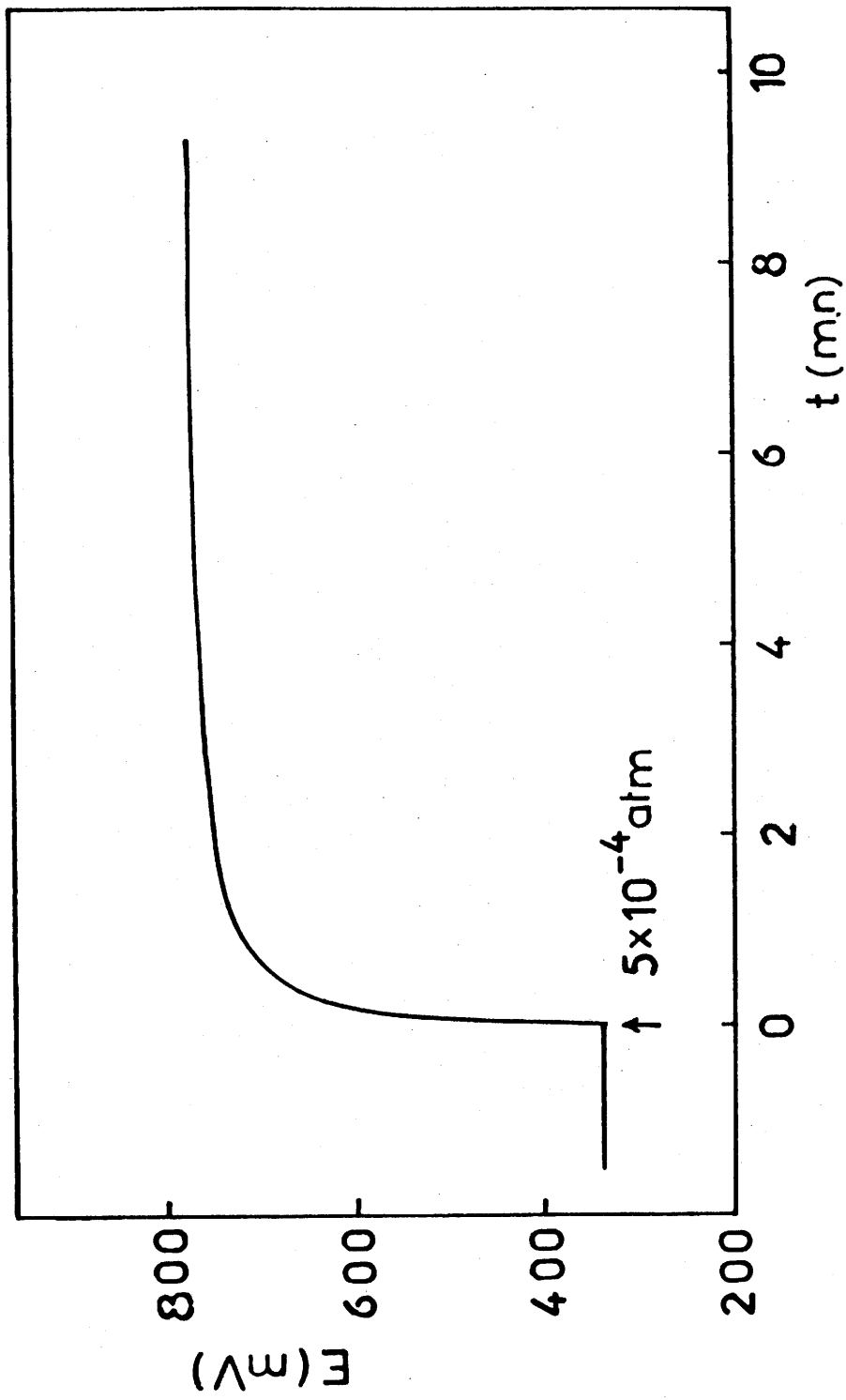


Fig. 7 Voltage response to addition of chlorine at 5×10^{-4} atm.

4 Conclusions

This study shows that silver conducting glasses can be used in electrochemical devices as electrolyte. Easy to prepare and to shape, with a good chemical durability they can replace RbAg_4I_5 in batteries and chemical sensors.

REFERENCES

- [1] S. Saito and S. Kashihara, "Problems in solid electrolyte batteries with silver ion conductors", in "Applications of solid electrolytes" T.Takahashi and A. Kozawa ed., JEC press (1980)
- [2] S.Sinha and D.W. Murphy, Solid State Ionics, 20, 81 (1986)
- [3] G. Hötzel and W. Weppner, Solid State Ionics, 18-19, 1223 (1986)
- [4] J.M. Réau, B.Tanguy, J.J. Videau, J. Portier and P. Hagenmuller, Solid State Ionics, 28, 782 (1986)
- [5] H. W. Sun, B. Tanguy, J.M. Réau, J.J. Videau and J.Portier, Mat. Res. Bull., 22, 823 (1987)
- [6] Liu Jun, J. Portier, B. Tanguy, J-J. Videau and C.A. Angell, Solid State Ionics, (in press).
- [7] Sun Hongwei, Thesis, University of Bordeaux I, (1986)
- [8] J.Fouletier, Sensors and Actuators, 3 (1982/83) 295.
- [9] G.Velasco, J.Ph.Schnell and M.Croset, Sensors and Actuators, 2 (1982) 371.
- [10] Wang Yong-Neng, Tan Fu-Bin and Jia Neng-Cheng, Solid State Ionics, 22 (1987) 151.
- [11] M.Gauthier, A.Bélangier, Y.Meas and M.Kleitz, in Solid Electrolytes, P.Hagenmuller and W.Van Gool eds. Academic Press, New York, 1978, p497.
- [12] M.Kleitz, A.Pelloux and M.Gauthier, in Fast Ion Transport in Solids, P.Vashishta, J.N.Mundy and G.K.Shenoy eds., New York, 1979, p69.
- [13] W.Weppner, Sensors and Actuators, 12 (1987) 107.

Chapitre 7 CONCLUSIONS GENERALES

Table des Matières

Chapitre 7 CONCLUSIONS GENERALES

125

Chapitre 7

CONCLUSIONS GENERALES

Lors de ce travail, nous avons étudié de nouveaux matériaux vitreux issus des systèmes formés entre le sulfure d'arsenic ou le phosphate d'argent et divers sulfures et iodures. Nous avons recherché systématiquement les relations entre composition, structure et propriétés de transport ionique.

Nous avons tout d'abord étudié les verres formés par hypertrempe par interaction du sulfure d'arsenic et du sulfure et de l'iode d'argent. Nous pensions en effet que ces verres posséderaient des performances supérieures à leurs homologues antimoniés étudiés précédemment. Cet espoir s'est avéré fallacieux, l'effet bénéfique de la covalence renforcée du réseau vitreux étant compensé par un encombrement stérique plus grand.

Nous avons ensuite étudié des verres à base de phosphate d'argent. L'interaction de ce composé avec le sulfure du même élément a conduit à des verres possédant le même comportement électrique que les verres iodés étudiés précédemment. Il avait été expliqué par la formation d'agrégats dont la structure mimerait celle du superconducteur ionique $\text{AgI-}\alpha$. Nous avons montré qu'il n'en était rien dans le cas de nos matériaux. Nous avons proposé un modèle alternatif : coordinence faible des ions argent comme dans les variétés haute température du sulfure et de l'iode dans un réseau lâche comme celui des phosphate à chaînes.

Les verres homologues à base d'iodure et de sulfure de thallium ont également fait l'objet d'investigation. Un échange argent- thallium a été observé en accord avec les acidités et basicité respectives des ions mis en jeu.

Nous avons pu montrer qu'il était possible d'introduire des ions Cu^+ dans ces matériaux par une méthode électrochimique.

Enfin, compte tenu des performances électriques de ces nouveaux verres, nous avons voulu tester leur possibilité d'utilisation dans des dispositifs électrochimiques. Des batteries et des capteurs de gaz ont donc été réalisés.

Les performances électriques les plus élevées ont été obtenues dans le cas des systèmes impliquant le sulfure et l'iodure d'argent au voisinage de la composition Ag_3SI . Des conductivités supérieures à $10^{-2}(\Omega.\text{cm})^{-1}$ ont été observées à température ambiante. Nous n'avons pas cependant surpassé les performances des systèmes à base de sulfure d'antimoine précédemment étudiés. On peut se demander s'il s'agit d'une limite physique à la conductivité ionique dans les solides amorphes. L'état d'avancement des recherches théoriques sur le sujet ne permet pas de répondre à cette question.

LISTE DES FIGURES

	page
CHAPITRE 2	
Fig. 1: Schématisation du modèle de Anderson-Stuart d'après Martin et Angell [12]	9
Fig.2: Variation de la conductivité en fonction de la température réciproque pour les verres conducteurs de l'ion argent. Comparaison avec quelques phases cristallisées.	14
CHAPITRE 3	
Ch.3.1	
Fig.1: Variation of log. vs. reciprocal temperature for various glasses belonging to the (1-x) As₂S₃-xAg₂S system.	22
Fig.2: Variation of logσ_{25°C} vs. molar rate of Ag₂S. Comparison with KAWAMOTO's results [9].	23
Fig.3: Variation of the activation energy at 25°C vs. molar rate of Ag₂S. Comparison with KAWAMOTO's results [9].	24
Fig.4: Far-infrared spectra for the crystallized compounds As₂S₃ and Ag₂S and various glasses belonging to the (1-x) As₂S₃-x Ag₂S system	26
Fig.5: Infrared absorption spectra for the AgAsS₂ and Ag₃AsS₃ crystallized phases.	28
Ch 3.2	
Fig.1: (1a) Glassy domain in the As₂S₃-Ag₂S-AgI system <—> Glasses obtain by rapid quenching <---> Glasses prepared in a silica tube. (1b) Corresponding domain in the Sb ₂ S ₃ -Ag ₂ S-AgI system (1c) Location in the ternary system of glasses described with the general formula:(As ₂ S ₃ -pAg ₂ S) _{1-y} (AgI) _y	33
Fig.2: Variation of logσ_{25°C} (a) and ΔE (b) versus y for glasses (As₂S₃-pAg₂S)_{1-y}(AgI)_y corresponding to constant values of p.	36

Ch.3.3

Fig.1: Variation de $\log\sigma_{25^\circ\text{C}}$ (a) et ΔE (b) en fonction de y pour les verres $(\text{Sb}_2\text{S}_3\text{-pAg}_3\text{S})_{1-y}(\text{AgI})_y$	39
---------------------------------------------------------------------------------------------------------------------------------------------------------------------------------------	----

Ch.3.4

Fig.1: Chemical composition of the vitreous samples studied by infrared spectroscopy. The continuous line corresponds to the limit of the vitreous domain obtained by hyperquenching of 10^{60}C/s rate.	43
------------------------------------------------------------------------------------------------------------------------------------------------------------------------------------------------------------------------	----

Fig.2: Infrared absorption spectra of glasses corresponding to $p \geq 9$ (a : $p = 19, y = 0.27$; b : $p = 13, y = 0.57$; c : $p = 9, y = 0.70$).	44
------------------------------------------------------------------------------------------------------------------------------------------------------------	----

Fig.3: Infrared absorption spectra of glasses corresponding to $p = 4$ (f : $y = 0.29$; e : $y = 0.45$).	45
-----------------------------------------------------------------------------------------------------------------	----

Fig.4: Infrared absorption spectra of glasses corresponding to $p = 2$ (f : $y = 0.21$; e : $y = 0.40$; h : $y = 0.55$; i : $y = 0.70$).	46
---------------------------------------------------------------------------------------------------------------------------------------------------	----

Fig.5: Infrared absorption spectra of glasses corresponding to $p = 1$ (j : $y = 0.15$; k : $y = 0.30$; l : $y = 0.50$; m : $y = 0.60$; n : $y = 0.80$).	48
--------------------------------------------------------------------------------------------------------------------------------------------------------------------	----

Fig.6: Infrared absorption spectra of glasses corresponding to $p = 4$ (o : $y = 0.20$; k : $y = 0.39$; s : $y = 0.50$; t : $y = 0.79$).	49
---------------------------------------------------------------------------------------------------------------------------------------------------	----

Fig.7: Infrared absorption spectra of vitreous As_2S_3 and crystalline $\text{AsI}_3, \text{AgI}, \text{Ag}_2\text{S}, \text{Ag}_3\text{AsS}_3$ and AgAsS_2	50
---------------------------------------------------------------------------------------------------------------------------------------------------------------------------------------------	----

Fig.8: Variation of $\log\sigma_{25^\circ\text{C}}$ vs. $r = \text{Ag/As}$ ratio for the glasses belonging to the $\text{As}_2\text{S}_3\text{-Ag}_2\text{S-AgI}$ system.	52
--------------------------------------------------------------------------------------------------------------------------------------------------------------------------------	----

Fig.9: Variation of $\log\sigma_{25^\circ\text{C}}$ vs. AgI molar fraction y for the glasses of the $\text{As}_2\text{S}_3\text{-Ag}_2\text{S-AgI}$ system.	54
--------------------------------------------------------------------------------------------------------------------------------------------------------------------	----

Fig.10: Isoconductivity curves in the $\text{As}_2\text{S}_3\text{-Ag}_2\text{S-AgI}$ system ($\sigma_{25^\circ\text{C}} = 10^{-2}, 10^{-3}$ and $10^{-4} (\Omega\text{cm})^{-1}$).	55
--------------------------------------------------------------------------------------------------------------------------------------------------------------------------------------------	----

CHAPITRE 4

Ch.4.1

Fig.1: Vitreous domain in $x\text{Ag}_2\text{S-(1-x)AgPO}_3$ system; (I) glass transition temperature (T_g) and (O) expansion coefficient (at 25°C).	63
------------------------------------------------------------------------------------------------------------------------------------------------------------------------------	----

Fig.2: Arrhenius plot of conductivity for $x\text{Ag}_2\text{S-(1-x)AgPO}_3$	65
------------------------------------------------------------------------------------	----

	page
glasses.	
Fig.3: Variation of conductivity at 25°C and activation energy of the $x\text{Ag}_2\text{S}-(1-x)\text{AgPO}_3$ glasses. Note extrapolations to values for supercooled crystalline Ag_2S in high temperature superionic form.	66
Fig.4: Infrared spectra of the glasses : (a) AgPO_3; (b) 0.3 $\text{AgI}-0.7\text{AgPO}_3$; (c) 0.3 $\text{Ag}_2\text{S}-0.7\text{AgPO}_3$.	69
Fig.5: Location of present pseudo-binary system in the ternary system $\text{Ag}_2\text{S}-\text{Ag}_2\text{O}-\text{P}_2\text{O}_5$.	71
Ch.4.2	
Fig.1: Représentation schématique des réseaux de AgPO_3, des verres $\text{AgPO}_3\text{-AgI}$ et $\text{AgPO}_3\text{-Ag}_2\text{S}$	78
CHAPITRE 5	
Chap 5.2	
Fig.1: The concentration profile of silver as a function of depth obtained with electron microprobe X-ray analysis.	86
Fig.2: The concentration profile of copper as a function of depth obtained with electron microprobe X-rays analysis.	86
Ch.5.3	
Fig.1: Vitreous domain (hatched area) and variation of T_g with iodide concentration in $x\text{TlI}-(1-x)\text{AgPO}_3$ (solid line) and $x\text{AgI}-(1-x)\text{AgPO}_3$ (dotted line).	93
Fig.2: Arrhenius plots of conductivities of TlI-AgPO_3 glasses (composition in mole % TlI).	94
Fig.3: Variation of the logarithm of the conductivities with % TlI of TlI-AgPO_3 glasses (solid line) compared with corresponding behavior of AgI-AgPO_3 glasses.	96
Fig.4: Variation of the activation energy for TlI-AgPO_3 glasses versus % TlI, compared with that for AgI-AgPO_3 glasses.	97
Fig.5: Infrared spectra of the glasses a) AgPO_3, b) 0.3 $\text{AgI}-0.7\text{AgPO}_3$, c) 0.3 $\text{TlI}-0.7\text{AgPO}_3$.	98
Ch.5.4	
Fig.1: Vitreous domain (hatched area) and variation of T_g (solid line) with Tl_2S concentration in $x\text{Tl}_2\text{S}-(1-x)\text{AgPO}_3$ system.	103

Fig.2: Arrhenius plots of conductivities of $Tl_2S-AgPO_3$ glasses (composition in mole % Tl_2S).	104
Fig.3: Variation of the logarithm of the conductivities at 25°C and the activation energy for $Tl_2S-AgPO_3$ glasses versus % Tl_2S	105
Fig.4: Infrared spectra of the glasses a) $AgPO_3$, b) $0.2Tl_2S-0.8AgPO_3$, c) $0.2Ag_2S-0.8AgPO_3$.	106
CHAPITRE 6		
Fig.1: Cross section of the battery test cell.	113
Fig.2: Discharge curve of the battery ($T = 25^\circ C$, current density = $10 \mu A/cm$).	114
Fig.3: Gas line used for testing the sensors : a) gas tank (high pressure), b) gas tank (low pressure), c) manometer, d) vacuum pump, e) mixture chamber, f) mixing gas device, g) cycling pump, h) test chamber, i) heater.	117
Fig.4: Schematic diagram of the investigated cell : a) sputtered Pt thin film, b) sputtered AgCl thin film, c) epoxy resin coating, d) Ag^+ conducting glass electrolyte, e) Ag reference electrode, f) Gold lead, g) Al_2O_3 ceramic substrate.	118
Fig.5: Sensor $Ag/Ag^+(glass)/Pt$ response : a) oxygen-argon at $93^\circ C$, b) H_2S-air at $92^\circ C$, c) H_2S-argon at $81^\circ C$.	119
Fig.6: Variation of EMF versus chlorine partial pressure ($T = 25^\circ C$) a) pure AgCl sensor, b) sensor coated with AgCl thick film, c) sensor coated with AgCl thin film.	121
Fig.7: Voltage response to addition of chlorine at 5×10^{-4} atm.	122

LISTE DES TABLEAUX

	page
CHAPITRE 2	
Tableau I : Un siècle de l'histoire de la conductivité ionique.	6
Tableau II : Ions mobiles et formateurs dans les principaux verres conducteurs ioniques.	7
CHAPITRE 3	
Ch.3.1	
TABLE I: Tg and Tc values for some compositions of the As₂S₃-Ag₂S system	21
TABLE II: Transport numbers of two glasses in the As₂S₃-Ag₂S system	21
Ch.3.2	
Table I: Tg values for some glasses in the As₂S₃-Ag₂S-AgI system.	35
Table II: Transport number of some glasses in the As₂S₃-Ag₂S-AgI system.	35
CHAPITRE 4	
Table I: Values of conductivity at 25°C, activation energy and pre-exponential term of the Ag₂S-AgPO₃ glasses.	67
Table II: Transport numbers of Ag⁺ ions in Ag₂S + AgPO₃ glasses	68
Table III: Chemical durability of 0.20 Ag₂S-0.80 AgPO₃ glass	68
CHAPITRE 5	
Table 1: Conductivity of the 0.67AgI-0.33Sb₂S₃ glass at 25°C	87

**Vu et approuvé
Talence, le
Le Président de l'Université
de BORDEAUX I.**